6-2011

Sphingolipids Containing Very-Long-Chain Fatty Acids Define a Secretory Pathway for Specific Polar Plasma Membrane Protein Targeting in *Arabidopsis*

Jonathan E. Markham
University of Nebraska-Lincoln, jmarkham3@unl.edu

Diana Molino
Institut National de la Recherche Agronomique–AgroParisTech

Lionel Gissot
Institut National de la Recherche Agronomique–AgroParisTech

Yannick Bellec
Institut National de la Recherche Agronomique–AgroParisTech

Kian Hématy
Institut National de la Recherche Agronomique–AgroParisTech

See next page for additional authors

Published in *The Plant Cell* 23 (June 2011), pp. 2362–2378; doi: 10.1105/tpc.110.080473 http://www.plantcell.org

Submitted October 13, 2010; revised April 15, 2011; accepted May 20, 2011; published June 10, 2011.

Sphingolipids Containing Very-Long-Chain Fatty Acids Define a Secretory Pathway for Specific Polar Plasma Membrane Protein Targeting in *Arabidopsis*

Jonathan E. Markham,[1] Diana Molino,[2] Lionel Gissot,[2] Yannick Bellec,[2] Kian Hématy,[2] Jessica Marion,[3] Katia Belcram,[2] Jean-Christophe Palauqui,[2] Béatrice Satiat-JeuneMaître,[3] and Jean-Denis Faure [2]

1. Donald Danforth Plant Science Center, St. Louis, Missouri 63132, USA (Current address: Department of Biochemistry, University of Nebraska–Lincoln, N146 Beadle Center, Lincoln, NE 68588, USA)
2. Institut Jean-Pierre Bourgin, Unité Mixte de Recherche 1318, Institut National de la Recherche Agronomique–AgroParisTech, Centre de Versailles-Grignon, 78000 Versailles, France
3. Institut des Sciences du Végétal, Centre National de la Recherche Scientifique, F-91198 Gif-sur-Yvette Cedex, France

Authors Markham and Molino contributed equally to this work.

Corresponding author — J.-D. Faure, email faure@versailles.inra.fr

Abstract

Sphingolipids are a class of structural membrane lipids involved in membrane trafficking and cell polarity. Functional analysis of the ceramide synthase family in *Arabidopsis thaliana* demonstrates the existence of two activities selective for the length of the acyl chains. Very-long-acyl-chain (C > 18 carbons) but not long-chain sphingolipids are essential for plant development. Reduction of very-long-chain fatty acid sphingolipid levels leads in particular to auxin-dependent inhibition of lateral root emergence that is associated with selective aggregation of the plasma membrane auxin carriers AUX1 and PIN1 in the cytosol. Defective targeting of polar auxin carriers is characterized by specific aggregation of Rab-A2^{a}– and Rab-A1^{e}–labeled early endosomes along the secretory pathway. These aggregates correlate with the accumulation of membrane structures and vesicle fragmentation in the cytosol. In conclusion, sphingolipids with very long acyl chains define a trafficking pathway with specific endomembrane compartments and polar auxin transport protein cargoes.

Introduction

Sphingolipids are essential for eukaryotic life (Holthuis et al., 2001). Current theory suggests this is due, at least in part, to their role in protein sorting and secretion. Evidence indicates that, within the diverse membrane composition of the Golgi body, sphingolipids coalesce into microdomains or lipid rafts where, together with cholesterol and saturated phospholipids, they attract a unique subset of proteins and together are transported to the plasma membrane (PM; Klemm et al., 2009). In animal epithelial cells, this property of sphingolipids is exploited to maintain cell polarity through the regulation of vesicle trafficking and endocytosis at the apical membrane (Maier and Hoekstra, 2003; Nyasae et al., 2003). Sphingolipid sterol–rich microdomains are similarly recruited in the budding yeast *Saccharomyces cerevisiae* to establish cell polarity during mating and budding (Bagnat and Simons, 2002).

The ability of sphingolipids to form microdomains may be attributed to their unique physical properties compared with the glycerolipids. Sphingolipids consist of three primary components: an acyl amino alcohol or long-chain base (LCB), a fatty acid attached via the amino group, and a head group attached to carbon-1 (C1) of the LCB. Additional hydroxyl groups at C2 on the fatty acid and C4 on the LCB promote hydrogen bonding between sphingolipids that is not available to glycerolipids (Pascher, 1976). Furthermore, the fatty acid component of sphingolipids often consists of a saturated or monounsaturated very-long-chain fatty acid (VLCFA) of >18 carbons and up to 26 carbons in length (C26). The presence of VLCFA in sphingolipids increases their hydrophobicity, membrane leaflet interdigitation, and the transition from a fluid to a gel phase, which is a requirement for microdomain formation. This important property of VLCFA in membrane organization is supported by the observation that *S. cerevisiae* mutants unable to synthesize sphingolipids can be rescued by the *SLC1-1* mutation, which allows for the transfer of C26 fatty acids to the *sn-2* position of glycerolipids. C22 fatty acids are unable to support the functions performed by C26 fatty acids, indicating the sensitivity of the system to fatty acid chain length (Gaigg et al., 2005, 2006). As a result, yeast mutants in which fatty acid elongation beyond C16 is abolished are not viable (Oh et al., 1997).

The incorporation of fatty acids into sphingolipids is catalyzed by the enzyme ceramide synthase (sphinganine *N*-acyltransferase). Ceramide synthases are encoded by the *LAG1* gene family (named after longevity assurance gene 1); members of which have been found in all eukaryotes so far examined from fungi to animals and plants (Winter and Ponting, 2002). In animals, several ceramide synthases have been characterized (CERS1-6) and shown to have different substrate specificities with respect to the length of the acyl chain of the fatty acid (Riebeling et al., 2003; Mizutani et al., 2005, 2006). *S. cerevisae* contains two *LAG1* family mem-

bers, *LAG1* and *LAC1*, and deletion of both of these genes causes strongly reduced cell growth, cell wall defects, and delayed endoplasmic reticulum (ER)-to-Golgi transport of glycosylphosphatidylinositol-anchored proteins (Barz and Walter, 1999; Guillas et al., 2001; Schorling et al., 2001). These phenotypes can be complemented by homologous genes from *Homo sapiens, Caenorhabditis elegans,* and *Solanum lycopersicum* (Jiang et al., 1998; Spassieva et al., 2002), indicating that *LAG1* homologs serve as ceramide synthases. Recent studies on the role of the mammalian ceramide synthase CERS2 indicate that it is responsible for the incorporation of the majority of VLCFAs into the sphingolipids of the liver and brain (Imgrund et al., 2009; Pewzner-Jung et al., 2010). Interestingly, the alteration in sphingolipid profile resulting from CERS2 disruption bears some resemblance to that obtained when challenged by the ceramide synthase inhibitor fumonisin B1 (FB1), suggesting that FB1 may specifically inhibit the incorporation of VLCFA into sphingolipids, thereby mimicking the disruption of CERS2 activity (Pewzner-Jung et al., 2010).

Recent studies have identified several mutants of acyl-CoA elongation in plants that show phenotypes that have been attributed to depletion of VLCFA in sphingolipids. These mutants include *cer*10 (Zheng et al., 2005), g*urke/pasticcino3* (*pas3*; Baud et al., 2004), *pas2* (Bach et al., 2008), and *pas1* (Roudier et al., 2010). In all these mutants, the level of VLCFA in sphingolipids is reduced, and this reduction is coupled with important morphological changes in the plant. In the *cer10* mutant, which is deficient in elongation-specific enoyl reductase, endosomal compartments were shown to accumulate, indicating abnormal vesicle trafficking (Zheng et al., 2005). In the case of the *pas1* mutant, abnormal trafficking of the auxin polar efflux carrier PIN1 was associated with decreased VLCFA in sphingolipids (Roudier et al., 2010). PIN1 is one of several proteins with a polar localization within the root tissues of *Arabidopsis thaliana* responsible for forming auxin gradients that in turn control root elongation and lateral root formation. While VLCFAs are involved in other metabolic processes in plants, such as wax biosynthesis or seed storage lipid biosynthesis, defects in neither of these lead to the extreme defects in plant and seed morphology in these elongase mutants leaving sphingolipids as the prime candidate.

Several lines of evidence suggest that sphingolipid sterol–rich microdomains exist in plant membranes and that they may be involved in the polar targeting of proteins to the PM (Fischer et al., 2004). However, the precise role of sphingolipids in such processes has only been tangentially addressed in plants. As in animals, plant sphingolipids are a complex family of lipids with various acyl chain lengths, LCBs, and head groups moieties, although the specific role of each moiety is still uncertain. Complete structural analysis of sphingolipids has been carried out in several plant species, identifying four main classes: ceramide, hydroxyceramides, glucosylceramides, and glucosylinositolphosphorylceramides (Markham et al., 2006). Although several steps of plant sphingolipid biosynthesis have been identified and modified genetically, their effects on protein trafficking have not been adequately assessed. Recently, however, inhibition of glucosylceramide synthase activity was shown to correlate with protein trafficking in tobacco (*Nicotiana tabacum*), suggesting that alteration in plant sphingolipid synthesis can result in abnormal protein sorting (Melser et al., 2010).

The goal of this study was to identify the genes responsible for ceramide synthase activity in *Arabidopsis* and to examine the influence of sphingolipid content on the biology of a multicellular organism. We discovered that the three *Arabidopsis LAG1* homologs have different acyl chain substrate specificities and that VLCFA sphingolipids are essential for plant development. By combining genetic and pharmacological approaches, we show that VLCFA-containing sphingolipids are required for organogenesis and, more specifically, for auxin-dependent lateral root outgrowth. Finally, we demonstrate that the depletion of ceramides led to defective secretory targeting of AUX1 and PIN1 to the PM by altering the Rab-A2^a early endosomal pathway, suggesting that VLCFA sphingolipids define specific endomembrane compartments for targeting specific polar cargo proteins.

Results

Identification of Genes for Ceramide Synthase in Arabidopsis

The first ceramide synthase identified from plants is the tomato gene *Asc-1* (for *Alternaria* stem canker resistance-1) that gives resistance to the ceramide synthase inhibitor FB1 (Brandwagt et al., 2000; Spassieva et al., 2002). A tBLASTn search of the completed *Arabidopsis* genome identified three *Asc-1*/*LAG1* homologs in *Arabidopsis*, At3g25540, At3g19260, and At1g13580, subsequently referred to as *LOH1, LOH2,* and *LOH3*, respectively (*LAG* One Homologue). A potential fourth homolog (At1g26200) was also identified; however, it contains some highly variable sequences not found in any other *LAG1* homologs that may suggest a different function yet to be discerned (see Supplemental Figure 1A). The protein sequences of the identified LAG1 homologs were aligned with the known full-length proteins from tomato and the LAG1 and LAC1 proteins from yeast to identify conserved structural features (Figure 1A). The alignments show strong conservation in the LAG1p motif and predicted transmembrane helices, suggesting that the *LOH* genes encode ceramide synthases. A phylogenetic tree derived from an alignment of all known full-length protein sequences of the eudicot plant *LAG1* homologs along with the *LAG1*/*LAC1* proteins from yeast and the CerS proteins from human was constructed (see Supplemental Figures 1A and 1B and Supplemental Data Set 1). The tree showed that LOH1 and LOH3 are closely related and cluster into a group along with the majority of other plant LAG1 homologs (see Supplemental Figure 1B). On the other hand, LOH2 appears to be evolutionarily distinct from LOH1 and LOH3. In order to investigate the function of the *LOH* genes, genetic disruptions were characterized for each gene.

Arabidopsis LAG1 Homologs LOH1 and LOH3 Are Essential for Plant Growth

T-DNA insertion mutants were identified from the Wisconsin (Krysan et al., 1999) (*loh1-1*, *loh2-1*, and *loh3-1*) and Salk (Alonso et al., 2003) (*loh1-2*, *loh2-2*, and *loh3-2*) collections for each of the three *Arabidopsis LOH* genes (Figure 1B). Both alleles *loh1-1* and *loh3-1* are insertions in the 5′-untranslated region of their respective genes (at −3 and −10 bp from the ATG

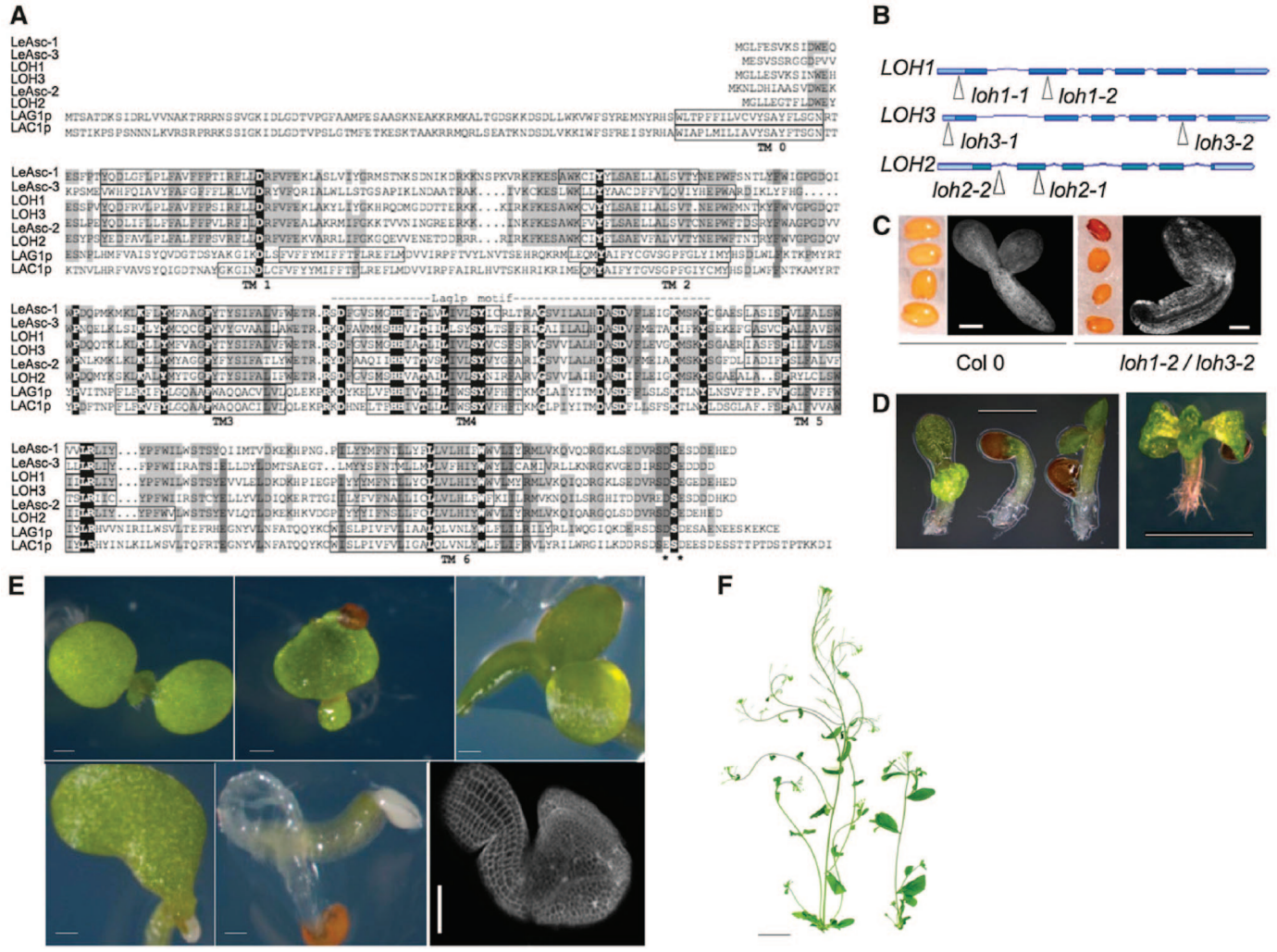

Figure 1. LOH1 and LOH3 Are Essential for Plant Development.

(A) Alignment of ceramide synthase protein sequences from *Arabidopsis* (LOH), tomato (Le ASC), and *S.s cerevisae* (Lag1p and Lac1p). Boxes indicate predicted transmembrane domains; an extratransmembrane domain, TM0, is predicted in *S. cerevisae*. Black shading shows the residues completely conserved among the ceramide synthase family, and gray shading indicates partial conservation (dark and light gray for seven and four to six residues, respectively, conserved out of eight).

(B) Structure of the *Arabidopsis LOH* genes and alleles. Boxes represent introns, with dark blue representing the coding region. The positions of identified T-DNA insertions in the different alleles are marked by triangles.

(C) Seeds and embryos from the wild type (left) and *loh1-2 loh3-2* double mutants (right) showing shrunken seeds and abnormal embryo development. Bars = 100 μm

(D) Germinating *loh1-2 loh3-2* seedlings showing very slow growth at 2 weeks (left) and no root development and abnormal leaf shape at 4 weeks (right). Bars = 2 mm.

(E) Phenotype of *loh1-1 loh3-1* mutants compared with the wild type (top left). Mutants show developmental defects ranging from modification of cotyledon number (top right) or shape (top middle and bottom left) to complete arrest of growth (bottom middle) and even severely impaired embryo morphology (bottom right). Bars = 300 μm.

(F) Adult *loh1-1 loh3-1* mutants showed reduced size with smaller rosette and shorter stems. Bar = 3 cm.

start, respectively) leading to knockdown of wild-type mRNA levels (see Supplemental Figure 2A). All other mutants are caused by insertions in an exon of their respective genes and result in undetectable wild-type mRNAs and are therefore true knockouts (see Supplemental Figures 1A and 1B).

Despite this, each single mutant showed a normal phenotype under standard growth conditions (see Supplemental Figure 2C). Similarly, combinations of double mutants between *loh2* and *loh1* or *loh3* null alleles did not show any significant differences of growth or development (see Supplemental Figure 2C). By contrast, the cross between the knockout alleles *loh1-2* and *loh3-2* resulted in ~1:16 seeds that were darker and smaller with a poor germination rate in the F2 progeny (n = 300). This phenotype was confirmed in the F3 progeny of the sesqui-mutant combinations *loh1-2*$^{-/-}$ *loh3-2*$^{+/-}$ (n = 96) or *loh1-2*$^{+/-}$ *loh3-2*$^{-/-}$ (n = 79), which pro-

duced 18 and 12% abnormal seeds, respectively (Figure 1C). The embryo morphology in these seeds was often strongly altered with thicker hypocotyls and a single cotyledon (Figure 1C). No double *loh1-2 loh3-2* mutant was recovered from seeds sown on soil, suggesting that the combination of mutations is lethal. However, when sown on solid media containing Suc, seedlings of the *loh1-2*$^{-/-}$ *loh3-2*$^{-/-}$ genotype could sometimes be recovered, albeit after a prolong incubation of several weeks. The resulting seedlings showed severely deformed plants with no roots and a deformed leaf shape that did not further develop, indicating that *LOH1* and *LOH3* are essential for root growth (Figure 1D). Despite transfer to fresh media, none of the seedlings were able to survive longer than 4 weeks.

As the *loh1-2 loh3-2* double mutant is lethal, the cross between the knockdown alleles *loh1-1* and *loh3-1* was also examined. Like the *loh1-2 loh3-2* seeds, *loh1-1 loh3-1* seeds showed reduced viability, and those that did germinate gave rise to seedlings with highly variable phenotype ranging from triple cotyledon, single deformed cotyledon, or undeveloped cotyledon (Figure 1E). Plants with relatively normal development showed smaller, wrinkled leaves, early senescence, delayed flowering, and reduced primary bolt length (Figure 1F; see Supplemental Figures 2G and 3D). Embryos dissected from seeds that did not germinate showed very strong alteration of cotyledon morphology with often single cotyledon embryos (Figure 1E) similar to the phenotypes observed in the progeny of sesqui-mutant combinations. To confirm that these phenotypes were indeed caused by the loss of *LOH1* and *LOH3* function, native *LOH1* and *LOH3* genes were transformed into the *loh1-1 loh3-1* or sesqui *loh1-2* 3-2$^{+/-}$ mutants under the control of the native promoter (see Supplemental Figures 3A and 3E). Plants with a wild-type phenotype were recovered upon transformation with either *LOH1* or *LOH3* (see Supplemental Figures 3B to 3D), indicating that the mutations in the *LOH1* and *LOH3* genes are responsible for the phenotypes observed in each of the double mutants. Overall, these data demonstrate that, out of the three different *LOH* genes, *LOH1* and *LOH3* are redundant and essential for plant growth, while *LOH2* has no obvious effect on plant development, indicative of a different role for LOH2 versus LOH1 and LOH3 in sphingolipid metabolism.

LOH Genes Encode Ceramide Synthases with Different Specific Activities

To investigate the role of the different *LOH* genes in sphingolipid metabolism and the biochemical basis for the phenotypes of the loh mutants, a complete sphingolipid analysis was performed for each line (Markham and Jaworski, 2007). For the lethal *loh1-2 loh3-2* double mutant, sphingolipid analysis performed on 2-week-old germinated seeds grown on solid media showed that all the classes of sphingolipids from these mutants were almost completely devoid of VLCFA (Figure 2A; see Supplemental Figure 4) and instead contained mostly 16:0 fatty acids. To confirm these results, sphingolipid analysis was performed on seedlings from the knockdown *loh1-1 loh3-1* double mutant. As expected, this mutant combination showed a less drastic reduction in VLCFA containing sphingolipids, ~30 mol % in total (Figure 2B; see Supplemental Figure 4A). Single *loh1-2* or *loh3-2* mutants had sphingolipid profiles almost identical to the wild type, indicating that LOH1 and LOH3 have redundant activities specifically targeted toward VLCFA sphingolipids (see Supplemental Figure 4A). The combined loss of *LOH1* and *LOH3* was also associated with a very strong accumulation of saturated free LCBs consistent with reduced ceramide synthase activity in these mutants (Figure 2C). Free LCBs also accumulated in the *loh1-1 loh3-1* mutants, albeit less pronounced than for *loh1-2 loh3-2* (see Supplemental Figure 4B).

Because disruption of *LOH1* and *LOH3* leads to an almost complete absence of VLCFA in sphingolipids, this suggests that the remaining ceramide synthase in these plants, LOH2, must be specific for 16:0. In support of this, sphingolipid profiling of *loh2-1* and *loh2-2* seedlings showed a strong reduction of 16:0 fatty acid in ceramide and other sphingolipids and a significant increase in VLCFA containing sphingolipids (Figure 2A; see Supplemental Figure 4A). Altogether, these results demonstrate the existence of at least two different ceramide synthase activities in *Arabidopsis*: LOH1 and LOH3 are specific for VLCFA, while LOH2 is specific for 16:0 fatty acids. Interestingly, disruption of *LOH1* and *LOH3* leads to high accumulation of free LCBs, similar to what was seen when CERS2 is disrupted in mice (Pewzner-Jung et al., 2010) and reminiscent of the effect of ceramide synthase inhibitors such as FB1 and AAL toxin (Abbas et al., 1994).

FB1 Mimics the Disruption of VLCFA-Specific Ceramide Synthases

FB1 and AAL toxins are sphingoid-base analog mycotoxins that have a strong and specific inhibitory effect on ceramide synthases (Merrill et al., 1993; Spassieva et al., 2002). Previous studies in animal systems have suggested that FB1 may be selective in its inhibition of ceramide synthase activity because treatment with FB1 changes the profile of fatty acids incorporated into sphingolipids (Venkataraman et al., 2002). The effect of 0.5 μM FB1 on the sphingolipid profile of *Arabidopsis* seedlings was examined (Figure 2D). Counterintuitively, after 9 d of growth on FB1, *Arabidopsis* seedlings contained higher amount of total sphingolipids than control plants, but the majority of the extra sphingolipids consisted of 16:0 species with a decrease in VLCFA containing species (Figure 2D). Exposure to FB1 for 24 h or less did not cause excessive 16:0-ceramide to be synthesized; however, a small, but significant, reduction in VLCFA-containing ceramide was noticeable by 16 to 24 h (see Supplemental Figure 5A). Inhibition of ceramide synthase by FB1 was detectable even after short exposure to FB1, judging by the rapid accumulation of the free trihydroxy (t) LCBs t18:0 after 4 h of treatment (see Supplemental Figures 5B and 5C). Accumulation of t18:0 and the dihydroxy (d) d18:0 was directly correlated with the time of exposure to FB1 with a maximum at 8 and 16 h for t18:0 and d18:0, respectively. Application of FB1 for 16 h and longer was saturating as shown by free LCB levels (see Supplemental Figure 5B). The effect of FB1 was also dose dependent, as shown by the analysis of total LCB hydrolyzed from sphingolipids after 9 d exposure to 0.4 and 0.8 μM FB1 (see Supplemental Figure 5D). Together, these data indicate that FB1 exposure rapidly inhibits ceramide synthase, elevating free LCB levels and depleting VLCFA-containing ceramides. Eventually, free LCBs are rerouted into 16:0-ceramides similar to the disruption of sphingo-

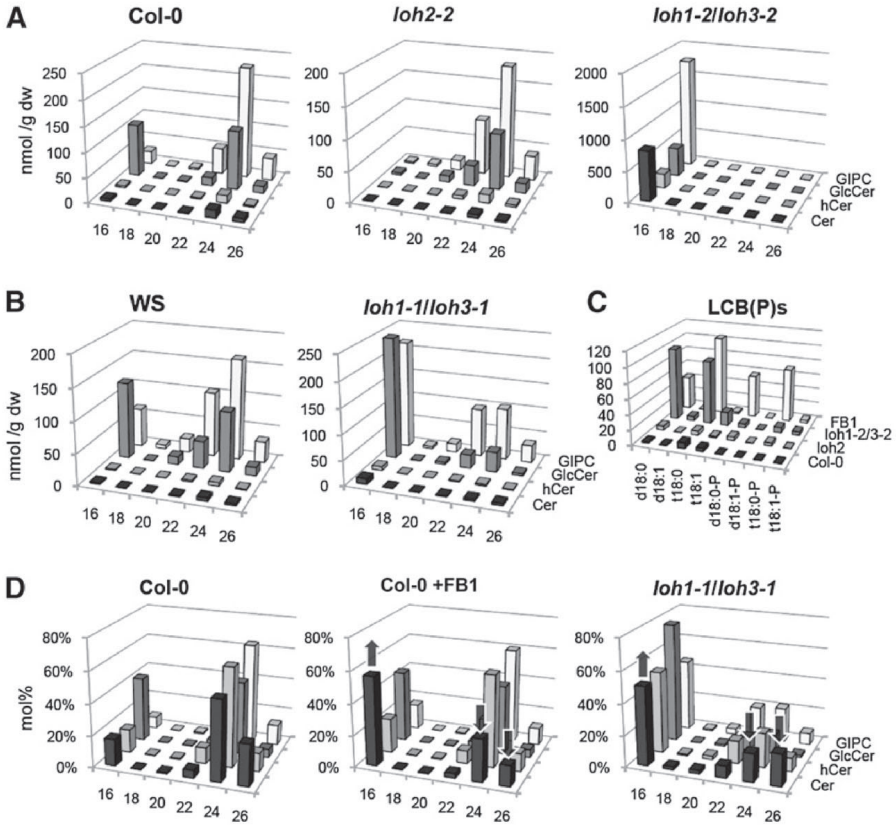

Figure 2. Disruption of LOH Activity by Knockout or FB1 Treatment Alters Sphingolipid Content.

(A) Total sphingolipid content of *loh2-2* and *loh1-2 loh3-2* compared with their related control (Col-0). Sphingolipid content is shown according to the four different classes (ceramides, hydroxyceramides, glucosylceramides, and glucosylinositolphosphorylceramides) and the length and saturation of the fatty acid chain.

(B) Total sphingolipid content of *loh1-1 loh3-1* compared with their related control (WS). Sphingolipid content is shown as in **(A)**.

(C) Free LCB levels of *loh2-2, loh1-2 loh3-2,* and wild-type seedlings grown in the presence of 0.5 μM FB1 for 9 d compared with the Col-0 wild type.

(D) Total sphingolipid content of wild-type (Col-0) seedlings grown in presence or absence of 0.5 μM FB1 for 9 d was compared with the *loh1-1 loh3-1* mutant and its corresponding wild-type seedlings (Ws). Sphingolipid levels are shown as in **(A)**.

LCB(P)s are referred to using standard sphingolipid annotation as explained by Markham and Jaworski (2007). Measurements are the average of three to five replicates.

lipid metabolism seen in the *loh1 loh3* double mutants. As expected, knockdown *loh1-1 loh3-1* double mutants treated with FB1 showed stronger depletion of VLCFA sphingolipids and enhanced accumulation of 16:0 sphingolipids, confirming the specific targeting of *LOH1* and *LOH3* ceramide synthases by FB1 (see Supplemental Figure 5E).

Wild-type seedlings germinated for 9 d on FB1 concentrations of 1 μM or higher showed global inhibition of growth (Figure 3A). At 0.5 μM FB1, primary root length was only moderately reduced (30% reduction compared with untreated control), but a strong reduction of lateral root emergence could be observed on 1 μM FB1 with 80% reduction compared with untreated control (Figure 3B). Likewise, knockdown *loh1-1 loh3-1* mutants, displaying abnormal cotyledon symmetry, also showed a 60% reduction in lateral root numbers compared with wild-type controls, as did the two different combinations of sesqui-mutants involving the *loh1-2 loh3-2* alleles (*loh1-2*$^{-/-}$ *loh3-2*$^{-/+}$ or *loh1-2* $^{-/+}$ *loh3-2*$^{-/-}$) (Figure 3C; see Supplemental Figure 2D). The weakest mutant phenotype could be mimicked by decreasing FB1 concentration to 0.25 μM, leading to 50% inhibition of lateral root growth (Figure 3B). FB1 application reduced lateral root primordia outgrowth but not the initiation stages as detected by the auxin reporter *DR5:β-glucuronidase* (*GUS*) (see Supplemental Figure 2E). Lateral root formation and growth is known to be very dependent on auxin, suggesting that the strong morphological changes observed in the *loh1/loh3* mutants could be related to an altered auxin physiology. Interestingly, the *pas1* mutant has reduced VLCFAs in sphingolipids and showed auxin-related inhibition of lateral root formation (Roudier et al., 2010). Primary root growth of *pas1* was found to be more sensitive to FB1 compared with the wild type, supporting the involvement of VLCFA sphingolipids in auxin-dependent lateral root formation (see Supplemental Figure 6A).

Very-Long-Chain Ceramides Are Required for Polar Auxin Distribution

In order to analyze the effect of sphingolipid composition on auxin distribution, we analyzed *DR5:GUS* expression in roots grown in presence of FB1 (Swarup et al., 2008). *DR5:GUS* ex-

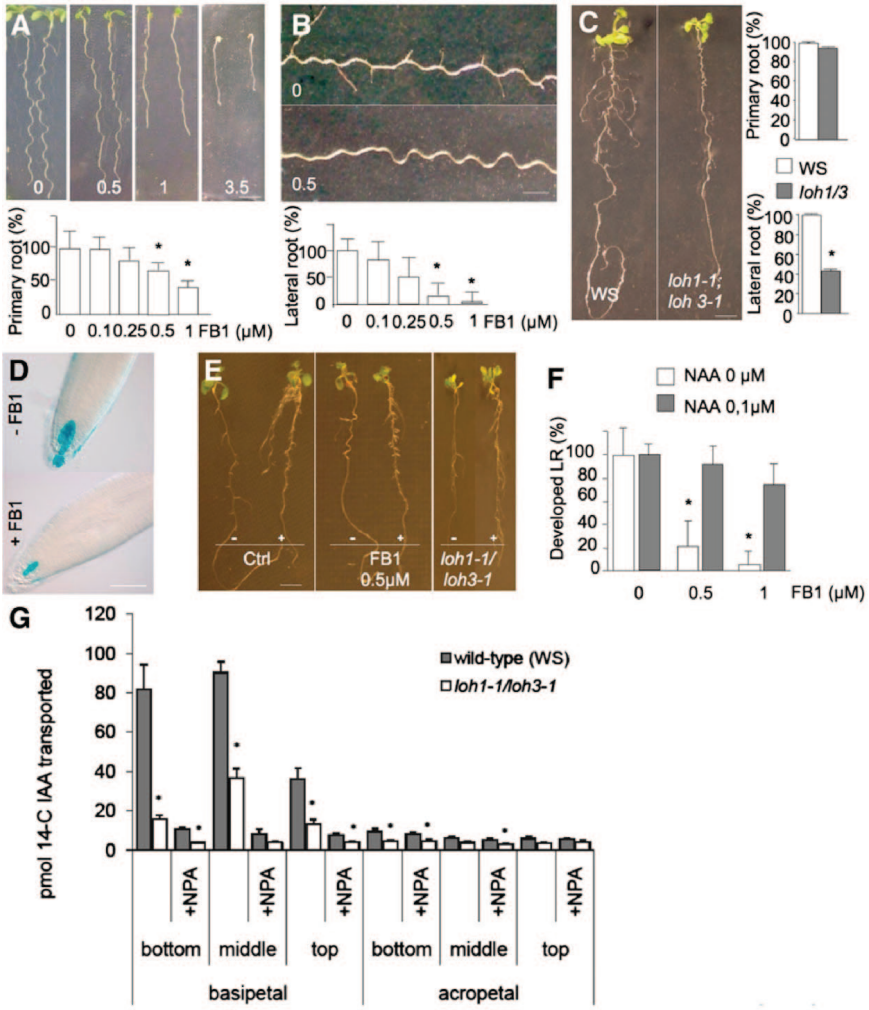

Figure 3. Inhibition of Ceramide Synthase Leads to Altered Root Development and Auxin Transport.

(A) and **(B)** Primary **(A)** or lateral **(B)** root length of *Arabidopsis* seedlings grown in the presence of various concentrations (0, 0.5, 1, and 3.5μM) of FB1. Shown is the average of 17 to 35 measurements plus standard error. Bars = 3 mm in **(A)** and 1 mm in **(B)**.

(C) Measurement of primary root growth and lateral root development in wild-type (Ws) and *loh1-1 loh3-1* mutant plants of 9 d. Number of lateral roots is the average of 16 to 35 plants normalized against wild-type plus standard error. Bar = 3 mm.

(D) DR5:GUS staining in 7-d-old wild-type primary root meristems treated (+) or not treated (−) with 2.5 μM FB1 for 16 h. Bar = 100 μm.

(E) and **(F)** Wild-type (Ws), FB1-treated, or *loh1-1 loh3-1* mutant plants grown in the absence (−) or presence (+) of the auxin analog NAA. The effect of exogenous NAA treatment on lateral root development in the presence of FB1 was quantified by counting the lateral roots in 18 to 23 plants and normalizing against the wild type **(F)**. Shown are the mean plus standard error. Bars in **(E)** = 3 mm.

(G) Transport of exogenous auxin through stem segments of wild-type plants (Ws, gray bars) and *loh1-1 loh3-1* mutant plants (white bars). Transport was measured in segments taken from different portions of the inflorescence stem (bottom, middle, and top) and in a basipetal or acropetal direction and in the presence (+NPA) or absence of NPA. Significant ($P \leq 0.05$; Student's *t* test) differences from control plants are indicated by an asterisk.

pression was reduced in root tips of seedlings grown for 9 d in the presence of 1 μM FB1 (see Supplemental Figure 2F) or simply treated with 2.5 μM FB1 for 16 h (Figure 3D). To check if auxin was directly involved in the root response to inhibition of ceramide synthase, we tested the effect of the permeable auxin analog naphthalene acetic acid (NAA) on lateral root development of FB1-treated seedlings and *loh1-1 loh3-1* double mutants. In both cases, NAA was able to restore lateral root outgrowth, suggesting that auxin transport and not auxin response was most likely impaired in FB1-treated roots (Figures 3E and 3F).

To investigate the role of VLCFA-containing sphingolipids in auxin transport, the transport of radiolabeled auxin along stem segments of wild-type and *loh1-1 loh3-1* mutants was measured. Stem segments of 2.5 cm in length were incubated for 16 h in the dark with the top/flower end (basipetal) or bottom/rosette end (acropetal) in a 20-μL solution of ^{14}C-labeled indole-3-acetic acid, the native auxin. The basipetal or acropetal auxin movements were subsequently quantified by measuring the amount of labeled auxin in the distal 5 mm along the stem. Controls for ruling out possible diffusion or metabolism of indole-3-acetic acid were performed by including 10 μM naphthylphalamic acid (NPA), an inhibitor of polar auxin transport. As expected, labeled auxin showed significant, NPA-sensitive, basipetal transport along the different sections of the wild-type stem (Figure 3G). In the *loh1-1 loh3-1* mutant, the auxin

flux was strongly affected compared with the wild type with the amount of auxin transported reduced by 50 to 75% along the stem (Figure 3G). Together, these data show that polar auxin transport is impaired by the reduction in VLCFA in the *loh1-1 loh3-1* mutant or by the inhibition of ceramide synthase in the FB1-treated plants.

Sphingolipid Synthesis Is Required for the Targeting of Specific Auxin Carriers to the PM

Polar auxin transport is mediated through a family of PM polar auxin transporters involved in cellular influx (AUX1 family members) or efflux of auxin (PIN family members). Polar localization of auxin transporters was thus investigated in the context of sphingolipid depletion either in the *loh1 loh3* mutant or in FB1-treated seedlings. To minimize possible artifactual response at the cellular level induced by long FB1 treatment, we designed a shorter FB1 treatment leading to ceramide synthase inhibition. We found that the application of 2.5 μM FB1 for 16 h (subsequently referred as FB1-16h) led to an accumulation of t18:0 and d18:0 that was identical to that induced by 9 d of treatment with 0.5 μM (see Supplemental Figure 5B). Since FB1 was described to induce cell death at high concentration, we verified that our short FB1 treatment was not impairing cell viability. We monitored cell viability in both primary and lateral roots using the fluorodiacetate (FDA) test, which labels viable cells by monitoring fluorescein release from ester bond hydrolysis of apolar FDA. In our conditions, FB1-treated roots were still showing fluorescein labeling, demonstrating their viability (see Supplemental Figure 6B). This experimental setting allowed the study of cellular responses in lateral root tip, which was found to be more sensitive to ceramide synthase inhibition than the primary root (Figures 3A and 3B).

We first analyzed AUX1-yellow fluorescent protein (YFP) distribution since *aux1* mutants showed reduced lateral root development similar to FB1-treated plants (Marchant et al., 2002). FB1 treatment for 16 h led to an accumulation of *pAUX1:AUX1-YFP* fluorescence inside meristematic, protophloem, and epidermal cells of lateral roots (Figures 4A and 4B). Similar aggregation of AUX1-YFP was observed in the primary root of sesqui *loh1-2*$^{+/-}$ *loh3-2*$^{-/-}$ mutants but not in the weak *loh1-1 loh1-3* (Figure 4C). PM targeting of AUX1-YFP was also impaired in lateral root primordia of *loh1-2*$^{+/-}$ *loh3-2*$^{-/-}$ (see Supplemental Figure 7A). Interestingly, FB1 treatment led to partial relocalization of AUX1-YFP into lateral membrane of epidermal and protophloem cells (Figures 4A and 4C, inset, arrows). We also investigated whether inhibition of ceramide synthase would have a similar effect on the subcellular distribution of LAX3-green fluorescent protein (GFP), since this AUX1-like influx carrier was described to be also essential for lateral root outgrowth (Swarup et al., 2008). But contrary to AUX1-YFP, FB1 did not modify LAX3-GFP targeting to the PM (see Supplemental Figures 7B and 7C).

We then checked the effect of FB1-16h treatment on the subcellular distribution of auxin efflux carriers in protophloem and epidermal cells. Like AUX1-YFP, PIN1-GFP was found to aggregate both in vascular and root meristem cells of lateral roots in presence of FB1 or in the most affected primary root of the weak *loh1-1 loh3-1* mutant (Figure 4D; see Supplemental Figures 8A and 8B). In the most severe cases, PIN1-GFP or PIN1 immunolocalization labeling showed PIN1 almost exclusively in cytosolic aggregates and no or only a weak signal could be detected at the PM (Figure 4D; see Supplemental Figure 8C). However, subcellular distributions of other efflux carriers, such as the ABC1-GFP and ABC19-GFP auxin pumps, were not affected by FB1-16h treatment (Figures 4E and 4F). The auxin efflux carrier PIN2-GFP was also insensitive to FB1 (see Supplemental Figure 7D); however, this was unrelated to its epidermal localization because PIN1-GFP expression in the epidermis led to aggregates as in the stele (see Supplemental Figure 7E). We also checked PM proteins not involved in auxin transport, such as the nonpolar LTi6b-GFP and PIP2-GFP fusion proteins. As for ABCs, PIN2, or LAX3 proteins, the localization of these markers was insensitive to FB1 treatment (see Supplemental Figures 7F and 7G). Altogether, these results indicate that ceramide synthase inhibition modified membrane targeting of specific protein cargoes. Interestingly, even if AUX1 and PIN1 are targeted to different sites within the PM, both proteins gathered partially into the same or closely associate aggregates upon FB1 application (Figure 4G; see Supplemental Figure 8C).

Inactivation of LOH activity led not only to decreased VLCFA-containing ceramide and sphingolipid contents but also to the accumulation of free LCBs. To exclude a possible role of free LCBs in the aggregation of AUX1 and PIN1 proteins, we treated *Arabidopsis* AUX1-YFP and PIN1-GFP seedlings with myriocin, an inhibitor of serine palmitoyltransferase, the first step of sphingolipid synthesis, leading to the depletion of both free LCBs and ceramides (Miyake et al., 1995). Like FB1, myriocin treatment led to similar accumulation of AUX1-YFP in cytosolic aggregates, demonstrating that inhibition of de novo sphingolipid synthesis and not LCB accumulation was responsible for the specific mistargeting of protein cargoes (see Supplemental Figure 8D). In conclusion, our results showed that inhibition of sphingolipid synthesis impaired normal trafficking of AUX1-YFP and PIN1-GFP proteins in the protophloem, meristem, and epidermal root cells, explaining the reduction of polar auxin transport and auxin-dependent lateral root outgrowth.

Inhibition of Sphingolipid Synthesis Disrupts Early Endosomes

Inhibition of ceramide synthase induced the aggregation of membrane and proteins in a structure that could be referred to as FB1 compartment by analogy with compartments induced by the anterograde transport inhibitor brefeldin A (BFA). We therefore investigated the different endomembrane markers recruited in the formation of these compartments. GFP marker lines for different endomembrane compartments were tested for their sensitivity to FB1. First, we investigated the effect of FB1 on the ER, since it is the site of de novo LCB, ceramide, and probably glucosylceramide biosynthesis (Marion et al., 2008). We examined the distribution of the ER markers YFP-NIP1 and AXR4-GFP. AXR4-GFP was of special interest since axr4 mutant aggregated AUX1 into cytosolic compartments, blocking its targeting to the PM (Dharmasiri et al., 2006). No obvious ER containing aggregates could be observed upon FB1-16h treatment for both markers, although enhanced AXR4-GFP signal was often observed in the perinuclear region (Figure 5A). We then evaluated the localization

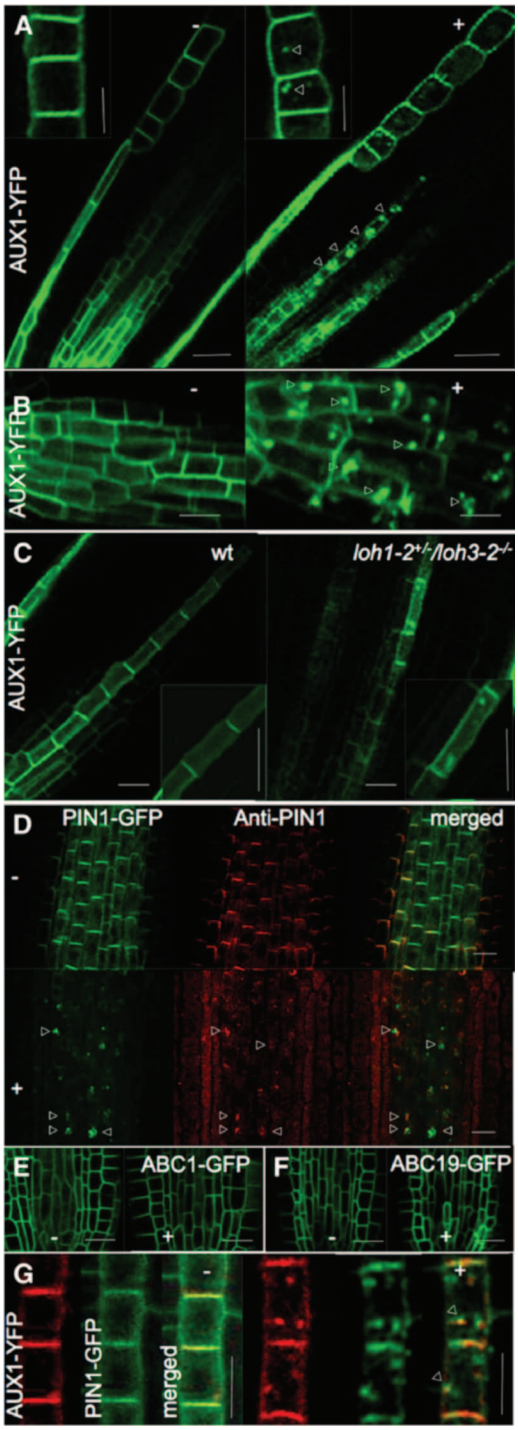

of several markers labeling the ER/*cis*-Golgi and Golgi apparatus, but none of them showed any significant aggregation in presence of FB1 (Figure 5). By contrast, the early endosomal markers YFP-Rab-A2^a and YFP-RabA1^e were clearly aggregated by FB1-16h treatment (Figure 5). The RabA2^a compartment extensively overlapped with the *trans*-Golgi network (TGN)-resident VHAa1 (Chow et al., 2008). As expected, partial colocalization of YFP-RabA2^a and VHAa1-RFP could also be observed in FB1-induced aggregates (Figure 5B). Endosomal subpopulations labeled by YFP-ARA7/RabF2^b or SNX1-GFP, defined as late endosomes, were insensitive to FB1 application. Similarly, late endosome vacuolar YFP-RabG3^C or YFP-RabG3^F or specific vacuolar marker YFP-VAMP711 were also insensitive to FB1 (Figure 5A; see Supplemental Figure 8E). Altogether, these results indicated that inhibition of ceramide synthase modified subcellular distribution only of the early endosomal/TGN resident markers, suggesting the involvement of sphingolipid synthesis in the maintenance of specific endomembrane compartments.

The modifications of endomembrane structures observed with GFP markers were confirmed by transmission electron microscopy. The organization of the Golgi apparatus as well as the mitochondria and plastids were not modified by FB1-16h treatment and by *loh1-1 loh3-1* mutations (Figure 6; see Supplemental Figures 9A and 9B). The ER network was clearly visible, and it seemed to be larger and more branched, an observation that could correlate with higher fluorescence of ER markers after FB1 treatment. The most dramatic changes were the presence of small vesicular structures looking like dismantled vacuole or fused vesicles (Figure 6D). Since fluorescent vacuolar markers did not show major macroscopic changes in vacuolar structure while early endosomal markers formed large aggregates, these accumulations of membrane materials could result from fusion of endosomal compartments.

Sphingolipid Synthesis Is Not Required for Endocytosis

AUX1-YFP and PIN1-GFP aggregates in the cytosol most probably result from altered TGN and/or early endosomal trafficking. However, PIN1 and AUX1, apart from being localized in the opposite side of the cell, are characterized by different dynamics with PIN1 undergoing active recycling, while AUX1 showed a slower turnover at the PM (Kleine-Vehn et al., 2006). We thus reasoned that the aggregation of both proteins upon ceramide synthesis inhibition would preferentially result from secretory pathway impairment rather than

Figure 4. Inhibition of Ceramide Synthesis Alters the AUX1-YFP and PIN1-GFP Targeting in Lateral Roots.

(A) and **(B)** AUX1-YFP aggregates (arrowheads) in the cytosol in presence of 2.5 μM FB1 for 16 h **(A)**. Detail of untreated (left, −) and treated lateral root cells (right, +). Details of epidermal cells are given in insets. Details of protophloem region of untreated and treated lateral roots are shown in **(B)**.

(C) AUX1-YFP aggregates (arrowheads) in the cytosol of meristematic and protophloem cells in the primary root of sesqui-mutants *loh1-2*$^{-/-}$ *loh3-2*$^{+/-}$ (right) compared with the wild type (wt; left).

(D) PIN1-GFP aggregates (arrowheads) in the cytosol of FB1-treated cells (bottom, +) compared with control (top, −). PIN1 aggregates were also confirmed by immunolocalization (anti-PIN1). Note that FB1 treatment depleted PIN1 from PM.

(E) ABC1-GFP expression in untreated (left, −) and FB1-treated cells (right, +).

(F) ABC19-GFP expression in untreated (left, −) and FB1-treated cells (right, +).

(G) AUX1-YFP (red) and PIN1-GFP (green) distribution in absence (left, −FB1) and in presence of FB1 (right, +FB1). Merged images are also shown. AUX1-YFP and PIN1-GFP aggregates colocalize partially (arrowheads).

Bars = 20 μm in **(A)**, **(F)**, and **(G)** and 10 μm in inset of **(A)** to **(E)** and **(H)**.

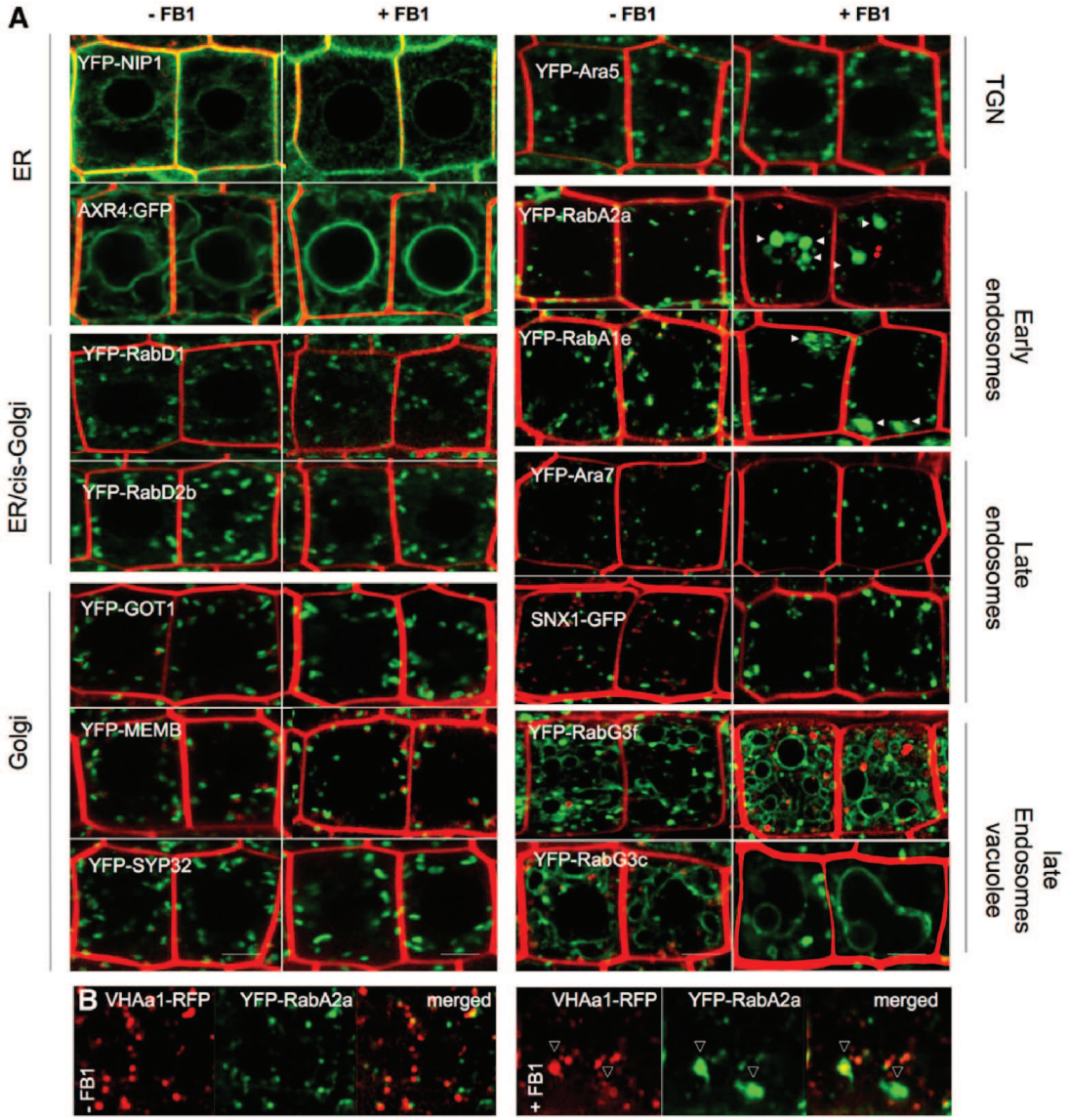

Figure 5. Inhibition of Ceramide Synthase Affects Specific Endomembrane Compartments.

(A) Fluorescence micrographs showing the subcellular localization of different endomembrane marker-XFP fusions in the lateral roots of untreated transgenic lines (−FB1) or after treatment with FB1 (+FB1). The subcellular compartment to which the marker has previously been localized is annotated far right or left, and the marker-XFP fusion being examined is shown in the top left of each set of micrographs. Note the aggregations under FB1 treatment for the early endosome markers (arrowheads). Bars = 5 μm.

(B) TGN marker VHAa1-RFP partially colocalizes with YFP-RabA2^a in the presence of FB1. Bars = 5 μm.

PM recycling. To first evaluate the involvement of recycling membrane material in ceramide-depleted endomembrane pools, we checked whether endocytosed membrane material was associated with FB1 compartments. Early endosomes like Rab-A2^a rapidly colocalized with endocytosed FM4-64 (Chow et al., 2008). However, when treated with FB1, the aggregated YFP-Rab-A2^a–labeled endosomes showed close proximity with FM4-64 but did not seem to colocalize, indicating that endocytosis provides only a minor contribution to the formation of FB1 compartments (see Supplemental Figure 10A). This was confirmed by comparing BOR1-GFP internalization upon boron application in presence or not of FB1-16h treatment (Takano et al., 2005). BOR1-GFP–labeled endosomes appeared with similar kinetics in the presence or absence of FB1, indicating that endocytosis was not severely impaired by FB1-16h treatment (see Supplemental Figure 10B). The origin of the FB1 compartment was directly probed using point mutations in Rab-A2^a that modify its subcellular distribution (Chow et al., 2008). To rule out possible interaction of GTPase activity with FB1 treatment, we monitored the subcellular distribution in a YFP-Rab-A2^a[N125I] mutant that is a nucleotide-free dominant-negative mutant that has the same subcellular distribution as wild-type YFP-Rab-A2^a but lower expression levels. YFP-Rab-A2^a[N125I] was as sensitive to FB1 as wild-type YFP-Rab-A2^a, demonstrating that FB1 sensitivity was independent of GTPase ac-

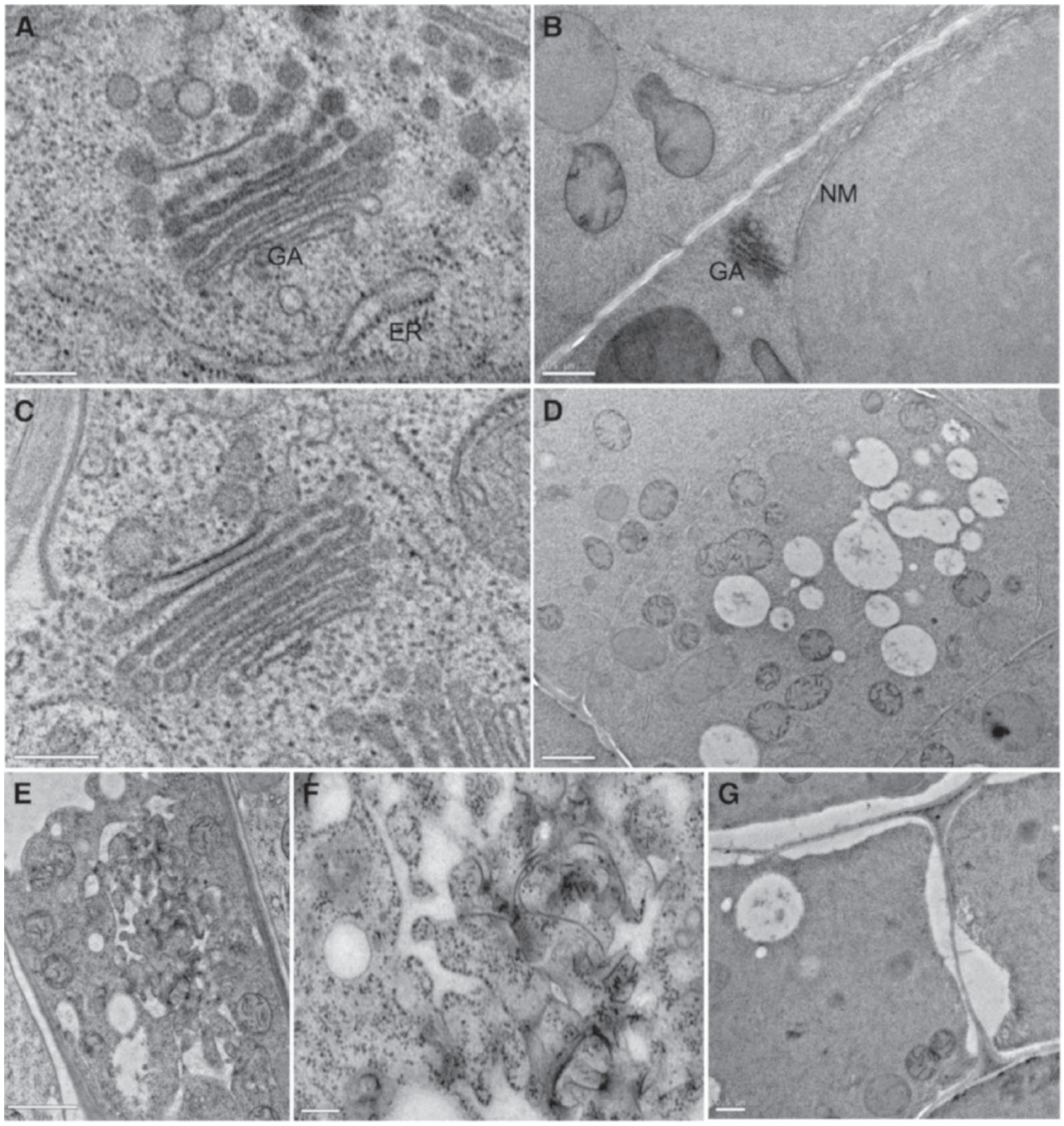

Figure 6. Inhibition of Ceramide Synthase Alters Endomembrane Ultrastructure.
(A) and **(B)** Control cells exhibiting characteristic tubular ER and a Golgi stack (GA) surrounded by secretory vesicles **(A)**. Detail of control cells exhibiting a narrow cell wall domain and a straight cell surface between two cells **(B)**. NM, nuclear membrane.
(C) to **(G)** Cells from roots of seedlings grown on 0.5 μM FB1 for 9 d.
(C) Golgi ultrastructure is not affected by FB1 treatment.
(D) Cytoplasm is often filled with small, deconvoluted vacuole-like structures.
(E) and **(F)** The ER exhibits a larger and more branched network compared with control cells.
(G) The PM is detached from the cell wall, and a large and irregular periplasmic space between the cell wall and PM is observed.
Bars = 200 nm in **(A)**, **(C)**, **(D)**, and **(F)**, 500 nm in **(B)** and **(G)**, and 1 μm in **(C)** and **(E)**.

tivity (see Supplemental Figure 10C). Then, we analyzed the S26N or Q71L mutations that stabilize YFP-Rab-A2^a into the inactive GDP-bound state or the constitutively active GTP-bound state. These mutations relocate YFP-Rab-A2^a mainly to the Golgi for YFP-Rab-A2^a[S26N] and the PM for YFP-Rab-A2^a[Q71L]. The Golgi YFP-RabA2^a[S26N] was still sensitive to FB1 by forming aggregates, while the PM-localized YFP-Rab-A2^a[Q71L] was insensitive, demonstrating that FB1 aggregates recruited YFP-Rab-A2^a from the Golgi but not the PM (see Supplemental Figure 10C). Altogether, these results indicate that FB1-16h compartments are not formed from recycled PM materials.

Sphingolipid Synthesis Is Required for the AUX1 and PIN1 Secretory Pathway

The alternative pathway for FB1 compartments would be the secretory route. BFA inhibits anterograde transport, resulting also in the aggregation of early endosomes with the TGN to form BFA compartments (Ritzenthaler et al., 2002; Geldner et al., 2003). BFA was thus applied to FB1-treated PIN-GFP and AUX1-YFP roots stained with FM4-64. In vascular cells, AUX1-YFP and PIN1-GFP FB1-induced aggregates appeared to be distinct from BFA compartments, suggesting that FB1 impaired a distinct post-Golgi compartment

than did BFA (Figures 7A to 7D; see Supplemental Figures 11A to 11D). To address the involvement of de novo synthesis in FB1 aggregates, we directly monitored aggregate formation through whole-cell fluorescence recovery after photobleaching (FRAP) analysis. We performed FRAP analysis of FB1-16h–treated PIN1-GFP and AUX1-YFP secondary root cells. FB1-16h– treated cells with PIN1-GFP localized in aggregates and at the PM were completely bleached (Figure 7E). Recovery of PIN1-GFP in aggregates was clearly visible after 30 min, and PM labeling was observed after aggregate recovery usually 30 to 45 min after bleaching. A similar finding was observed with AUX1-YFP, albeit with a reduced recovery (see Supplemental Figure 11E). FRAP analysis showed that FB1 delayed but also reduced PIN1-GFP recovery at the PM (Figure 7E, left). However, PIN1-GFP recovery in aggregates showed similar kinetics than the recovery of PIN1-GFP at PM in untreated samples (Figure 7E, right), indicating that the primary effect of FB1 is to block secretion by aggregating PIN1-GFP prior to its PM localization. Altogether, these results show that PIN1-GFP, like AUX1-YFP, aggregation occurs along the secretory pathway.

Finally, we investigated the involvement of VLCFA sphingolipids in protein secretion in the apoplast by analyzing the localization of tomato arabinogalactan fusion protein LeAGP1-GFP (see Supplemental Figure 11F). It was previously demonstrated that this fusion protein provided a robust marker for secretion in *Arabidopsis* (Estévez et al., 2006). FB1-16h treatment did not modify LeAGP1 accumulation in the apoplast, confirming that VLCFA sphingolipids are involved in the traffic of specific cargoes along the secretory pathway.

Discussion

Functional analysis of *Arabidopsis LAG1* homologs 1 through 3 demonstrated that the three *LOH* genes encode ceramide synthases. The three LOH proteins showed high sequence identity with the yeast *LAG1*p and LAC1p but also with tomato Le Asc1, which was demonstrated to complement yeast *lag* mutants (Spassieva et al., 2002). Sphingolipid analysis of the different *loh* mutants demonstrated how the different LOH proteins contribute to ceramide biosynthesis and more specifically, the sphingolipid fatty acid chain length. Complete loss of LOH2 function led to specific reduction in C16-ceramide, whereas the absence of both LOH1 and LOH3 activity caused complete depletion of ceramides with an acyl chain longer than C18. Altogether, these results show that *Arabidopsis* possesses two different ceramide synthase activities. *LOH2* encodes long-acyl-chain ceramide synthase, whereas *LOH1* and *LOH3* encode ceramide synthases with very-long-acyl-chain specificity. The role of the distinct LAG1 homolog At2g26200 in plant biology remains somewhat of an enigma as *LOH1*, *2*, and *3* would appear to account for VLCFA and c16-specific ceramide synthase activity in leaf tisues. This functional distinction is supported by the phylogenetic analysis of plant LOH proteins, with LOH2 representative of a distinct clade. It will be interesting to see if other members of the LOH2 clade are also specific for C16-fatty acids and to dissect the amino acid differences between LOH2 and VLCFA-specific ceramide synthases. Similar

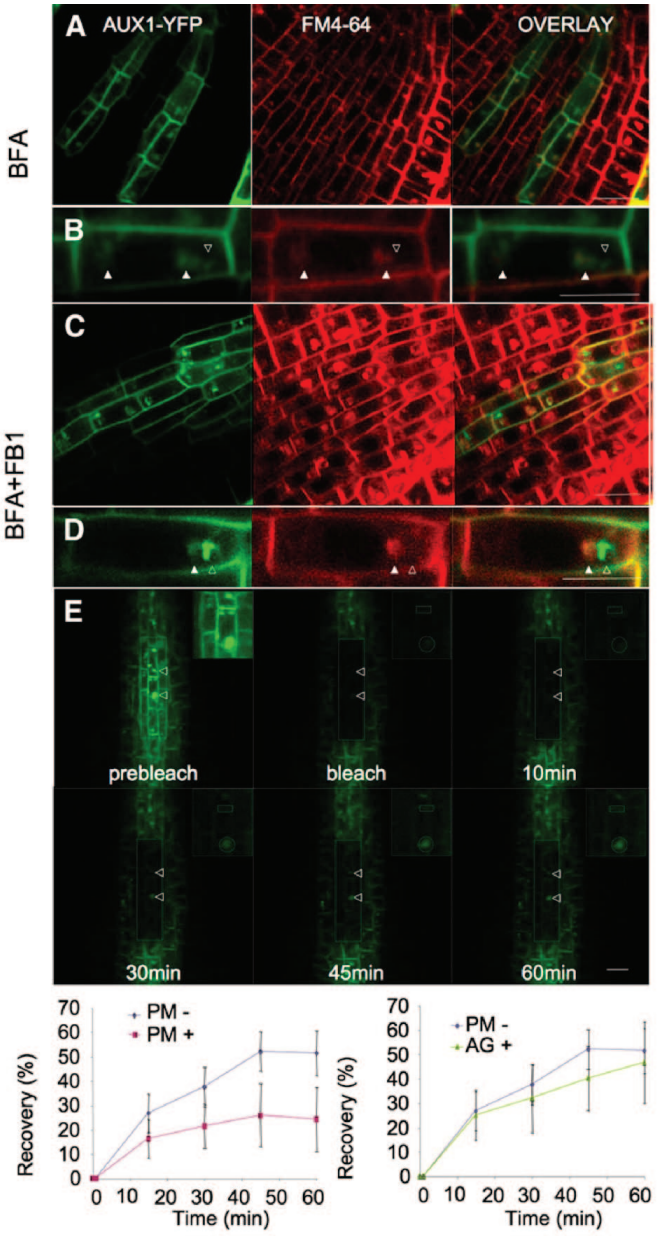

Figure 7. Inhibition of Ceramide Synthase Modifies Vesicle Trafficking.

(A) Partial localization of pAUX1:AUX1-YFP and FM4-64 staining in the presence of 50 μM BFA.

(B) Detail of BFA compartments with presence (open arrowhead) or absence (closed arrowhead) of colocalization between FM4-64 and AUX1-YFP.

(C) FM4-64 staining of aggregates in FB1-16h–treated pAUX1:AUX1-YFP cells in the presence of BFA. Partial colocalization is observed (arrowheads).

(D) Detail of FM4-64 staining of aggregates in FB1-treated pAUX1:AUX1-YFP cells showing partial colocalization of AUX1-YFP with FM4-64 in FB1/BFA compartments.

(E) FRAP analysis of FB1-16h cells expressing PIN1-GFP. Lateral root cells expressing PIN1-GFP (prebleach) were bleached, and recovery of PIN1-GFP was monitored for 60 min. Aggregates are shown (arrows). Fluorescence recovery was quantified on transverse membranes in the absence (PM−) or the presence of FB1 (PM +) as well on aggregates (AG+) (n = 10, average + sd). Inset shows the two types of ROI used for FRAP quantification.

Bars = 10 μm in **(A)**, **(C)**, and **(E)** and 5 μm in **(B)** and **(D)**.

differences of acyl chain specificity were also described for mammalian ceramide synthase CERS (Teufel et al., 2009). CERS5 and 6, like LOH2, display a preference for long-chain acyl-CoA, while CERS2 or 4 is specifically involved in the synthesis of C22- and C22-C24-ceramides, respectively.

In yeast, both ceramide synthases are specific to very-long-chain ceramides with mainly C26 acyl chains (Guillas et al., 2001). However, this specificity can be modified by disrupting the enzymes responsible for VLCFA synthesis, namely, ELO2 and ELO3. Similarly, in the *Arabidopsis pas3* mutant, elongation is affected by the reduced cytoplasmic acetyl-CoA carboxylase activity, and increased levels of C20 and C18 fatty acids are found in sphingolipids (Roudier et al., 2010). These observations indicate that there is a close relationship between the specificity of the ceramide synthase reaction and the acyl-CoA pool feeding that reaction; however, the nature of that relationship remains to be understood.

Disruption of *LOH1* and *LOH3* also has a marked affect on the total amount of sphingolipids. Free LCBs accumulate to high levels and drive the synthesis of excessive amounts of 16:0-containing sphingolipids. Similar findings were observed in the CERS2 knockout mouse, which is depleted in VLCFA sphingolipids but has overall normal sphingolipid content due to the accumulation of C16-sphingolipids (Pewzner-Jung et al., 2010). Likewise, the reduction of the VLCFA-CoA pool in the elongation mutants *pas1* and *pas3* led to an increase of C16-ceramides (Roudier et al., 2010). Interestingly, sphingoid base hydroxylases mutants that lacked t18:0 showed also enhanced C16-sphingolipids (Chen et al., 2008). In that article, a model was proposed whereby disruption of t18:0 biosynthesis caused d18:0 to accumulate, which drove the synthesis of C16:0-containing sphingolipids through a C16:0-dependent ceramide synthase. It was also suggested that t18:0-VLCFA–containing sphingolipids negatively regulate serine palmitoyltransferase activity, regulating the amount of sphingolipid that the cell synthesizes. This work further refines that idea by identifying the C16:0-dependent ceramide synthase as *LOH2* and indicating that VLCFA-containing sphingolipids are capable of affecting total sphingolipid content.

Our work demonstrated that the length of the ceramide acyl chain has an important effect on the biological function of the sphingolipid molecules. While loss of *LOH2* function did not lead to any obvious developmental phenotype, the *loh1-2 loh3-2* double mutant was impaired in embryo development and germination, indicating that very-long-chain but not long-chain ceramides are critical for plant growth. Fine-tuning of ceramide synthase activity could be efficiently achieved with the sphingoid base analog FB1. FB1 is a mycotoxin from *Fusarium moniliforme* that inhibits ceramide synthase and is responsible for several naturally and experimentally induced animal and human diseases (Desai et al., 2002; Stockmann-Juvala and Savolainen, 2008). FB1 was found to inhibit ceramide synthase and to lead to free LCB accumulation (Abbas et al., 1994; Spassieva et al., 2002). Sensitivity to FB1 was also described to directly correlate with the activity of tomato *LAG1* homolog *Asc-1* (Brandwagt et al., 2000, 2002; Spassieva et al., 2002).

Here, we demonstrated that FB1 selectively inhibits very-long-acyl-chain ceramide synthesis in *Arabidopsis*. Moreover, our results demonstrate that, at the concentrations used, the most of the effects of FB1 can be attributed to the inhibition of de novo ceramide synthesis since many FB1 phenotypes were observed in the *loh1 loh3* mutant. Interestingly, lateral roots were more sensitive to FB1 than primary roots. Contrary to primary roots that are of embryogenic origin, lateral roots are developed from nondividing pericycle cells and exhibit extensive plasticity associated with differential response to environmental cues, like phosphate or nitrate (Linkohr et al., 2002; Jain et al., 2007). Lateral roots could thus be more sensitive to protein secretion at the PM to respond to these different environmental stimuli.

The use of FB1 to inhibit ceramide synthesis in a short window of time demonstrates the role of these lipids in the secretory pathway in particular for two specific cargoes, PIN1-GFP and AUX1-YFP. The normal expression and subcellular distribution of AXR4-GFP in the presence of FB1 indicates that the effect of sphingolipid depletion on AUX1-YFP targeting is independent of the AXR4 pathway. Interestingly, PIN1, but not AUX1, targeting was also impaired in VLCFA-defective mutants *pas1* and *3* (Roudier et al., 2010). The fact that PIN1-GFP was more sensitive to BFA in *pas1* mutant suggests that PIN1 recycling was selectively altered. The differences observed between *pas1* and FB1 or loh1 loh3 plants could be explained by the nature of the VLCFA lipids involved since *pas1* mutation impacts potentially all the VLCFA-containing lipids and even among sphingolipids *pas1* was found to reduce more the levels of glucosylceramides than glucosylinositolphosphorylceramides (Roudier et al., 2010). PIN1 membrane localization was found to be dependent on sterol levels, as illustrated by polarity defects in sterol methyltransferase mutant *smt1*^{orc} (Willemsen et al., 2003). The role of sterols in AUX1 polarity is debated since conflicting results were obtained with smt1^{orc} (Willemsen et al., 2003; Kleine-Vehn et al., 2006). Nonetheless, the application of filipin, a specific sterol binding drug, was able to specifically reduce sterol levels at the PM and resulted in changes in AUX1 polar distribution and caused its cytosolic aggregation similarly to what was found with FB1 (Kleine-Vehn et al., 2006).

Interestingly, PIN2 polarity was also dependent on sterol levels since PIN2 localized to apical, basal, and lateral membranes in the sterol biosynthetic mutant *cpi-1* (Men et al., 2008). In contrast with defects in sterol biosynthesis, inhibition of ceramide synthase did not seem to alter PIN2-GFP targeting, indicating a potentially differential sensitivity of the membrane proteins to the nature of their lipid environment. Similarly, we showed that FB1 treatment specifically altered the Rab-A2^{a}– and Rab-A1^{e}–labeled early endosome populations. The fact that both markers are targeted to the cell plate (Chow et al., 2008) indicates that VLCFA sphingolipids might directly impact cytokinesis, as recently suggested in BY2 cells (Aubert et al., 2011). The existence of lipid sorting at the TGN was recently demonstrated in yeast with specific enrichment of sphingolipids and sterols in post-Golgi vesicles transporting raft proteins (Klemm et al., 2009). Not surprisingly, PIN1 was found to be associated with detergent-resistant membrane fractions that are usually rich in sterols and sphingolipids (Mongrand et al., 2004; Borner et al., 2005; Titapiwatanakun et al., 2009). Detergent-resistant membrane, enriched in sterol and sphingolipids, cofrationate with PM and Golgi but not with ER proteins (Laloi et al., 2007). Inhibition of ceramide synthase did not seem to alter the ER and Golgi structure even though *Arabidopsis* ceramide synthases were found to localize in the ER (Marion et al., 2008). However, the reduction of ceramide syn-

thesis could impair the assembly of lipid domains in the ER or Golgi, leading to subsequent disorganization of specific endosomal populations.

Recently, FB1 was reported to induce ER-derived aggregates and to block ER to Golgi cargo delivery in BY2 cells (Aubert et al., 2011). The nature of the sphingolipids involved remain to be found, but the acyl chain length was found to be critical for polar targeting and trafficking and could not be compensated for by shorter chain ceramides. Importantly, very-long-chain ceramides were a determinant of protein cargoes and endosomal specificity. Very-long-chain fatty acyl chains were also described to be involved in polar auxin transport in *Arabidopsis* (Roudier et al., 2010). Reduction of the acyl chain length in particular in sphingolipids resulted in PIN1-GFP but not AUX1-YFP cytosolic aggregation. The relative insensitivity of AUX1-YFP to VLCFA depletion in that report might be explained by a lesser reduction of very-long-acyl-chain sphingolipids compared with that achieved in this work by FB1 treatment or the effect of the *loh1-1 loh3-1* double mutant. However, enhanced sensitivity of PIN1 compared with AUX1 was also observed in this work, as PIN1 was aggregated in both weak and strong *loh1 loh3* double mutants, while AUX1 distribution was only impaired in the strong *loh1-2 loh3-2* mutant. These data suggest that AUX1 sensitivity to lipid environment might be more complex than for PIN1.

The VLCFA content of lipids has been shown to affect membrane bending during yeast nuclear pore formation and membrane plasticity during furrow ingression in *Drosophila melanogaster* (Schneiter et al., 1996; Szafer-Glusman et al., 2008). Simulation of lipid bilayers comprising common sphingomyelins showed that increasing acyl chain length enhances bilayer thickness and lipid packing but reduces lateral diffusion because of acyl chain interdigitations (Niemelä et al., 2006). Impairment of yeast fatty acid elongation leading to reduced C26-sphingolipid levels decreased lipid packing and membrane order in yeast cell but also prevented liquid ordered phase separation in model membranes from total lipid extracts (Klose et al., 2010). Such structural properties of the acyl chains of sphingolipids could infer specific membrane features like vesicular mobility or fusions that could define some endosomal populations and PM subdomains. However, the molecular mechanisms underlying these specificities remain to be explored to fully understand the structural role of sphingolipids in membrane dynamics.

Methods

Bioinformatics and Phylogenetic Analysis

GenBank and the tomato genome database (http://mips.helmholtz-muenchen.de/plant/tomato/index.jsp) were searched using the tBLASTn algorithm and the *Asc-1* protein sequence AJ312131 using default parameters, except the filter for low complexity was turned off. The GenBank sequence for *Arabidopsis lyrata* XM_002890624 was manually extended using the A. lyrata sequence available at http://genome.jgi-psf.org/Araly1/Araly1.home.html. Full-length eudicot sequences were identified and the protein sequences aligned using ClustalW. Gaps were condensed and edited using the BioEdit sequence software. Phylogenetic relationships between sequences were established using the MEGA4 software program with parameters set to the default values (Tamura et al., 2007). Transmembrane domains were predicted with TMPred (Hofmann and Stoffel, 1993).

Plant Growth Condition and Drug Treatments

Seedlings were grown on *Arabidopsis thaliana* agar medium (Estelle and Somerville, 1987) for phenotyping, genotyping, and drug treatment. FB1 (Sigma-Aldrich) short treatment was performed by incubating 9-d-old seedlings in liquid *Arabidopsis* media for 16 to 20 h in the presence of 2.5 μM FB1. Due to batch variability, each FB1 stock solution was calibrated with a root growth response curve and variation of drug concentration never exceeded 2.5 ± 1 μm for a short incubation. For long FB1 treatment, seedling were directly germinated on *Arabidopsis* solid media supplemented with 0.25 to 3.5 μM FB1. BFA (Sigma-Aldrich), which inhibits anterograde vesicular transport, was used in liquid *Arabidopsis* media at 50 μM for 1 h on 9-d-old seedlings. After each drug treatment, seedlings where washed before mounting for imaging.

Complementation of the lateral root defect of the *loh1-1 loh3-1* mutant or FB1-treated seedlings was obtained with 0.1 μM NAA (Sigma-Aldrich) supplemented in solid *Arabidopsis* media with or without 0.5 μM FB1.

The different transgenic lines used in this study were as follows: *pPIN1:PIN1-GFP* (Benková et al., 2003), *pPIN2:PIN2-GFP* (Abas et al., 2006), *pPIN2:PIN1-GFP* (Wisniewska et al., 2006), *pAUX1:AUX1-YFP* (Swarup et al., 2004), *pLAX3:LAX3-GFP* (Swarup et al., 2008), *35S:PIP2:GFP* and *35S:LTi6b:GFP* (Cutler et al., 2000), *pABC19:ABC19-GFP* and *pABC1:ABC1-GFP* (Titapiwatanakun et al., 2009), *pSNX1:SNX1-GFP* (Jaillais et al., 2006), and *pAXR4:AXR4-GFP* (Dharmasiri et al., 2006). The lines from the Wave Marker collection lines containing the UBQ10 promoter were as follows: wave6 (*YFP-NIP1*), wave29Y (*YFP-ARA5/RabD2*^{a}), wave33Y (*YFP-RAbD2*^{b}), wave18Y (*YFP-GOT1*), wave127Y (*YFP-MEMB*), wave22Y (*YFP-SYP32*), wave34Y (*YFP-RABA1*^{e}), wave2Y (*YFP-ARA7*), wave5Y (*YFP-RABG3*^{F}), wave9Y (*YFP-VAMP711*), and wave11Y (YFP-RabG3^{C}) (Geldner et al., 2009). The Rab-A2^{a} mutant constructs were the following: pRab-A2^{a}:YFP-pRab-A2^{a}, pRab-A2^{a}:YFP-Rab-A2^{a}[N125I], pRab-A2^{a}:YFP-Rab-A2^{a}[S26N], pRab-A2^{a}:YFP-Rab-A2^{a}[Q71L] (Chow et al., 2008), pBOR1-BOR1-GFP (Takano et al., 2005), and p35S:LeAGP1-GFP (Estévez et al., 2006).

Insertion Mutants

Two *Arabidopsis* ecotypes Columbia-0 (Col-0) and Wassilewskija (Ws) were used. *loh1-1*, *loh2-1,* and *loh3-1* are in the Ws background and were isolated by screening the original collection of 60,480 T-DNA insertions described by Krysan et al. (1999) using the following primers: *loh1-1* (5′-TCTTTTATCTCATTCTCCTTTGCTCTGCT-3′; 5′-GAACCAAAAAAAACCCCAAGAAAATTCAT-3′), *loh2-1* (5′-AGTCAGTAAGGTAATGAAGCTGAAAACAA-3′; 5′-AAAAAGAAAGAAGGTCTGTGAGATCCCAA-3′), and *loh3-1* (5′-ATTCGATTTCTCCTCGATAGATTCGTCTT-3′; 5′-ACAACGTGCTTTTACATTTCTATCTACCT-3′) in combination with the left border primer JL202 (5′-CATTTTATAATAACGCTGCGGACATCTAC-3′). *loh1-2* (N580371), *loh2-2* (N524192), and *loh3-2* (N650849) were obtained from the Salk collection. The genotyping of SALK *loh* was performed with the following primers: *loh1* (5′-TTCCTTCTTATGTGATTGTAAAGAGAA-3′; 5′-AAAAACCCCAAGAAAATTCATTTAG-3′), *loh2* (5′-TTTCGGATTCTTCTTCTTGA-3′, 5′-AAAGACATCACTTGCATCATG-3′), and *loh3* (5′-TGGTTTAAAGAGAGGATTTTACGG-3′, 5′-CAAAATTTGTTCAGACTACAATTCAA-3′).

Lipid Analysis

Free and total LCB analysis was performed by HPLC after fluorescent derivatization (Bach et al., 2008). Complete sphingolipid analysis was performed by mass spectrometry as described (Markham and Jaworski, 2007).

Auxin Transport Measurements

Auxin transport was measured through sections cut from 12- to 15-cm-long inflorescence bolts as previously described (Brown et al., 2001). Ws and *loh1-1 loh3-1* plants were grown for 5 to 6 weeks until the bolts were 12 to 15 cm high. Sections 25 mm in length were cut using a sharp razor blade from the bottom, the middle, and 10 mm below the top of the bolt. The stem section was immediately placed in a tube containing 20 µL of 5 mM MES, pH 5.5, 1% Suc, 0.05% Tween 20, 19 nCi 1-^{14}C-indole acetic acid (9 mCi/mmol) with or without the addition of 10 µM NPA such that one end of the stem segment was immersed in the solution. To measure basipetal transport, the stem segment was placed in the inverted orientation, that is, with the top of the stem segment in the solution. Stem segments were incubated for 16 h in the dark after which the upper 5 mm of the stem was excised, immersed in scintillation fluid, and the dpm measured in a scintillation counter.

Live-Cell Imaging

Excitation/emission of YFP (514 nm, 520 to 560 nm) GFP (488 nm, 490 to 550 nm), and FM4-64 (488 or 514 nm, 600 to700 nm) was performed on LSM 710 (Zeiss) and SP2 (Leica) confocal microscopes. Root tip imaging was performed with seedlings mounted in water, and high magnification images were taken with a ×63 objective lens (water immersion) with a line averaging of 8. Roots were stained with 2 µM FM4-64 and directly mounted on the microscope slide. Spectral separation of PIN1:GFP and AUX1:YFP was conducted according the GFP and YFP emission profile and the LSM software spectral mode. GUS and propidium iodide staining was performed as described previously (Harrar et al., 2003; Truernit et al., 2008). FRAP analysis of PIN1-GFP and AUX1-YFP was performed on 10- to 12-d-old secondary root tips of pPIN1:PIN1-GFP and pAUX1:AUX1-YFP seedlings treated with 2.5 µM FB1. The FRAP experiment was performed using a Zeiss LSM710 with a ×40 oil objective. A prebleach scan was done with either a 488-nm laser excitation (5%) for PIN1-GFP or a 514-nm laser excitation (3.5%) for AUX1-YFP with a pinhole of 82.2 and a 512 × 512 (8-bit) acquisition mode with a pixel dwell of 1.27 µs, 8 line average, and a 2× zoom. Fluorescence bleaching was performed after three prebleach scans with a double scan at 100% laser 488 and 514 nm and a pixel dwell of 177.32 µs. Confocal pictures were processed using ImageJ V1.44m. The pictures corresponding to prebleach, postbleach, and each recovery time point (15, 30, 45, and 60 min) were assembled into a time-lapse picture stack. Occasional drifting of the sample was corrected using the StackReg plugin. About two to four cells were quantified per root. Fluorescence intensity was measured on cell apical/basal membranes either as rectangular region of interest (ROI) in the case of PMs or as circular ROI in the case of FB1 aggregates. A nonbleached PM ROI was measured and used to correct fluorescence decrease due to photobleaching during acquisition. Fluorescence recovery was expressed as percentage of fluorescence increase of the bleached region corrected by the acquisition bleaching factor of the whole sample.

High-Pressure Freezing, Freeze Substitution, and Embedding Processes

For electron microscopy, root tips (3 mm) were cut in 1-hexadecene, transferred to 200-µm size cupules (Leica) containing 1-hexadecen, and frozen with a high-pressure freezer apparatus (EMPACT2; Leica). Freeze substitution was performed (Leica freeze substitution unit AFS2) in acetone supplemented with 2% osmium tetroxide warming up progressively from −90 to −30°C (specimens are left at −90°C for 27 h, then warmed up to −60°C over 15 h). Specimens stayed in a −60°C bath for 8 h, before the next warm-up step to −30°C over 15 h, where they remain for additional 8 h. Root tips were finally infiltrated and embedded in epoxy resin (low viscosity Premix Kit medium, agar) at room temperature according to the manufacturer's instructions. For polymerization, they were placed in flat plastic molds and polymerized for 17 h at 60°C.

Electron Microscopy Observations

The 70-nm ultrathin sections (Ultracut UC6; Leica) were collected on formvar-coated copper grids and poststained with aqueous 2% uranyl acetate/lead citrate as described by Hawes and Satiat-Jeunemaitre (2001). They were examined with a JEOL 1400 transmission electron microscope operating at 120 kV. Images were acquired using a postcolumn high-resolution (11 megapixels) high-speed camera (SC1000 Orius; Gatan).

Experimental Procedures for Supplemental Data

The mRNA levels of *LOH1*, *2*, and *3* were checked via RT-PCR for *loh1-2*, *loh2-2*, and *loh3-2* and via RNA gel blot on total RNA for *loh1-1*, *loh2-1*, and *loh3-1* using an RNA probe constructed from the cloned cDNA for each gene (see Supplemental Figures 2A and 2B).

Myriocin treatment was performed for 16 to 20 h on 9-d-old seedlings at 7 µM directly dissolved in liquid *Arabidopsis* media.

The FDA test was performed on 9-d-old Col-0 or AUX1:YFP seedlings treated with FB1 (16-h treatment at 2.5 µM). Seedlings were treated with 2 µM FDA for 15 min and then washed and directly mounted in 2 µM FM 4-64 for visualization (see Supplemental Figure 6B). Esterase activity of cells was monitored in the green and FM4-64 in red channel. Both were activated with a 488-nm argon laser.

To test the effect of FB1 treatment on endocytosis, BOR11-GFP seedlings grown for 5 d on agar medium were treated or not with 2.5 mM FB1 (16 h) in water and mounted (t = 0) in 100 µM boric acid (±2.5 µM FB1) (see Supplemental Figure 10B). To test the effect of FB1 treatment on secretion, 12-d-old seedlings (35S:LeAGP1-GFP) treated or not with 2.5 mM FB1 (16 h) were plasmolysed using 0.4 mM mannitol with 3 µM propidium Iodide during 5 min and then mounted (see Supplemental Figure 11F).

Accession Numbers

Sequence data from this article can be found in the GenBank/EMBL database or the *Arabidopsis* Genome Initiative database under the following accession numbers: *Arabidopsis* (At) LOH1 (At3g25540), LOH2 (At3g19260), LOH3 (At1g13580), and LOH4 (At1g26200). Accession numbers of tomato (Le) Asc1, Asc2, and Asc3 and yeast Lag1p and Lac1p used in Figure 1A are AJ312131, SL1.00sc02793_15.1.1, SL1.00sc02749_302.1.1, SCU08133, and NM_001179574, respectively. The accession numbers of the *Arabidopsis* mutants used in this study are as follows: *loh1-2* (N580371), *loh2-2* (N524192), *loh3-2* (N650849), *loh1-1* (CS66113), *loh2-1* (CS66114), and *loh3-1* (CS66115).

Acknowledgments — D.M. and this work were supported by the Agence Nationale de la Recherche Programe Blanc Sphingopolar (07-BLAN-202) and the European training program Marie Curie (European Union Versailles-Evry Research Training program). J.E.M. was supported by National Science Foundation Grant MCB 0312559 under the guidance of J.G. Jaworski and by the University of Groningen in the laboratory of J. Hille. We thank Thierry Gaude, Jan Traas, Markus Geisler, Christian Luschnig, and Jiří Friml for the gifts of p35S:YFP-RAB-F2b, pPIN1-PIN1:GFP, pABCs:ABCs-GFP, pPIN2:PIN2-GFP, and pPIN2:PIN1-GFP transgenic lines, respectively. We thank Niko Geldner for all the wave lines. We thank Ranjan Swarup for the gift of pAXR4:AXR4-GFP and pLAX3:LAX3-GFP and for helpful discussion. We are grateful to Ian Moore for providing the different pRab-A2:YFP-Rab-A2^a mutant lines, to José Estevez for the LeAGP1-GFP line, and to Junpei Takano for the BOR1-GFP line. We thank Bruno Letarnec for taking care of the plants. We

used the cytology and imaging facility of the Plateforme de Cytologie et Imagerie Végétale and the Plateforme de Chimie du Végétal of Institut Jean-Pierre Bourgin (supported by Région Ile de France and Conseil Général des Yvelines) and the electron microscopy facilities and cell biology unit of the Imagif platform (Centre National de la Recherche Scientifique), supported by the Conseil Général de l'Essonne.

Supplemental Data

The following materials are presented following the **References** to this article:

- **Supplemental Figure 1.** Protein Sequence Alignment of 29 LAG1 Homologs and Phylogenetic Relationship among LAG1 Homologs.
- **Supplemental Figure 2.** Characterization of loh Mutants.
- **Supplemental Figure 3.** Complementation of the *loh1 loh3* Double Mutant.
- **Supplemental Figure 4.** Fatty Acid Content of Total Sphingolipids and Free LCBs from *loh* Mutants.
- **Supplemental Figure 5.** Sphingolipid Analysis of FB1-Treated Seedlings .
- **Supplemental Figure 6.** Effect of FB1 on Root Growth and Viability .
- **Supplemental Figure 7.** FB1 Has No Effect on Several Membrane Markers.
- **Supplemental Figure 8.** Subcellular Distribution of PIN1-GFP and AUX1-YFP and YFP-VAMP711 upon Sphingolipid Depletion .
- **Supplemental Figure 9.** Endomembrane Ultrastructure Is Altered in *loh1-1*/*loh3-1* Root Cells .
- **Supplemental Figure 10.** Involvement of Endocytosis in YFP-RabA2^a Aggregation .
- **Supplemental Figure 11.** Involvement of Endocytic and Secretory Pathways in YFP-RabA2^a Aggregation .
- **Supplemental Data Set 1.** Text File of the Sequences and Alignment Used for the Phylogenetic Analysis Shown in Supplemental Figure 1B.

References

Abas, L., Benjamins, R., Malenica, N., Paciorek, T., Wiśniewska, J., Moulinier-Anzola, J. C., Sieberer, T., Friml, J., and Luschnig, C. (2006). Intracellular trafficking and proteolysis of the *Arabidopsis* auxin-efflux facilitator PIN2 are involved in root gravitropism. Nat. Cell Biol. **8:** 249–256. Erratum. Nat. Cell Biol. **8:** 424.

Abbas, H. K., Tanaka, T., Duke, S.O., Porter, J. K., Wray, E. M., Hodges, L., Sessions, A. E., Wang, E., Merrill, A. H., Jr., and Riley, R. T. (1994). Fumonisin- and AAL-Toxin-Induced Disruption of Sphingolipid Metabolism with Accumulation of Free Sphingoid Bases. Plant Physiol. **106:** 1085–1093.

Alonso, J.M., et al. (2003). Genome-wide insertional mutagenesis of *Arabidopsis thaliana.* Science **301:** 653–657.

Aubert, A., Marion, J., Boulogne, C., Bourge, M., Abreu, S., Bellec, Y., Faure, J.-D., and Satiat-Jeunemaître, B. (2011). Sphingolipids involvement in plant endomembrane differentiation: The BY2 case. Plant J. **65:** 958–971.

Bach, L., et al. (2008). The very-long-chain hydroxy fatty acyl-CoA dehydratase PASTICCINO2 is essential and limiting for plant development. Proc. Natl. Acad. Sci. USA **105:** 14727–14731.

Bagnat, M., and Simons, K. (2002). Lipid rafts in protein sorting and cell polarity in budding yeast *Saccharomyces cerevisiae*. Biol. Chem. **383:** 1475–1480.

Barz, W. P., and Walter, P. (1999). Two endoplasmic reticulum (ER) membrane proteins that facilitate ER-to-Golgi transport of glycosylphosphatidylinositol-anchored proteins. Mol. Biol. Cell **10:** 1043– 1059.

Baud, S., Bellec, Y., Miquel, M., Bellini, C., Caboche, M., Lepiniec, L., Faure, J.-D., and Rochat, C. (2004). gurke and pasticcino3 mutants affected in embryo development are impaired in acetyl-CoA carboxylase. EMBO Rep. **5:** 515–520.

Benková, E., Michniewicz, M., Sauer, M., Teichmann, T., Seifertová, D., Jürgens, G., and Friml, J. (2003). Local, efflux-dependent auxin gradients as a common module for plant organ formation. Cell **115:** 591–602.

Borner, G. H., Sherrier, D. J., Weimar, T., Michaelson, L. V., Hawkins, N. D., Macaskill, A., Napier, J. A., Beale, M. H., Lilley, K. S., and Dupree, P. (2005). Analysis of detergent-resistant membranes in *Arabidopsis*. Evidence for plasma membrane lipid rafts. Plant Physiol. **137:** 104–116.

Brandwagt, B. F., Kneppers, T. J., Nijkamp, H. J., and Hille, J. (2002). Overexpression of the tomato *Asc-1* gene mediates high insensitivity to AAL toxins and fumonisin B1 in tomato hairy roots and confers resistance to *Alternaria alternata* f. sp. *lycopersici* in *Nicotiana umbratica* plants. Mol. Plant Microbe Interact. **15:** 35–42.

Brandwagt, B. F., Mesbah, L. A., Takken, F. L., Laurent, P. L., Kneppers, T. J., Hille, J., and Nijkamp, H. J. (2000). A longevity assurance gene homolog of tomato mediates resistance to *Alternaria alternata* f. sp. *lycopersici* toxins and fumonisin B1. Proc. Natl. Acad. Sci. USA **97:** 4961–4966.

Brown, D. E., Rashotte, A. M., Murphy, A. S., Normanly, J., Tague, B. W., Peer, W. A., Taiz, L., and Muday, G. K. (2001). Flavonoids act as negative regulators of auxin transport *in vivo* in *Arabidopsis.* Plant Physiol. **126:** 524–535.

Chen, M., Markham, J. E., Dietrich, C. R., Jaworski, J. G., and Cahoon, E. B. (2008). Sphingolipid long-chain base hydroxylation is important for growth and regulation of sphingolipid content and composition in *Arabidopsis.* Plant Cell **20:** 1862–1878.

Chow, C. M., Neto, H., Foucart, C., and Moore, I. (2008). Rab-A2 and Rab-A3 GTPases define a trans-Golgi endosomal membrane domain in *Arabidopsis* that contributes substantially to the cell plate. Plant Cell **20:** 101–123.

Cutler, S. R., Ehrhardt, D. W., Griffitts, J. S., and Somerville, C. R. (2000). Random GFP:cDNA fusions enable visualization of subcellular structures in cells of *Arabidopsis* at a high frequency. Proc. Natl. Acad. Sci. USA **97:** 3718–3723.

Desai, K., Sullards, M. C., Allegood, J., Wang, E., Schmelz, E. M., Hartl, M., Humpf, H. U., Liotta, D. C., Peng, Q., and Merrill, A. H., Jr. (2002). Fumonisins and fumonisin analogs as inhibitors of ceramide synthase and inducers of apoptosis. Biochim. Biophys. Acta **1585:** 188–192.

Dharmasiri, S., Swarup, R., Mockaitis, K., Dharmasiri, N., Singh, S. K., Kowalchyk, M., Marchant, A., Mills, S., Sandberg, G., Bennett, M. J., and Estelle, M. (2006). AXR4 is required for localization of the auxin influx facilitator AUX1. Science **312:** 1218–1220.

Estelle, M., and Somerville, C. (1987). Auxin-resistant mutants of *Arabidopsis thaliana* with an altered morphology. Mol. Gen. Genet. **206:** 200–206.

Estévez, J.M., Kieliszewski, M. J., Khitrov, N., and Somerville, C. (2006). Characterization of synthetic hydroxyproline-rich proteoglycans with arabinogalactan protein and extensin motifs in *Arabidopsis.* Plant Physiol. **142:** 458–470.

Fischer, U., Men, S., and Grebe, M. (2004). Lipid function in plant cell polarity. Curr. Opin. Plant Biol. **7:** 670–676.

Gaigg, B., Timischl, B., Corbino, L., and Schneiter, R. (2005). Synthesis of sphingolipids with very long chain fatty acids but not ergosterol is required for routing of newly synthesized plasma membrane ATPase to the cell surface of yeast. J. Biol. Chem. **280:** 22515–22522.

Gaigg, B., Toulmay, A., and Schneiter, R. (2006). Very long-chain fatty acid-containing lipids rather than sphingolipids per se are required for raft association and stable surface transport of

newly synthesized plasma membrane ATPase in yeast. J. Biol. Chem. **281:** 34135–34145.

Geldner, N., Anders, N., Wolters, H., Keicher, J., Kornberger, W., Muller, P., Delbarre, A., Ueda, T., Nakano, A., and Ju¨ rgens, G. (2003). The *Arabidopsis* GNOM ARF-GEF mediates endosomal recycling, auxin transport, and auxin-dependent plant growth. Cell **112:** 219–230.

Geldner, N., Dénervaud-Tendon, V., Hyman, D. L., Mayer, U., Stierhof, Y. D., and Chory, J. (2009). Rapid, combinatorial analysis of membrane compartments in intact plants with a multicolor marker set. Plant J. **59:** 169–178.

Guillas, I., Kirchman, P. A., Chuard, R., Pfefferli, M., Jiang, J. C., Jazwinski, S. M., *and Conzelmann, A. (2001). C26-CoA-dependent ceramide synthesis of Saccharomyces cerevisiae* is operated by Lag1p and Lac1p. EMBO J. **20: 2655–2665.

Harrar, Y., Bellec, Y., Bellini, C., and Faure, J.-D. (2003). Hormonal control of cell proliferation requires PASTICCINO genes. Plant Physiol. **132:** 1217–1227.

Hawes, C., and Satiat-Jeunemaître, B. (2005). The plant Golgi apparatus—going with the flow. Biochim. Biophys. Acta **1744:** 93–107.

Hofmann, K., and Stoffel, W. (1993). TMbase - A database of membrane spanning proteins segments. Biol. Chem. Hoppe Seyler **374:** 166.

Holthuis, J. C., Pomorski, T., Raggers, R.J., Sprong, H., and Van Meer, G. (2001). The organizing potential of sphingolipids in intracellular membrane transport. Physiol. Rev. **81:** 1689–1723.

Imgrund, S., Hartmann, D., Farwanah, H., Eckhardt, M., Sandhoff, R., Degen, J., Gieselmann, V., Sandhoff, K., and Willecke, K. (2009). Adult ceramide synthase 2 (CERS2)-deficient mice exhibit myelin sheath defects, cerebellar degeneration, and hepatocarcinomas. J. Biol. Chem. **284:** 33549–33560.

Jaillais, Y., Fobis-Loisy, I., Miège, C., Rollin, C., and Gaude, T. (2006). AtSNX1 defines an endosome for auxin-carrier trafficking in *Arabidopsis.* Nature **443:** 106–109.

Jain, A., Poling, M. D., Karthikeyan, A. S., Blakeslee, J. J., Peer, W. A., Titapiwatanakun, B., Murphy, A. S., and Raghothama, K. G. (2007). Differential effects of sucrose and auxin on localized phosphate deficiency-induced modulation of different traits of root system architecture in *Arabidopsis.* Plant Physiol. **144:** 232–247.

Jiang, J. C., Kirchman, P. A., Zagulski, M., Hunt, J., and Jazwinski, S. M. (1998). Homologs of the yeast longevity gene *LAG1* in *Caenorhabditis elegans* and human. Genome Res. **8:** 1259–1272.

Kleine-Vehn, J., Dhonukshe, P., Swarup, R., Bennett, M., and Friml, J. (2006). Subcellular trafficking of the *Arabidopsis* auxin influx carrier AUX1 uses a novel pathway distinct from PIN1. Plant Cell **18:** 3171–3181.

Klemm, R. W., Ejsing, C. S., Surma, M. A., Kaiser, H. J., Gerl, M. J., Sampaio, J. L., de Robillard, Q., Ferguson, C., Proszynski, T.J., Shevchenko, A., and Simons, K. (2009). Segregation of sphingolipids and sterols during formation of secretory vesicles at the trans-Golgi network. J. Cell Biol. **185:** 601–612.

Klose, C., Ejsing, C. S., García-Sáez, A. J., Kaiser, H. J., Sampaio, J. L., Surma, M. A., Shevchenko, A., Schwille, P., and Simons, K. (2010). Yeast lipids can phase-separate into micrometer-scale membrane domains. J. Biol. Chem. **285:** 30224–30232.

Krysan, P. J., Young, J. C., and Sussman, M. R. (1999). T-DNA as an insertional mutagen in *Arabidopsis.* Plant Cell **11:** 2283–2290.

Laloi, M., et al. (2007). Insights into the role of specific lipids in the formation and delivery of lipid microdomains to the plasma membrane of plant cells. Plant Physiol. **143:** 461–472.

Linkohr, B. I., Williamson, L. C., Fitter, A. H., and Leyser, H. M. (2002). Nitrate and phosphate availability and distribution have different effects on root system architecture of *Arabidopsis.* Plant J. **29:** 751–760.

Maier, O., and Hoekstra, D. (2003). Trans-Golgi network and subapical compartment of HepG2 cells display different properties in sorting and exiting of sphingolipids. J. Biol. Chem. **278:** 164–173.

Marchant, A., Bhalerao, R., Casimiro, I., Eklöf, J., Casero, P. J., Bennett, M., and Sandberg, G. (2002). AUX1 promotes lateral root formation by facilitating indole-3-acetic acid distribution between sink and source tissues in the *Arabidopsis* seedling. Plant Cell **14:** 589–597.

Marion, J., Bach, L., Bellec, Y., Meyer, C., Gissot, L., and Faure, J.-D. (2008). Systematic analysis of protein subcellular localization and interaction using high-throughput transient transformation of *Arabidopsis* seedlings. Plant J. **56:** 169–179.

Markham, J. E., and Jaworski, J. G. (2007). Rapid measurement of sphingolipids from *Arabidopsis thaliana* by reversed-phase high-performance liquid chromatography coupled to electrospray ionization tandem mass spectrometry. Rapid Commun. Mass Spectrom. **21:** 1304–1314.

Markham, J. E., Li, J., Cahoon, E. B., and Jaworski, J. G. (2006). Separation and identification of major plant sphingolipid classes from leaves. J. Biol. Chem. **281:** 22684–22694.

Melser, S., Batailler, B., Peypelut, M., Poujol, C., Bellec, Y., Wattelet-Boyer, V., Maneta-Peyret, L., Faure, J.-D., and Moreau, P. (2010). Glucosylceramide biosynthesis is involved in Golgi morphology and protein secretion in plant cells. Traffic **11:** 479–490.

Men, S., Boutté, Y., Ikeda, Y., Li, X., Palme, K., Stierhof, Y. D., Hartmann, M. A., Moritz, T., and Grebe, M. (2008). Sterol-dependent endocytosis mediates post-cytokinetic acquisition of PIN2 auxin efflux carrier polarity. Nat. Cell Biol. **10:** 237–244.

Merrill, A. H., Jr., Wang, E., Gilchrist, D. G., and Riley, R. T. (1993). Fumonisins and other inhibitors of de novo sphingolipid biosynthesis. Adv. Lipid Res. **26:** 215–234.

Miyake, Y., Kozutsumi, Y., Nakamura, S., Fujita, T., and Kawasaki, T. (1995). Serine palmitoyltransferase is the primary target of a sphingosine-like immunosuppressant, ISP-1/myriocin. Biochem. Biophys. Res. Commun. **211:** 396–403.

Mizutani, Y., Kihara, A., and Igarashi, Y. (2005). Mammalian Lass6 and its related family members regulate synthesis of specific ceramides. Biochem. J. **390:** 263–271.

Mizutani, Y., Kihara, A., and Igarashi, Y. (2006). LASS3 (longevity assurance homologue 3) is a mainly testis-specific (dihydro)ceramide synthase with relatively broad substrate specificity. Biochem. J. **398:** 531–538.

Mongrand, S., Morel, J., Laroche, J., Claverol, S., Carde, J. P., Hartmann, M. A., Bonneu, M., Simon-Plas, F., Lessire, R., and Bessoule, J. J. (2004). Lipid rafts in higher plant cells: Purification and characterization of Triton X-100-insoluble microdomains from tobacco plasma membrane. J. Biol. Chem. **279:** 36277–36286.

Niemelä, P. S., Hyvönen, M. T., and Vattulainen, I. (2006). Influence of chain length and unsaturation on sphingomyelin bilayers. Biophys. J. **90:** 851–863.

Nyasae, L. K., Hubbard, A. L., and Tuma, P. L. (2003). Transcytotic efflux from early endosomes is dependent on cholesterol and glycosphingolipids in polarized hepatic cells. Mol. Biol. Cell **14:** 2689– 2705.

Oh, C. S., Toke, D. A., Mandala, S., and Martin, C. E. (1997). ELO2 and ELO3, homologues of the *Saccharomyces cerevisiae* ELO1 gene, function in fatty acid elongation and are required for sphingolipid formation. J. Biol. Chem. **272:** 17376–17384.

Pascher, I. (1976). Molecular arrangements in sphingolipids. Conformation and hydrogen bonding of ceramide and their implication on membrane stability and permeability. Biochim. Biophys. Acta **455:** 433–451.

Pewzner-Jung, Y., et al. (2010). A critical role for ceramide synthase 2 in liver homeostasis: I. Alterations in lipid metabolic pathways. J. Biol. Chem. **285:** 10902–10910.

Riebeling, C., Allegood, J. C., Wang, E., Merrill, A. H., Jr., and Futerman, A. H. (2003). Two mammalian longevity assurance gene (*LAG1*) family members, trh1 and trh4, regulate dihydroceramide synthesis using different fatty acyl-CoA donors. J. Biol. Chem. **278:** 43452–43459.

Ritzenthaler, C., Nebenführ, A., Movafeghi, A., Stussi-Garaud, C., Behnia, L., Pimpl, P., Staehelin, L. A., and Robinson, D. G. (2002). Reevaluation of the effects of brefeldin A on plant cells using tobacco Bright Yellow 2 cells expressing Golgi-targeted green fluorescent protein and COPI antisera. Plant Cell **14:** 237–261.

Roudier, F., et al. (2010). Very-long-chain fatty acids are involved in polar auxin transport and developmental patterning in *Arabidopsis.* Plant Cell **22:** 364–375.

Schneiter, R., Hitomi, M., Ivessa, A. S., Fasch, E. V., Kohlwein, S. D., and Tartakoff, A. M. (1996). A yeast acetyl coenzyme A carboxylase mutant links very-long-chain fatty acid synthesis to the structure and function of the nuclear membrane-pore complex. Mol. Cell. Biol. **16:** 7161–7172.

Schorling, S., Vallée, B., Barz, W. P., Riezman, H., and Oesterhelt, D. (2001). Lag1p and Lac1p are essential for the acyl-CoA-dependent ceramide synthase reaction in *Saccharomyces cerevisae*. Mol. Biol. Cell **12:** 3417–3427.

Spassieva, S. D., Markham, J. E., and Hille, J. (2002). The plant disease resistance gene *Asc-1* prevents disruption of sphingolipid metabolism during AAL-toxin-induced programmed cell death. Plant J. **32:** 561–572.

Stockmann-Juvala, H., and Savolainen, K. (2008). A review of the toxic effects and mechanisms of action of fumonisin B1. Hum. Exp. Toxicol. **27:** 799–809.

Swarup, K., et al. (2008). The auxin influx carrier LAX3 promotes lateral root emergence. Nat. Cell Biol. **10:** 946–954.

Swarup, R., et al. (2004). Structure-function analysis of the presumptive *Arabidopsis* auxin permease AUX1. Plant Cell **16:** 3069–3083.

Szafer-Glusman, E., Giansanti, M. G., Nishihama, R., Bolival, B., Pringle, J., Gatti, M., and Fuller, M. T. (2008). A role for very-longchain fatty acids in furrow ingression during cytokinesis in Drosophila spermatocytes. Curr. Biol. **18:** 1426–1431.

Takano, J., Miwa, K., Yuan, L., von Wirén, N., and Fujiwara, T. (2005). Endocytosis and degradation of BOR1, a boron transporter of *Arabidopsis thaliana*, regulated by boron availability. Proc. Natl. Acad. Sci. USA **102:** 12276–12281.

Tamura, K., Dudley, J., Nei, M., and Kumar, S. (2007). MEGA4: Molecular Evolutionary Genetics Analysis (MEGA) software version 4.0. Mol. Biol. Evol. **24:** 1596–1599.

Teufel, A., Maass, T., Galle, P. R., and Malik, N. (2009). The longevity assurance homologue of yeast lag1 (Lass) gene family (review). Int. J. Mol. Med. **23:** 135–140.

Titapiwatanakun, B., et al. (2009). ABCB19/PGP19 stabilises PIN1 in membrane microdomains in *Arabidopsis.* Plant J. **57:** 27–44.

Truernit, E., Bauby, H., Dubreucq, B., Grandjean, O., Runions, J., Barthélémy, J., and Palauqui, J. C. (2008). High-resolution whole-mount imaging of three-dimensional tissue organization and gene expression enables the study of Phloem development and structure in *Arabidopsis.* Plant Cell **20:** 1494–1503.

Venkataraman, K., Riebeling, C., Bodennec, J., Riezman, H., Allegood, J. C., Sullards, M. C., Merrill, A. H., Jr., and Futerman, A. H. (2002). Upstream of growth and differentiation factor 1 (uog1), a mammalian homolog of the yeast longevity assurance gene 1 (*LAG1*), regulates N-stearoyl-sphinganine (C18-(dihydro)ceramide) synthesis in a fumonisin B1-independent manner in mammalian cells. J. Biol. Chem. **277:** 35642–35649.

Willemsen, V., Friml, J., Grebe, M., van den Toorn, A., Palme, K., and Scheres, B. (2003). Cell polarity and PIN protein positioning in *Arabidopsis* require STEROL METHYLTRANSFERASE1 function. Plant Cell **15:** 612–625.

Winter, E., and Ponting, C.P. (2002). TRAM, *LAG1* and CLN8: members of a novel family of lipid-sensing domains? Trends Biochem. Sci. **27:** 381–383.

Wisniewska, J., Xu, J., Seifertová, D., Brewer, P. B., Ruzicka, K., Blilou, I., Rouquié, D., Benková, E., Scheres, B., and Friml, J. (2006). Polar PIN localization directs auxin flow in plants. Science **312:** 883.

Zheng, H., Rowland, O., and Kunst, L. (2005). Disruptions of the *Arabidopsis* Enoyl-CoA reductase gene reveal an essential role for very-long-chain fatty acid synthesis in cell expansion during plant morphogenesis. Plant Cell **17:** 1467–1481.

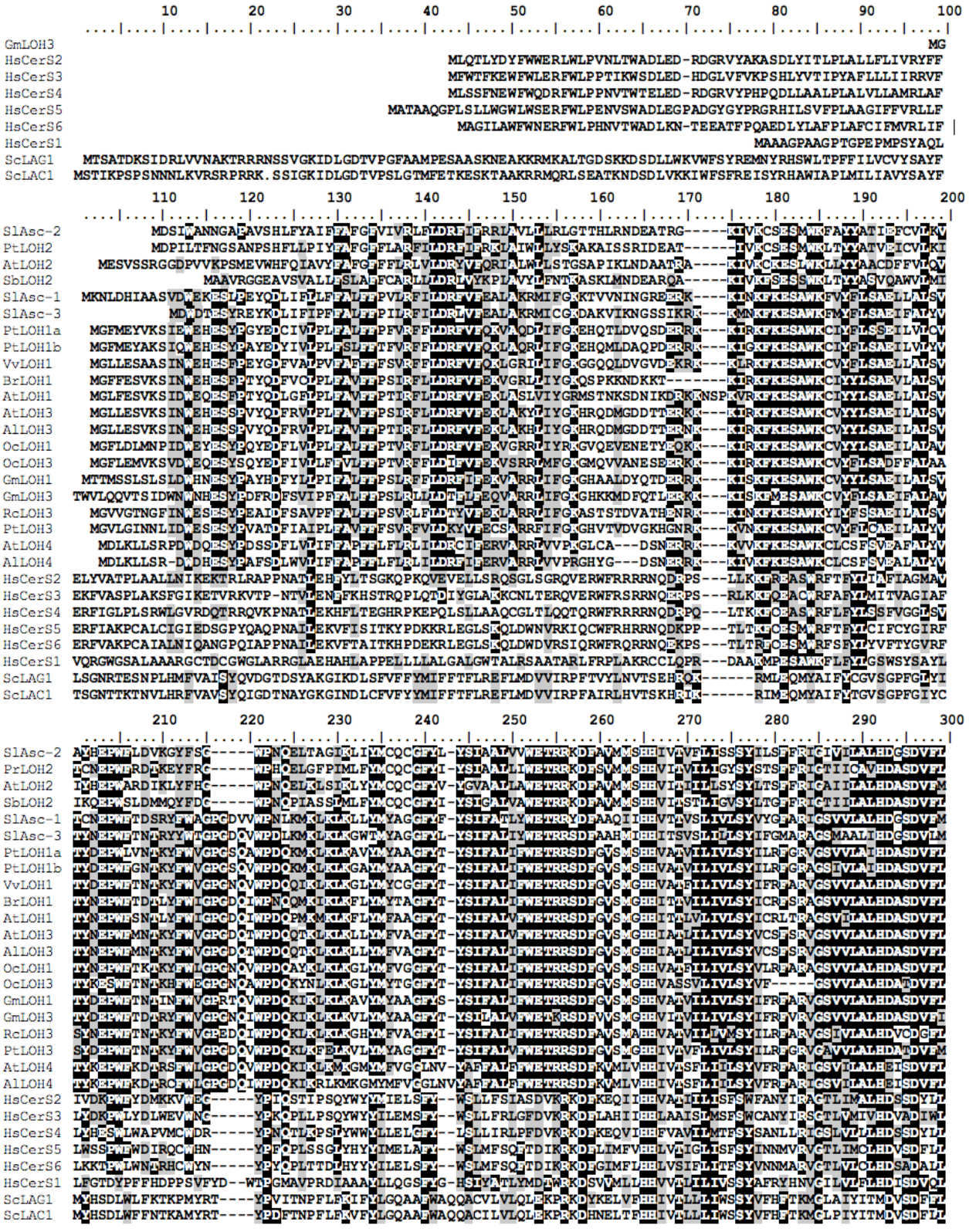

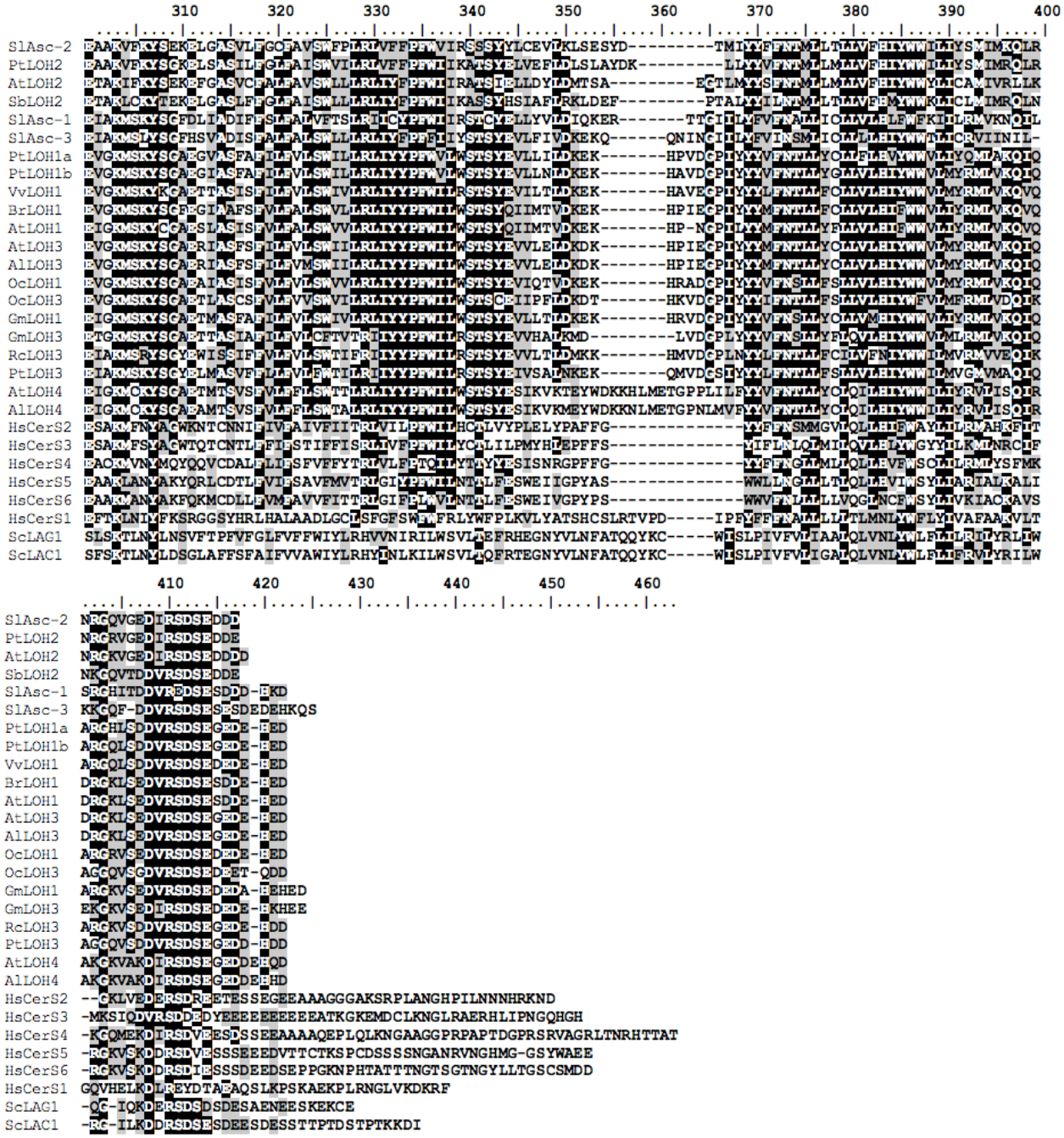

Supp. Fig. 1A. Protein sequence alignment of 29 LAG1 homologs.

Full length protein eudicot sequences are aligned with the CerS homologs from human (HsCerS1-6; #NM_021267, #NM_181746, #NM_178842, #NM_024552, #NM_147190, #NM_203463) and the LAG1 (#SCU08133) / LAC1 (#NM_001179574) sequences from *S.cerevisiae*. The two tomato sequences SlAsc-2 (#SL1.00sc02793_15.1.1) and SlAsc-3 (#SL1.00sc02749_302.1.1) are available from the tomato genome database http://mips.helmholtz-muenchen.de/plant/tomato/index.jsp. Other proteins are from *Arabidopsis lyrata*, (AlLOH3 # XM_002892714, AlLOH4 # XM_002890624); *Arabidopsis thaliana*, (AtLOH1-4, #NM_113450, #NM_112813, #NM_001035960 and #NM_001160896); *Brassica rapa* (BrLOH1 #EU186328); *Glycine max* (GmLOH1 #BT097014 and GmLOH3 #BT093554); *Orobance ceruna* (OcLOH1 #GQ181109 and OcLOH3 #GQ181110); *Populous trichocarpa* (PtLOH1a #XM_002311388, PtLOH1b #XM_002315949, PtLOH2 #XM_002330290, PtLOH3 #XM_002328643); *Riccinus communis* (RcLOH3 #XM_002511975); *Solanum lycopersicon* (SlAsc-1 #AJ312131); *Sorghum bicolor* (SbLOH2 #XM_002465463); *Vitis vinifera* (VvLOH1 #XM_002270764) Sequences are listed in Supplemental Dataset 1 online.

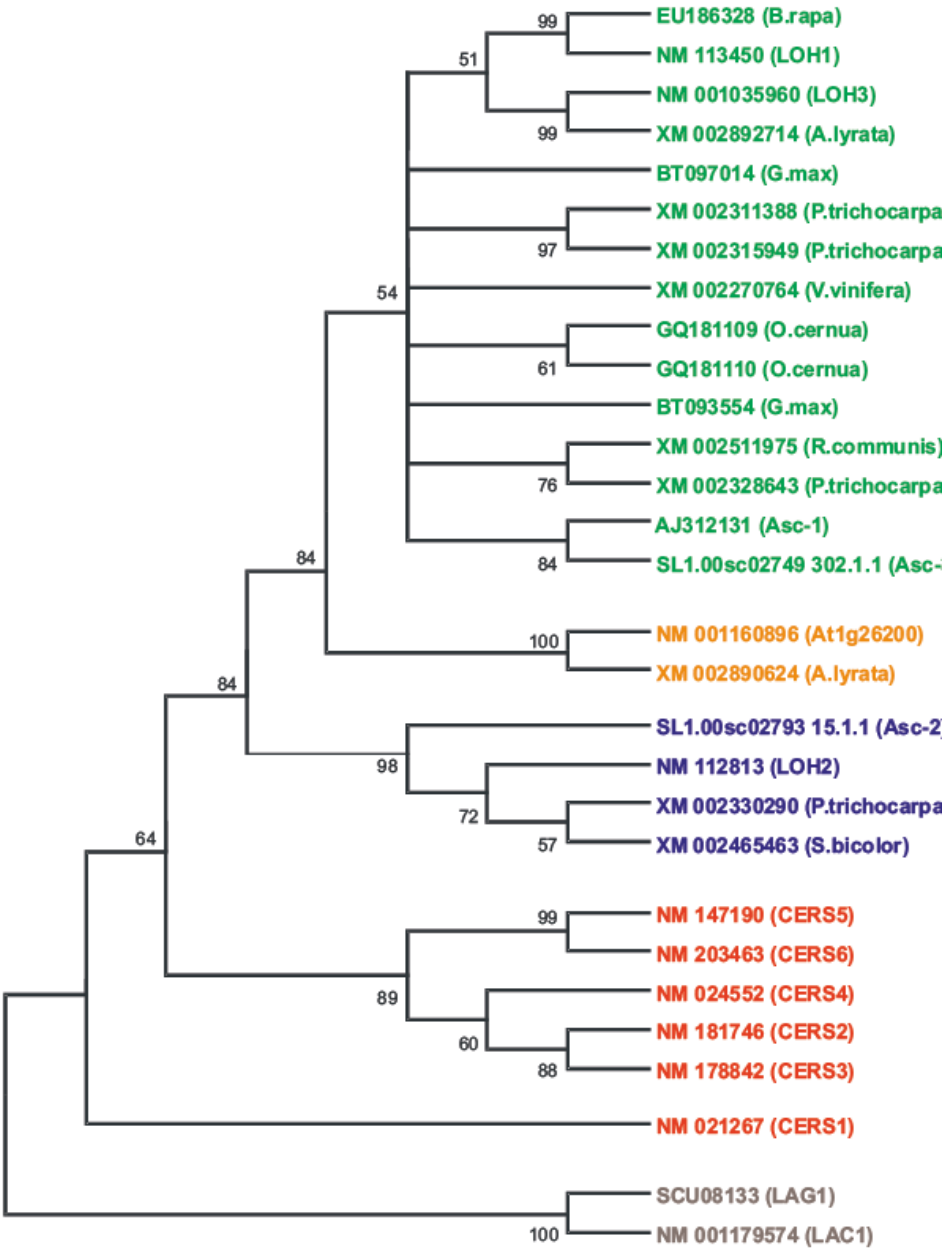

Supp. Fig. 1B. Phylogenetic relationship among LAG1 homologs.

The alignment shown in Fig. S1A was used to examine the phylogenetic relationship between LAG1 protein sequence homologs. Significant groupings are highlighted in colour. The region from 179 to 417 on the alignment ruler was used to establish the tree using Maximum Parsimony methods, gaps were excluded. The bootstrap consensus tree (1000 replicates) is shown, branches where divisions produced less than 50% of the time are collapsed. The percentage of trees where a particular branch occurred is shown next to each branch point. CERS1 is an unique link between the mammalian and fungal sequences and was selected as the root branch. Similar tree arrangements were produced using Maximum Likelihood and Neighbour-Joining algorithms. Alignment is shown in Supplemental Dataset 1 online.

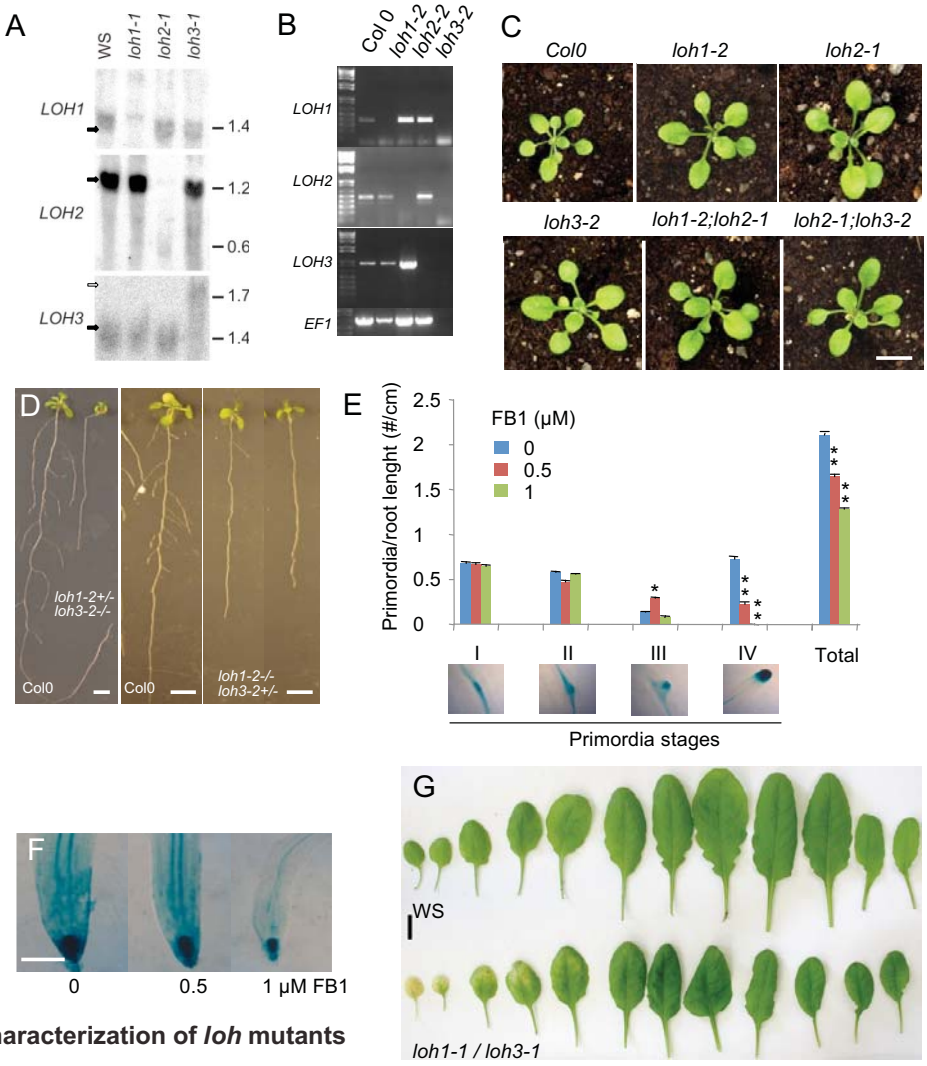

Supp. Fig. 2. Characterization of *loh* mutants

(A) Nothern blot with RNA from *loh1-1, loh2-1* and *loh3-1* and hybridized with *LOH1, LOH2* and *LOH3* probes. Transcript size (kb) are indicated by solid arrow and the abnormal *LOH3* transcript by an open arrow.

(B) Molecular analysis of *loh* alleles. RT- PCR of total RNAs from *loh1-2, loh2-2, loh3-2* with T-DNA flanking primers.

(C) Phenotype of 3 week-old rosettes of *loh* mutant. Scale bar, 1cm.

(D) Lateral root development is inhibited in sesqui mutants *loh1-2-/+;loh3-2-/-* and *loh1-2-/-;loh3-2-/+*. Plants were grown *in vitro* for two weeks. Scale bar, 1mm.

(E) Lateral root outgrowth but not initiation is inhibited by FB1 treatment. Number of lateral roots expressing DR5:GUS were classified according to different developmental stages (defined arbitrarily as I, first pericycle divisions; II, first periclinal divisions; III, primordia formation; IV, primordia outgrowth) in seedlings treated for 9 days with different concentrations of FB1. Data represent the mean of total lateral roots for 30 seedlings as shown in Fig.S2D. Significant differences between means (Student's t-test) are indicated by one (P≤0.05) or two (P≤0.01) asterisks.

(F) GUS staining in wild-type primary root meristems containing the DR5::GUS auxin reporter that were grown for 9 days in the presence of various concentrations (0, 0.5 and 1µM) of FB1. Scale bar, 100µm.

(G) Rosette leaves from wild-type (WS - top) and *loh1-1/loh3-1* mutant plants (bottom). Mutant leaves are smaller, wrinkled and show premature senescence. Scale bar, 10mm.

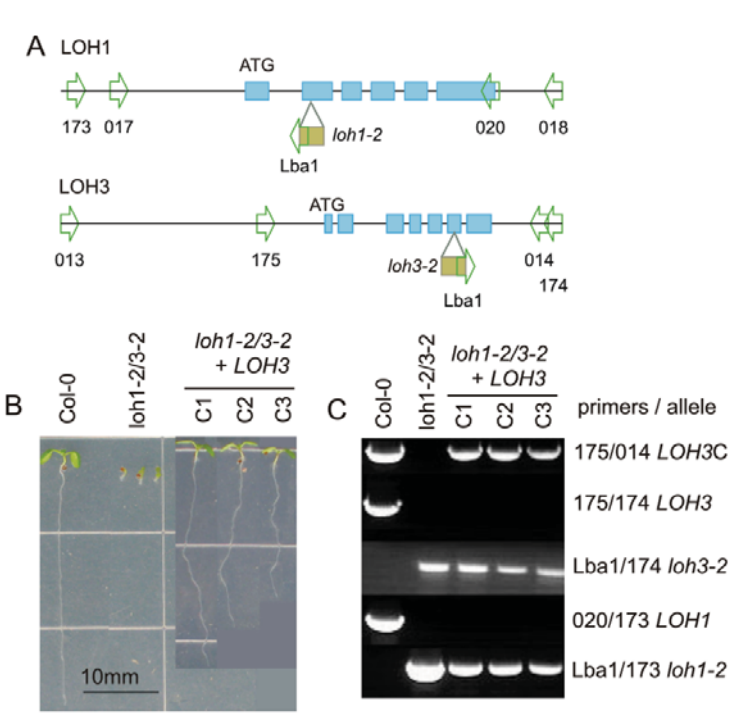

E

Primer #	sequence
013	5'-GCCTTTTTCAAGCGATAAGTGTCCTAAAA-3'
014	5'-GATGAATTTCAATTCAATTCCCAGAAAC-3'
017	5'-CTAATCAGAGAACCATTATCATCAAATAC-3'
018	5'-TTTTATCAAAATCTCACAGACCTGTAT-3'
020	5'-GAACCAAAAAAAACCCCAAGAAAATTCAT-3'
173	5'-CAGAAAACCATAATACCAAAACACAATCA-3'
174	5'-CACTTGTTCTTATTGCATCTCTAATCGAA-3'
175	5'-TAATAAAGATGCGGCTGGATAGATTCATA-3'
Lba1	5'-TGGTTCACGTAGTGGGCCATCG-3'

Supp. Fig. 3. Complementation of *loh1/loh3* double mutant.

A. Location of primers used to create *LOH* complementation constructs and analyze the complemented plants. Primers are shown as green arrows, the position of exons is indicated by blue boxes, the position of the T-DNA insertions in the *loh1-2* and *loh 3-2* allele are indicated.

B. Complementation of *loh1-2/loh3-2* by *LOH3*. Shown are a Col-0 wild-type plant, *loh1-2/loh3-2* seedlings and complemented *loh1-2/loh3-2* plants containing a transgenic copy of the *LOH3* allele.

C. PCR analysis of genomic DNA extracted from the plants shown in B. PCR reactions used the primers indicated on the right. Primers 175 and 014 detect the wild-type *LOH3* allele and the complementing *LOH3* containing T-DNA. Primers 175 and 174 detect only the wild-type LOH3 allele.

D. Complementation of *loh1-1/loh3-1* by *LOH1*. A *loh1-1/loh3-1* plant is shown in the left with typical delayed flowering and reduced rosette size. Plants containing the complementing LOH1 T-DNA do not show these phenotypes.

E. Primers used in making and analyzing the complemented plants.

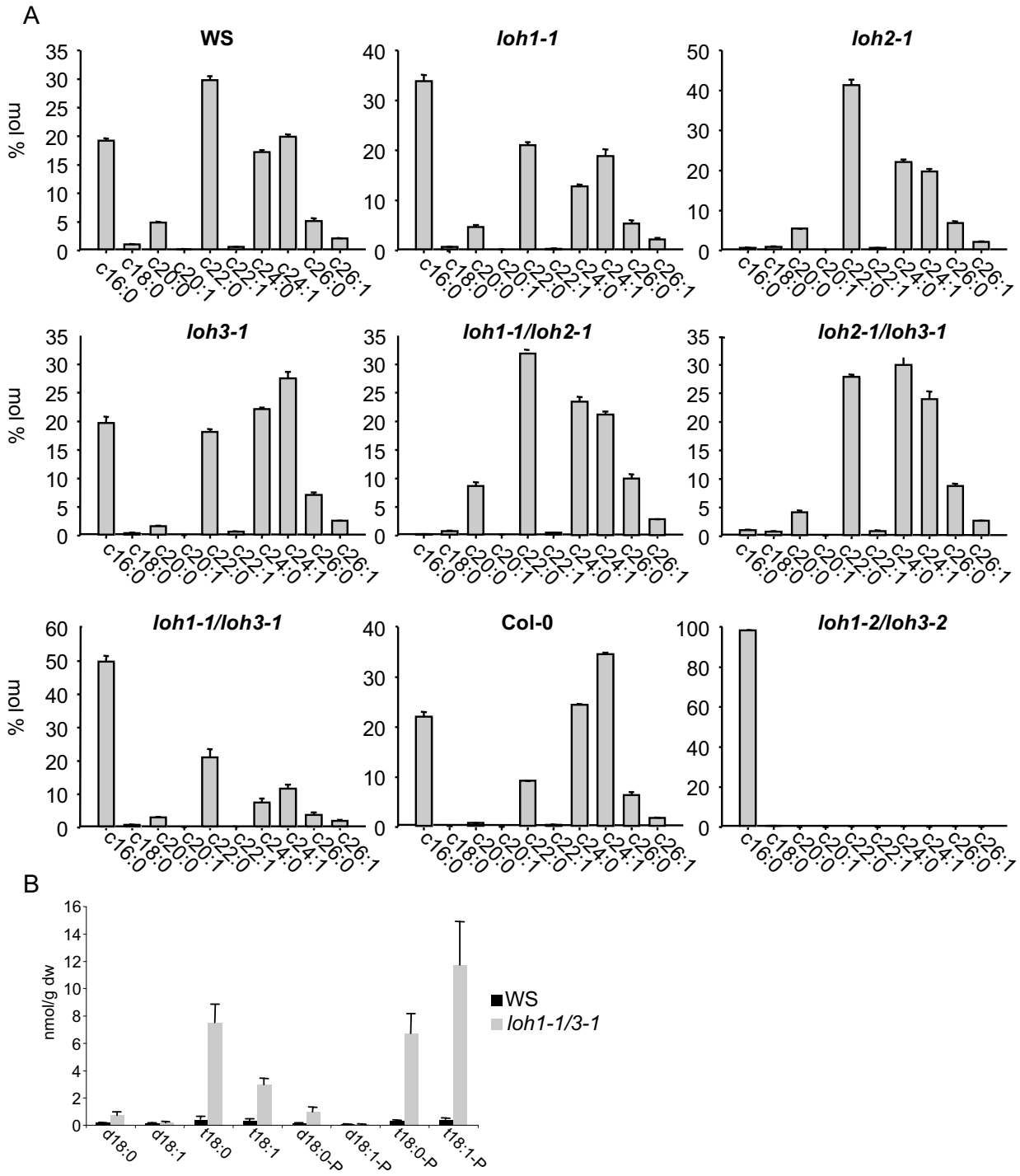

Supp. Fig. 4. Fatty acid content of total sphingolipids and free LCBs from *loh* mutants. (A) Total sphingolipids Total sphingolipid content of *loh* mutants compared to their related control (WS for *loh1-1, loh2-1* and *loh3-1*; Col0 for *loh1-2* and *loh3-2*). Sphingolipid content is shown according to the length and saturation of the fatty acid chain. (B) Free LCB content of *loh 1-1/loh3-1* compared to its related control (WS). Analyses were performed on 3-5 biological replicates. Data are the mean and standard error (n = 5).

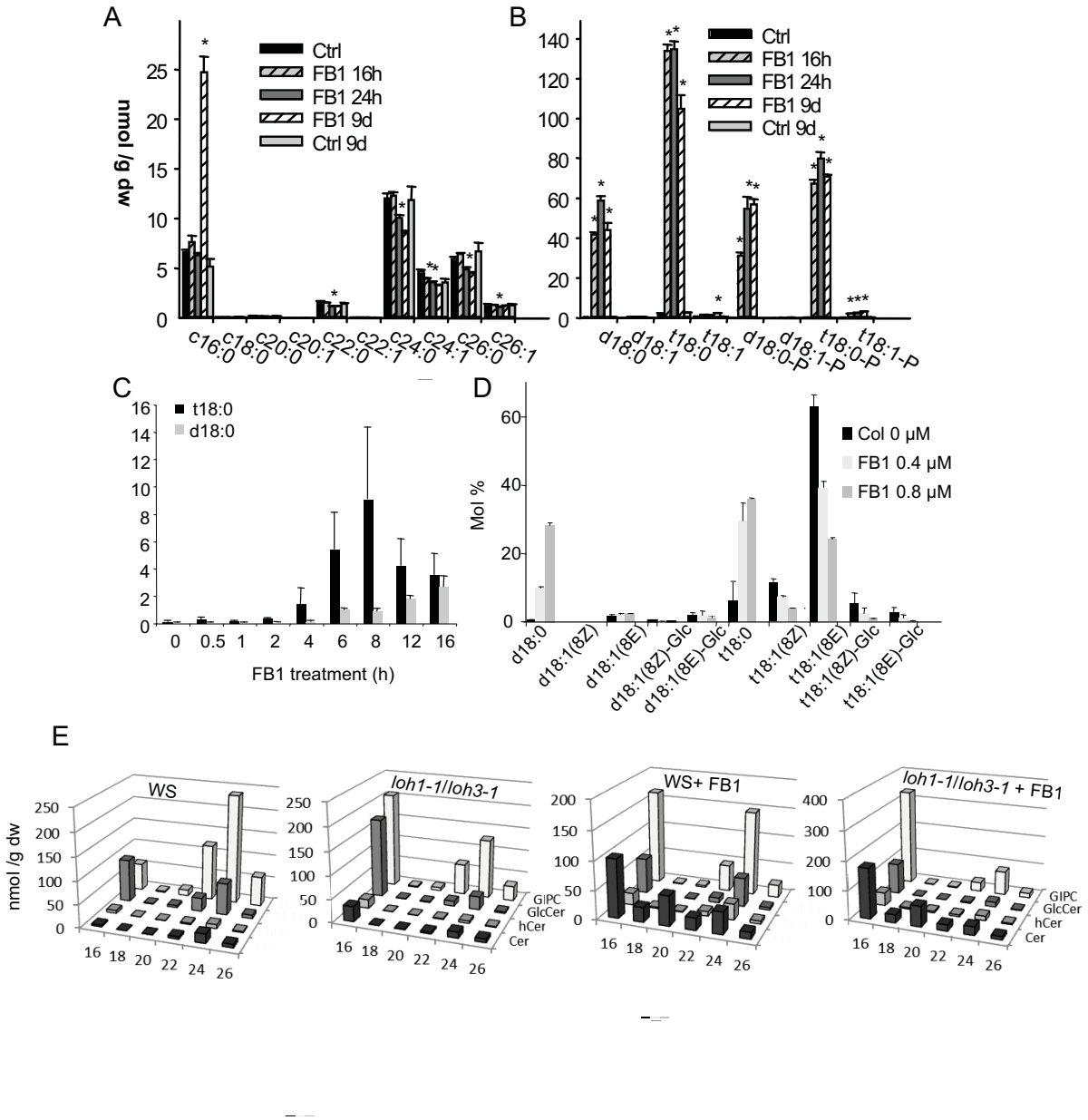

Supp. Fig. 5. Sphingolipid analysis of FB1 treated seedlings.

(A) Ceramide content in seedlings grown for several hours (16h, 24h) or 9 days (9d) on medium supplemented with 0.5 µM FB1 and compared to untreated seedlings.

(B) Free LCB content in seedlings grown for several hours (16h, 24h) or 9 days (9d) on medium supplemented with 0.5 µM FB1 and compared to untreated seedlings.

(C) Free t18:0 and d18:0 levels during time course treatment with 1µM FB1 (h, hours).

(D) Total LCB from seedlings treated with two FB1 concentrations for 9 days compared to untreated seedlings.

(E) Total sphingolipid content of WS and loh1-1/3-1 double mutant treated (+FB1) or not with 0.5µM FB1.

Data show mean plus one standard error and significant differences between means ($P \leq 0.05$, Student's t-test) are indicated by an asterisk.

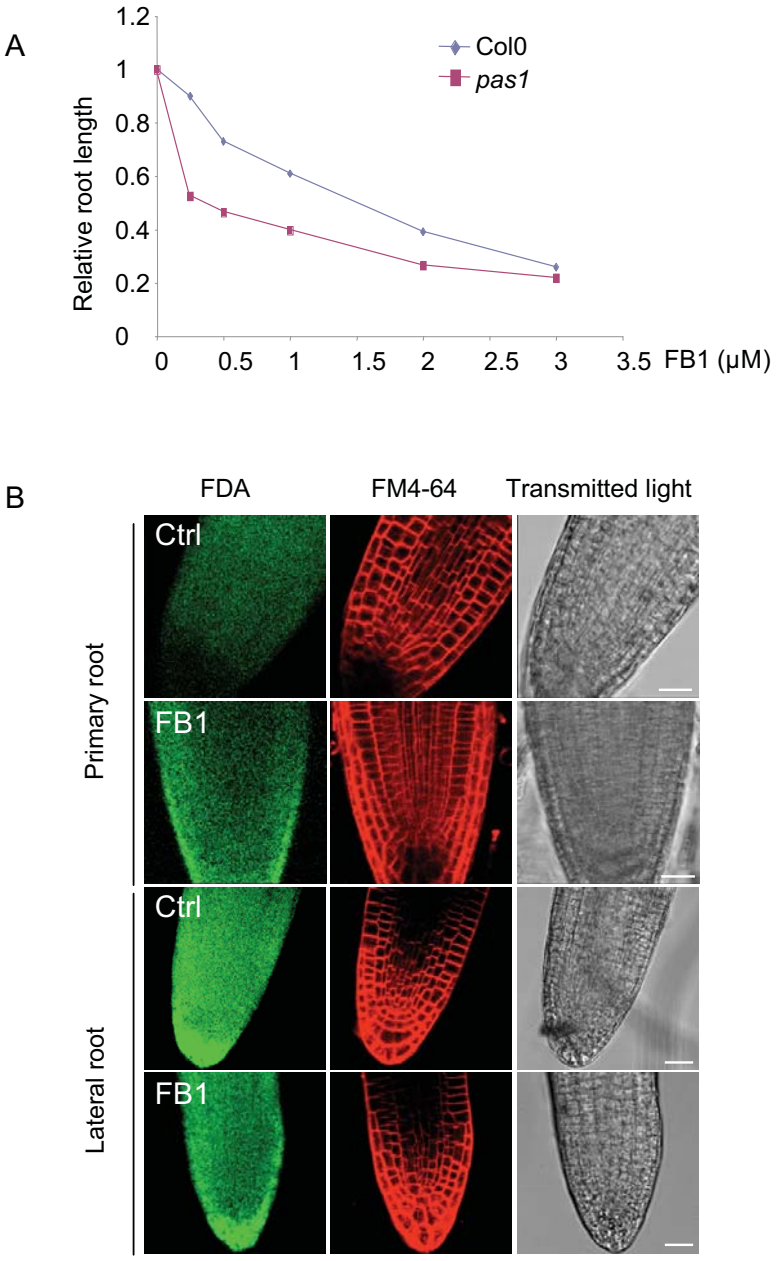

Supp. Fig. 6. Effect of FB1 on root growth and viability.

(A) *Pasticcino1* mutant root growth is more sensitive to FB1 than wild type. Seedlings were germinated and grown vertically on different concentrations of FB1 for 10 days. Data show root length relative to untreated control seedlings. Data are the mean of 25 to 33 seedling roots.

(B) Primary and secondary root viability upon FB1 treatment. Root tips treated or not with FB1 were stained with FM4-64 and FDA. Scale bar, 20µm.

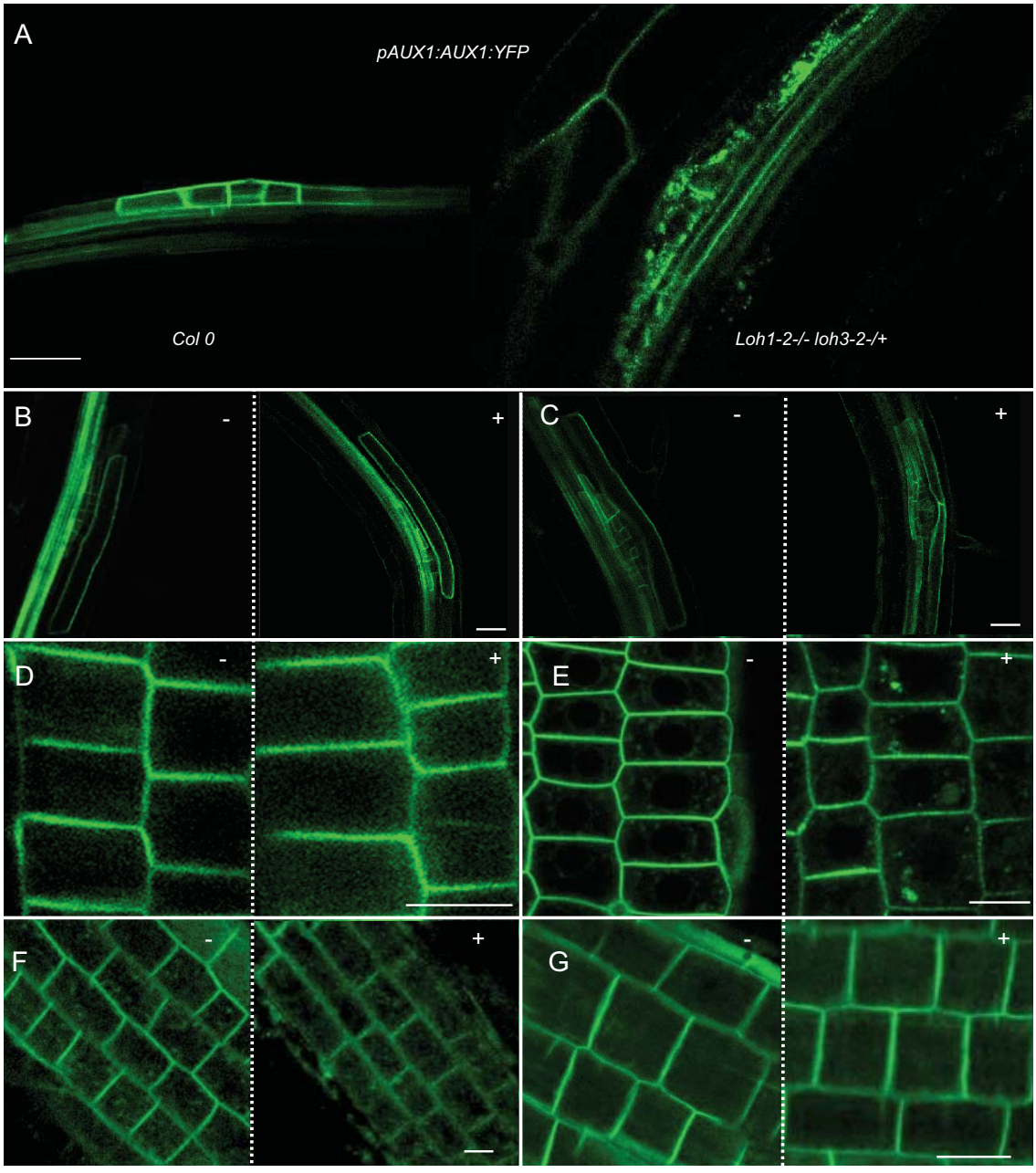

Supp. Fig. 7. FB1 has no effect on several membrane markers.

(A) Expression of *pAUX1:AUX1-YFP* in lateral root primordia of Col0 and *loh1-2*$^{-/-}$*/loh3-2*$^{-/+}$ double mutant. Note tha absence of membrane localization of AUX1-YFP in *loh1-2*$^{-/-}$*/loh3-2*$^{-/+}$. Scale bar, 10µm.

(B-C) Expression of *pLAX3:LAX3-GFP* in FB1-16h treated lateral roots (+) compared to untreated roots (-). *LAX3-GFP* expression was observed at two different developmental stages. Scale bar, 10µm. (B) the first anticlinal division of pericycle cells, and (C) the first periclinal cell divisions leading to the lateral root emergence.

(D-G) Plasma membrane markers in untreated (-) and FB1-16h treated (+) epidermal cells from lateral roots. (D) pPIN2:PIN2-GFP, (E) *pPIN2:PIN1-GFP,* (F) *35S:LTi6b-GFP* and (G) *35S:PIP2-GFP*. Scale bar, 10µm.

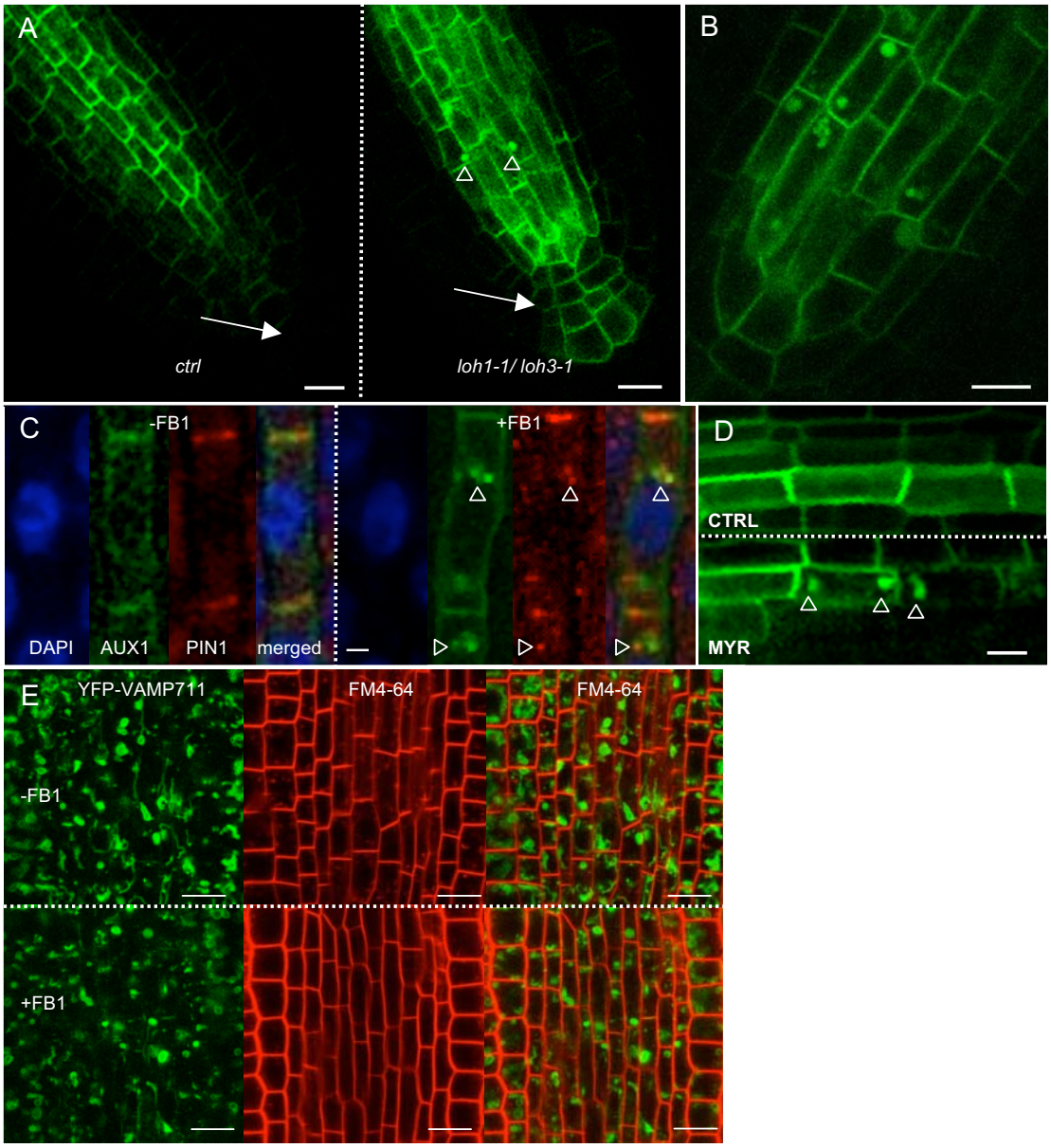

Supp. Fig. 8. Subcellular Distribution of PIN1-GFP and AUX1-YFP and YFP-VAMP711 upon sphingolipid depletion

(A) Expression of *pPIN1:PIN1-GFP* in control (ctrl) and *loh1-1/loh3-1* double mutant. Arrows indicate the columella and arrows head show the presence of PIN1-GFP aggregates.
(B) Detail of *pPIN1:PIN1-GFP* in *loh1-1/loh3-1* double mutant.
(C) Immunolocalization of PIN1 in *pAUX1:AUX1-YFP* secondary root cells treated (+FB1) or not (-FB1) with 2.5µM FB1 for 16h. Cells were counterstained with DAPI. Note that PIN1 aggregates in presence of FB1 and partially colocalize with AUX1-YFP.
(C) Myriocin treatment induces *pAUX1:AUX1:YFP* aggregation
(D) Expression of the vacuolar marker YFP-VAMP711 (Wave 9Y) in the root stele in presence (+FB1) or not of FB1-16h treatment.
Scale bar. 20µm in A, 10 µm in B and D, 2µm in C.

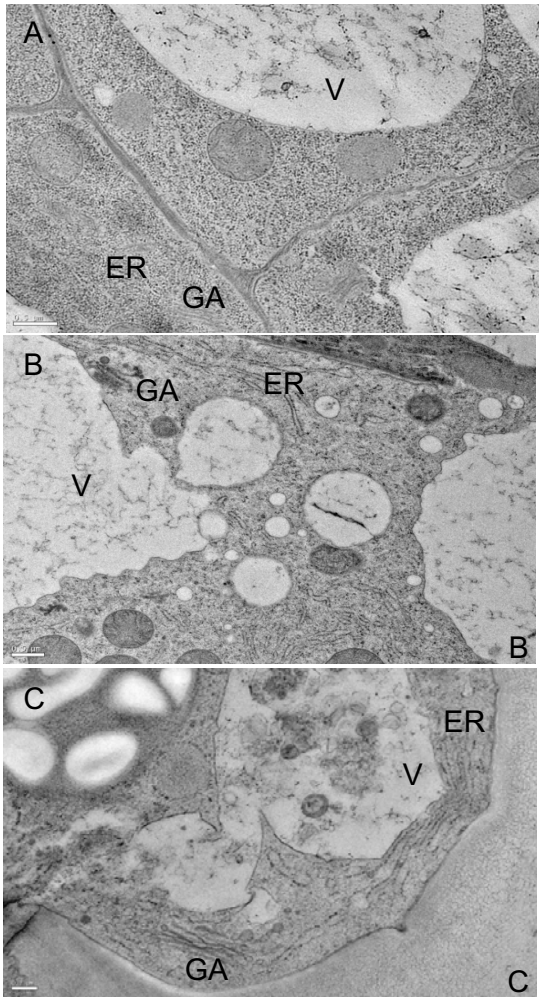

Supp. Fig. 9. Endomembrane ultrastructure is altered in *loh1-1/loh3-1* root cells.

(A) Control cells exhibiting characteristic tubular endoplasmic reticulum (ER), a Golgi stack (GA) and a large vacuole (V).

(B-C) In *loh 1* mutant (B) and *loh1-1/3-1* mutant (C), Golgi ultrastructure is not affected, cytoplasm is often filled with small convoluted vacuole-like structures, with modified ER network.

Scale bar, 200nm

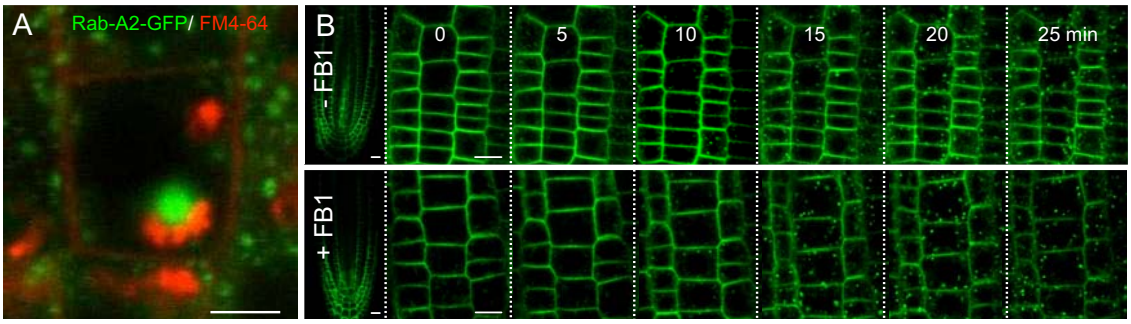

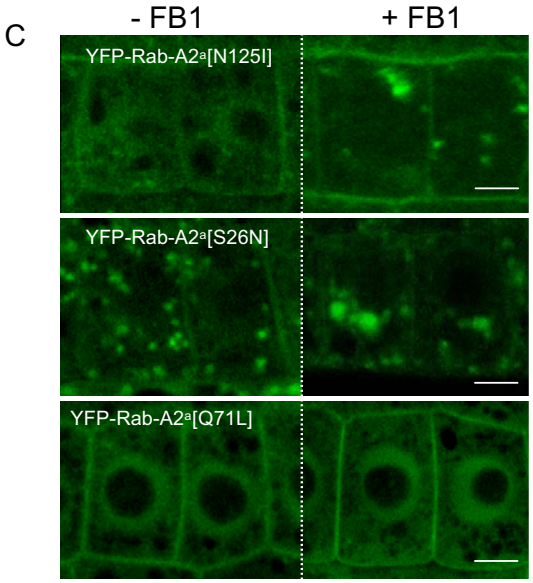

Supp. Fig. 10. **Involvement of endocytosis in YFP-RabA2^a aggregation**

(A) Proximity but no colocalisation between YFP-Rab-A2^a (green) and FM4-64 (red) in presence of FB1.

(B) Kinetics of BOR1-GFP endocytosis in the presence of boron. Five day-old BOR1-GFP seedlings were treated with 2.5µM FB1 for 16h and incubated in the presence of 100µM boric acid (t=0). Internalization of BOR1-GFP was then monitored in FB1 treated seedlings (+FB1) compared to untreated (- FB1). BOR1-GFP are clearly visible in both conditions 10 min after boron application.

(C) Subcellular distribution of Rab-A2^a mutants. YFP-Rab-A2^a[N125I] ^{I} is a nucleotide free mutant showing the same subcellular distribution as wild type YFP-Rab-A2^a but with lower protein levels. YFP-Rab-A2^a[S26N] is the GDP-bound inactive isoform localized exclusively in the cytosol and the Golgi. YFP-Rab-A2^a[Q71L]L is the GTP-bound constitutively active isoform present in the cytosol and at the plasma membrane.

Scale bar : A and C, 5µm; B ,10µm.

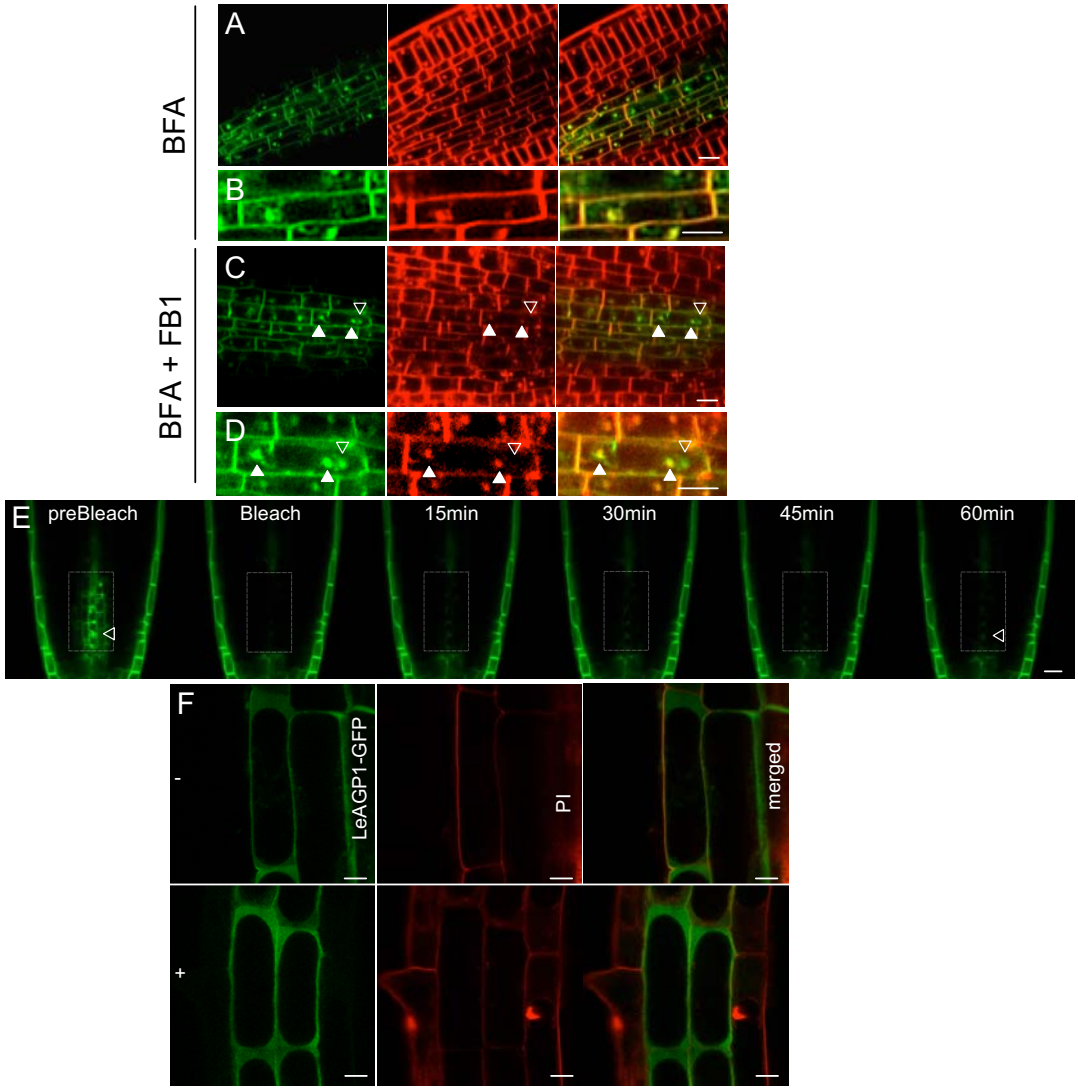

Supp. Fig. 11. Involvement of endocytic and secretory pathways in YFP-RabA2^a aggregation

(A) Partial localization of pPIN1:PIN1-GFP (left) and FM4-64 (right) staining in presence of BFA.

(B) Detail of BFA compartments with presence (open arrow head) or absence (closed arrow head) of colocalization between FM4-64 and PIN1-GFP.

(C) FM4-64 staining of aggregates in FB1-16h treated pPIN1:PIN1-GFP cells in presence of BFA. Partial colocalization is observed (arrow heads).

(D) Detail of FM4-64 staining of aggregates in FB1-treated pPIN1:PIN1-GFP cells showing partial colocalisation of PIN1-GFP with FM4-64 in FB1/BFA compartments.

(E) FRAP analysis of FB1-16h cells expressing pAUX1:AUX1-YFP. AUX1-YFP expressing lateral root (pre-bleach) was bleached and recovery of AUX1-YFP was monitored for 60min.

(F) LeAGP1-GFP expression in absence (-FB1) or presence of 2.5µM FB1 (+ FB1) in plasmolysed epidermal root cells. Cell wall was stained with propidium Iodide (PI).

Scale bar is 10 µm in A, C, E and F and 5µM in B and D.

Sequences (p. 1-5) and alignment (p. 6-10) used for phytogenetic analysis in Supplemental Figure 1B (FASTA format)

>SlAsc-2
MDSIWANNGAPAVSHLFYAIFFAFGFVIVRLFLDRFIFRRLAVLLLRLGTTHLRNDEATRGKIVKCSESM
WKFAYYATIEFCVLKVAYHEPWFLDVKGYFSGWPNQELTAGIKLIYMCQCGFYLYSIAALVVWETRRKDF
AVMMSHHIVTVFLISSSYILSFFRIGIVILALHDGSDVFLEAAKVFKYSEKELGASVLFGCFAVSWFPLR
LVFFPFWVIRSSSYYLCEVLKLSESYDTMIYYFFNTMLLTLLVFHIYWWILIYSMIMKQLRNRGQVGEDI
RSDSEDDD

>PtLOH2
MDPILTFNGSANPSHFLLPIYFAFGFFLARFILDRFIFRKLAIWLLYSKAKAISSRIDEATIVKCSESMW
KLTYYATVEICVLKITCNEPWFRDTKEYFRGWPHQELGFPIMLFYMCQCGFYIYSIAALLIWETRRKDFS
VMMSHHVITVILIGYSYSTSFFRIGTIICAVHDASDVFLEAAKVFKYSGKELSASILFGLFAISWVILRL
VFFPFWIIKATSYELVEFLDLSLAYDKLLYYVFNTMLLMLLVFHIYWWILIYSMIMRQLRNRGRVGEDIR
SDSEDDE

>AtLOH2
MESVSSRGGDPVVKPSMEVWHFQIAVYFAFGFFFLRLVLDRYVFQRIALWLLSTGSAPIKLNDAATRAKI
VKCKESLWKLLYYAACDFFVLQVIYHEPWARDIKLYFHGWPNQELKLSIKLYYMCQCGFYVYGVAALLAW
ETRRKDFAVMMSHHVITIILLSYSYLTSFFRIGAIILALHDASDVFMETAKIFKYSEKEFGASVCFALFA
VSWLLLRLIYFPFWIIRATSIELLDYLDMTSAEGTLMYYSFNTMLLMLLVFHIYWWYLICAMIVRLLKNR
GKVGEDIRSDSEDDDD

>SbLOH2
MAAVRGGEAVSVALLFSLAFFCARLLLDRLVYKPLAVYLFNTKASKLMNDEARQAKIVKFSESSWKLTYY
ASVQAWVLMIIKQEPWSLDMMQYFDGWPNQPIASSLMLFYMCQCGFYIYSIGALVAWETRRKDFAVMMSH
HVITSTLIGVSYLTGFFRIGTIILALHDASDVFLETAKLCKYTEKELGASLFFGLFAISWLLLRLIYFPF
WIIKASSYHSIAFLRKLDEFPTALYYILNTMLLTLLVFHMYWWKLICLMIMRQLNNKGQVTDDVRSDSED
DE

>SlAsc-1
MKNLDHIAASVDWEKESLPEYQDLIFLLFFALFFPVLRFILDRFVFEALAKRMIFGKKTVVNINGREERK
KINKFKESAWKFVYFLSAELLALSVTCNEPWFTDSRYFWAGPGDVVWPNLKMKLKLKLLYMYAGGFYFYS
IFATLYWETRRYDFAAQIIHHVTTVSLIVLSYVYGFARIGSVVLALHDGSDVFMEIAKMSKYSGFDLIAD
IFFSLFALVFTSLRIICYPFWIIRSTCYELLYVLDIQKERTTGIILYFVFNALLICLLVLHLFWFKIILR
MVKNQILSRGHITDDVREDSESDDDHKD

>SlAsc-3
MDWDTESYREYKDLIFIPFFALFFPILRFILDRLVFEALAKRMICGKDAKVIKNGSSIKRKKMNKFKESA
WKFMYFLSAEIFALYVTYNEPWFTNTRYYWTGPGDQVWPDLKMKLKLKGWTMYAGGFYLYSIFALIYWET
RRSDFAAHMIHHITSVSLILLSYIFGMARAGSMAALIHDGSDVLMEIAKMSLYSGFHSVADISFALFALS
WLLLRLIYFPFFIIYSTSYEVLFIVDKEKQQNINGIILYFVINSMLICLLLLHIYWWTLICRVIINILKK
GQFDDVRSDSESESDEDEHKQS

>PtLOH1a
MGFMEYVKSIEWEHESYPGYEDCIVLPLFALFFPFVRFFLDRFVFQKVAQDLIFGKEHQTLDVQSDERRK
KIRKFKESAWKCIYFLSSEILVLCVTYDEPWLVNTKYFWVGPGSQAWPDQKMKLKLKAVYMYAAGFYTYS
IFALIFWETRRSDFGVSMSHHVATVILIVLSYILRFGRVGSVVLAIHDASDVFLEVGKMSKYSGAEGVAS
FAFILFVLSWILLRLIYYPFWVLWSTSYEVLLILDKEKHPVDGPIYYYVFNTLLYCLLFLHVYWWVLIYQ
MLAKQIQARGHLSDDVRSDSEGEDEHED

>PtLOH1b
MGFMEYAKSIQWEHESYPAYEDYIVLPLFSLFFTFVRFFLDRFVFQKLAQRLIFGKEHQMLDAQPDERRK
KIGKFKESAWKCIYFLSAEILVLYVTYDEPWFGNTKYFWVGPGSQVWPDQKMKLKLKGAYMYAAGFYTYS
IFALIFWETRRSDFGVSMSHHVATVILIVLSYILRFGRAGSIVLAIHDASDVFLEVGKMSKYSGAEGIAS
FAFILFVLSWILLRLIYYPFWVLWSTSYEVLLNLDKEKHAVDGPIYYYVFNTLLYGLLVLHIYWWVLMYR
MLVKQIQARGQLSDDVRSDSEGEDEHED

>VvLOH1
MGLLESAASINWEHESFPEYGDFVALPVFAFFFFSVRFFLDRFVFQKLGRILIFGKGGQQLDVGVDEKRK
KLRKFKESAWKCVYFLSAELLALSVTYDEPWFTNTKYFWVGPGNQVWPDQQIKLKLKGLYMYCGGFYTYS
IFALIFWETRRSDFGVSMGHHVATFILIVLSYIFRFARVGSVVLALHDASDVFLEVGKMSKYKGAETTAS
ISFILFVLSWIVLRLIYYPFWILRSTSYEVILTLDKEKHAVEGPIYYYLFNTLLFCLLVLHIYWWVLMYR
MLVKQVQARGQLSDDVRSDSEDEDEHED

>BrLOH1
MGFFESVKSINWEHESFPTYQDFVCLPLFAVFFPSIRFLLDRFVFEKVGRLLIYGKQSPKKNDKKTKIRK
FKESAWKCIYYLSAEVLALSVTYNEPWFTDTLYFWIGPGDQIWPNQQMKIKLKFLYMYTAGFYTYSIFAL
IFWETRRSDFGVSMGHHITTVILIVLSYICRFSRAGSVVLALHDASDVFLEVGKMSKYSGFEGIAAFSFV
LFALSWVLLRLIYYPFWILWSTSYQIIMTVDKEKHPIEGPIYYYMFNTLLFCLLVLHIFWWVLIYRMLVK
QVQDRGKLSEDVRSDSESDDEHED

>AtLOH1
MGLFESVKSIDWEQESFPTYQDLGFLPLFAVFFPTIRFLLDRFVFEKLASLVIYGRMSTNKSDNIKDRKK
NSPKVRKFKESAWKCIYYLSAELLALSVTYNEPWFSNTLYFWIGPGDQIWPDQPMKMKLKFLYMFAAGFY
TYSIFALVFWETRRSDFGVSMGHHITTLVLIVLSYICRLTRAGSVILALHDASDVFLEIGKMSKYCGAES
LASISFVLFALSWVVLRLIYYPFWILWSTSYQIIMTVDKEKHPNGPILYYMFNTLLYFLLVLHIFWWVLI
YRMLVKQVQDRGKLSEDVRSDSESDDEHED

>AtLOH3
MGLLESVKSINWEHESSPVYQDFRVLPLFAVFFPSIRFLLDRFVFEKLAKYLIYGKHRQDMGDDTTERKK
KIRKFKESAWKCVYYLSAEILALSVTYNEPWFMNTKYFWVGPGDQTWPDQQTKLKLKLLYMFVAGFYTYS
IFALVFWETRRSDFGVSMGHHIATLILIVLSYVCSFSRVGSVVLALHDASDVFLEVGKMSKYSGAERIAS
FSFILFVLSWIILRLIYYPFWILWSTSYEVVLELDKDKHPIEGPIYYYMFNTLLYCLLVLHIYWWVLMYR
MLVKQIQDRGKLSEDVRSDSEGEDEHED

>AlLOH3
MGLLESVKSINWEHESSPVYQDFRVLPLFAVFFPTIRFLLDRFVFEKLAKHLIYGKHRQDMGDDTTERNK
KIRKFKESAWKCVYYLSAEILALSVTYNEPWFMNTKYFWVGPGDQTWPDQQTKLKLKLLYMFVAGFYTYS
IFALIFWETRRSDFGVSMGHHIATLILIVLSYVCSFSRVGSVVLALHDASDVFLEVGKMSKYSGAERIAS
FSFILFVMSWIILRLIYYPFWILWSTSYEVVLELDKDKHPIEGPIYYYMFNTLLYCLLVLHIYWWVLMYR
MLVKQIQDRGKLSEDVRSDSEGEDEHED

>OcLOH1
MGFLDLMNPIDWEYESYPQYEDFLVLPLFALFFPTVRFLLDRFVFEKVGRRLIYRKGVQEVENETYEQKK
KIRKFKESAWKCVYYLSAEILALAVTYNEPWFTKTKYFWLGPGNQVWPDQAYKLKLKGLYMFVGGFYTYS
IFALIFWETRRSDFGVSMSHHVATFILIVLSYVLRFARAGSVVLALHDASDVFLEVGKMSKYSGAEAIAS
ISFVLFVLSWVVLRLIYYPFWILWSTSYEVIQTVDKEKHRADGPIYYYVFNSLLFSLLVLHIYWWVLMYR
MLVKQIQARGRVSEDVRSDSEDEDEHED

>OcLOH3
MGFLEMVKSVDWEQESYSQYEDFIVLLFFVLFFPTVRFFLDIFVFEKVSRRLMFGKGMQVVANESEERKK
KIRKFKESAWKCVYFLSADFFALAATYKESWFTNTKHFWEGPGNQAWPDQKYNLKLKGLYMYTGGFYTYS

IFALIFWETRRSDFGVSMGHHVASSVLIVLSYVFGSVVLALHDATDVFLEVGKMSKYSGAETLASCSFVL
FVVSWVILRLIYYPFWILWSTSCEIIPFLDKDTHKVDGPIYYYIFNTLLFSLLVLHIYWFVLMFRMLVDQ
IKAGGQVSGDVRSDSEDEETQDD

>GmLOH1
MTTMSSLSLSLDWHNESYPAYHDFYLLPIFALFFPSLRFFLDRFIFEKVARRLIFGKGHAALDYQTDERR
KKISKFKESAWKCVYYLSAEILALSVTYDEPWFTNTINFWVGPRTQVWPDQKIKLKLKAVYMYAAGFYSY
SIFALIFWETRRSDFGVSMSHHVATVILIVLSYIFRFARVGSVVLALHDASDVFLEIGKMSKYSGAETMA
SFAFILFVLSWIVLRLIYYPFWILWSTSYEVLLTLDKEKHRVDGPIYYYVFNSLLYCLLVMHIYWWVLIY
RMLVKQIQARGKVSEDVRSDSEDEDAHEHED

>GmLOH3
MGTWVLQQVTSIDWNWNHESYPDFRDFSVIPFFALFFPSLRLLLDTFLFEQVARRLIFGKGHKKMDFQTL
ERKKKISKFMESAWKCVYFLSAEIFALAVTYDEPWFTDTRYFWVGPGNQIWPDQKIKLKLKVLYMYAAGF
YTYSILALVFWETKRSDFVVSMGHHVITVILIVLSYIFRFVRVGSVVLALHDASDVFIETGKMSKYSGAE
TTASIAFILFVLCFTVTRIIYYPFWILRSTSYEVVHALKMDLVDGPLYYYVFNSLLYFLQVLHIYWWVLM
LRMLVKQIQEKGKVSEDIRSDSEDEDEHKHEE

>RcLOH3
MGVVGTNGFINWESESYPEAIDFSAVPFFALFFPSVRLFLDTYVFEKLARRLIFGKASTSTDVATHENRK
KINKFKESAWKYIYFSSAEILALSVSYNEPWFTNTKYFWVGPEDQIWPDQKLKLKLKGHYMFVAGFYIYS
IFALIFWETRRSDFAVSMAHHVATVILLVMSYILRFARVGSIVLALHDVCDGFLEIAKMSRYSGYEWISS
IFFVLFVLSWTIFRIIYYPFWILRSTSYEVVLTLDMKKHMVDGPLNYYLFNTLLFCILVFNIYWWILMVR
MVVEQIKARGKVSDDVRSDSEGEDEHDD

>PtLOH3
MGVLGINNLIDWESESYPVATDFIAIPLFAVFFFSVRFVLDKYVFECSARRFIFGKGHVTVDVGKHGNRK
KVNKFKESAWKCVYFLCAEILALYVSYDEPWFTNTKYFWVGPGDQVWPDQKLKFELKVLYMYAGGFYTYS
IFALVFWETRRSDFGVSMGHHIVTVFLIVLSYILRFGRVGAVVLALHDATDVFMEIAKMSKYSGYELMAS
VFFLLFVLFWTILRIIYYPFWILRSTSYEIVSALNKEKQMVDGSIYYYLFNTLLFSLLVLHIYWWILMVG
MVMAQIQAGGQVSDDVRSDSEGEDDHDD

>AtLOH4
MDLKLLSRPDWDQESYPDSSDFLVLIFFAPFFLFLRLILDRCIFERVARRLVVPKGLCADSNERRKKVVK
FKESAWKCLCSFSVEAFALYVTYKEPWFKDTRSFWLGPGDQVWPDQKIKLKMKGMYMFVGGLNVYAFFAL
FFWETRRSDFKVMLVHHIVTSFLIILSYVFRFARIGSVILALHEISDVFLEIGKMCKYSGAETMTSVSFV
LFFLSWTTLRLIYYPFWILWSTSYESIKVKTEYWDKKHLMETGPPLILFYYVFNTLLYCLQILHIYWWIL
IYRVLISQIRAKGKVAKDIRSDSEGEDDEHQD

>AlLOH4
MDLKLLSRDWDHESYPAFSDLWVLIFFAPFFLFLRLILDRFIFERVARRLVVPRGHYGDSNERRKKIVKF
KESAWKCLCSFSVEALALYVTYKEPWFKDTRCFWLGPGDQIWPDQKIKRLKMKGMYMFVGGLNVYAFFAL
FFWETRRSDFKVMLVHHIVTSFLIILSYVFRFARIGSVILALHEISDVFLEIGKMCKYSGAEAMTSVSFV
LFFLSWTALRLIYYPFWILWSTSYESIKVKMEYWDKKNLMETGPNLMVFYYVFNTLLYCLQILHIYWWIL
IYRVLISQIRAKGKVAKDIRSDSEGEDDEHHD

>HsCerS2
MLQTLYDYFWWERLWLPVNLTWADLEDRDGRVYAKASDLYITLPLALLFLIVRYFFELYVATPLAALLNI
KEKTRLRAPPNATLEHFYLTSGKQPKQVEVELLSRQSGLSGRQVERWFRRRRNQDRPSLLKKFREASWRF
TFYLIAFIAGMAVIVDKPWFYDMKKVWEGYPIQSTIPSQYWYYMIELSFYWSLLFSIASDVKRKDFKEQI
IHHVATIILISFSWFANYIRAGTLIMALHDSSDYLLESAKMFNYAGWKNTCNNIFIVFAIVFIITRLVIL
PFWILHCTLVYPLELYPAFFGYYFFNSMMGVLQLLHIFWAYLILRMAHKFITGKLVEDERSDREETESSE

GEEAAAGGGAKSRPLANGHPILNNNHRKND

>HsCerS3
MFWTFKEWFWLERFWLPPTIKWSDLEDHDGLVFVKPSHLYVTIPYAFLLLIIRRVFEKFVASPLAKSFGI
KETVRKVTPNTVLENFFKHSTRQPLQTDIYGLAKKCNLTERQVERWFRSRRNQERPSRLKKFQEACWRFA
FYLMITVAGIAFLYDKPWLYDLWEVWNGYPKQPLLPSQYWYYILEMSFYWSLLFRLGFDVKRKDFLAHII
HHLAAISLMSFSWCANYIRSGTLVMIVHDVADIWLESAKMFSYAGWTQTCNTLFFIFSTIFFISRLIVFP
FWILYCTLILPMYHLEPFFSYIFLNLQLMILQVLHLYWGYYILKMLNRCIFMKSIQDVRSDDEDYEEEEE
EEEEEATKGKEMDCLKNGLRAERHLIPNGQHGH

>HsCerS4
MLSSFNEWFWQDRFWLPPNVTWTELEDRDGRVYPHPQDLLAALPLALVLLAMRLAFERFIGLPLSRWLGV
RDQTRRQVKPNATLEKHFLTEGHRPKEPQLSLLAAQCGLTLQQTQRWFRRRRNQDRPQLTKKFCEASWRF
LFYLSSFVGGLSVLYHESWLWAPVMCWDRYPNQTLKPSLYWWYLLELGFYLSLLIRLPFDVKRKDFKEQV
IHHFVAVILMTFSYSANLLRIGSLVLLLHDSSDYLLEACKMVNYMQYQQVCDALFLIFSFVFFYTRLVLF
PTQILYTTYYESISNRGPFFGYYFFNGLLMLLQLLHVFWSCLILRMLYSFMKKGQMEKDIRSDVEESDSS
EEAAAAQEPLQLKNGAAGGPRPAPTDGPRSRVAGRLTNRHTTAT

>HsCerS5
MATAAQGPLSLLWGWLWSERFWLPENVSWADLEGPADGYGYPRGRHILSVFPLAAGIFFVRLLFERFIAK
PCALCIGIEDSGPYQAQPNAILEKVFISITKYPDKKRLEGLSKQLDWNVRKIQCWFRHRRNQDKPPTLTK
FCESMWRFTFYLCIFCYGIRFLWSSPWFWDIRQCWHNYPFQPLSSGLYHYYIMELAFYWSLMFSQFTDIK
RKDFLIMFVHHLVTIGLISFSYINNMVRVGTLIMCLHDVSDFLLEAAKLANYAKYQRLCDTLFVIFSAVF
MVTRLGIYPFWILNTTLFESWEIIGPYASWWLLNGLLLTLQLLHVIWSYLIARIALKALIRGKVSKDDRS
DVESSSEEEDVTTCTKSPCDSSSSNGANRVNGHMGGSYWAEE

>HsCerS6
MAGILAWFWNERFWLPHNVTWADLKNTEEATFPQAEDLYLAFPLAFCIFMVRLIFERFVAKPCAIALNIQ
ANGPQIAPPNAILEKVFTAITKHPDEKRLEGLSKQLDWDVRSIQRWFRQRRNQEKPSTLTRFCESMWRFS
FYLYVFTYGVRFLKKTPWLWNTRHCWYNYPYQPLTTDLHYYYILELSFYWSLMFSQFTDIKRKDFGIMFL
HHLVSIFLITFSYVNNMARVGTLVLCLHDSADALLEAAKMANYAKFQKMCDLLFVMFAVVFITTRLGIFP
LWVLNTTLFESWEIVGPYPSWWVFNLLLLLVQGLNCFWSYLIVKIACKAVSRGKVSKDDRSDIESSSDEE
DSEPPGKNPHTATTTNGTSGTNGYLLTGSCSMDD

>HsCerS1
MAAAGPAAGPTGPEPMPSYAQLVQRGWGSALAAARGCTDCGWGLARRGLAEHAHLAPPELLLLALGALGW
TALRSAATARLFRPLAKRCCLQPRDAAKMPESAWKFLFYLGSWSYSAYLLFGTDYPFFHDPPSVFYDWTP
GMAVPRDIAAAYLLQGSFYGHSIYATLYMDTWRKDSVVMLLHHVVTLILIVSSYAFRYHNVGILVLFLHD
ISDVQLEFTKLNIYFKSRGGSYHRLHALAADLGCLSFGFSWFWFRLYWFPLKVLYATSHCSLRTVPDIPF
YFFFNALLLLLTLMNLYWFLYIVAFAAKVLTGQVHELKDLREYDTAEAQSLKPSKAEKPLRNGLVKDKRF

>ScLAG1
MTSATDKSIDRLVVNAKTRRRNSSVGKIDLGDTVPGFAAMPESAASKNEAKKRMKALTGDSKKDSDLLWK
VWFSYREMNYRHSWLTPFFILVCVYSAYFLSGNRTESNPLHMFVAISYQVDGTDSYAKGIKDLSFVFFYM
IFFTFLREFLMDVVIRPFTVYLNVTSEHRQKRMLEQMYAIFYCGVSGPFGLYIMYHSDLWLFKTKPMYRT
YPVITNPFLFKIFYLGQAAFWAQQACVLVLQLEKPRKDYKELVFHHIVTLLLIWSSYVFHFTKMGLAIYI
TMDVSDFFLSLSKTLNYLNSVFTPFVFGLFVFFWIYLRHVVNIRILWSVLTEFRHEGNYVLNFATQQYKC
WISLPIVFVLIAALQLVNLYWLFLILRILYRLIWQGIQKDERSDSDSDESAENEESKEKCE

>ScLAC1
MSTIKPSPSNNNLKVRSRPRRKSSIGKIDLGDTVPSLGTMFETKESKTAAKRRMQRLSEATKNDSDLVKK
IWFSFREISYRHAWIAPLMILIAVYSAYFTSGNTTKTNVLHRFVAVSYQIGDTNAYGKGINDLCFVFYYM

IFFTFLREFLMDVVIRPFAIRLHVTSKHRIKRIMEQMYAIFYTGVSGPFGIYCMYHSDLWFFNTKAMYRT
YPDFTNPFLFKVFYLGQAAFWAQQACILVLQLEKPRKDHNELTFHHIVTLLLIWSSYVFHFTKMGLPIYI
TMDVSDFLLSFSKTLNYLDSGLAFFSFAIFVVAWIYLRHYINLKILWSVLTQFRTEGNYVLNFATQQYKC
WISLPIVFVLIGALQLVNLYWLFLIFRVLYRILWRGILKDDRSDSESDEESDESSTTPTDSTPTKKDI

Alignment used for phylogenetic analysis in Supplemental Figure 1B

```
SlAsc-2  ------------------------------------------------------------
PtLOH2   ------------------------------------------------------------
AtLOH2   ------------------------------------------------------------
SbLOH2   ------------------------------------------------------------
SlAsc-1  ------------------------------------------------------------
SlAsc-3  ------------------------------------------------------------
PtLOH1a  ------------------------------------------------------------
PtLOH1b  ------------------------------------------------------------
VvLOH1   ------------------------------------------------------------
BrLOH1   ------------------------------------------------------------
AtLOH1   ------------------------------------------------------------
AtLOH3   ------------------------------------------------------------
AlLOH3   ------------------------------------------------------------
OcLOH1   ------------------------------------------------------------
OcLOH3   ------------------------------------------------------------
GmLOH1   ------------------------------------------------------------
GmLOH3   ------------------------------------------------------------
RcLOH3   ------------------------------------------------------------
PtLOH3   ------------------------------------------------------------
AtLOH4   ------------------------------------------------------------
AlLOH4   ------------------------------------------------------------
HsCerS2  ------------------------------------------MLQTLYDYFWWERLWLP
HsCerS3  ------------------------------------------MFWTFKEWFWLERFWLP
HsCerS4  ------------------------------------------MLSSFNEWFWQDRFWLP
HsCerS5  ----------------------------------MATAAQGPLSLLWGWLWSERFWLP
HsCerS6  ------------------------------------------MAGILAWFWNERFWLP
HsCerS1  ------------------------------------------------------------
ScLAG1   -MTSATDKSIDRLVVNAKTRRRNSSVGKIDLGDTVPGFAAMPESAASKNEAKKRMKALTG
ScLAC1   MSTIKPSPSNNNLKVRSRPRRK-SSIGKIDLGDTVPSLGTMFETKESKTAAKRRMQRLSE

SlAsc-2  ----------------------------------------------MDSIWANNGAP
PtLOH2   ----------------------------------------------MDPILTFNGSA
AtLOH2   ------------------------------------------MESVSSRGGDPVVKPSM
SbLOH2   ------------------------------------------------------MAAVR
SlAsc-1  ----------------------------------------MKNLDHIAASVDWEKESLP
SlAsc-3  ----------------------------------------------MDWDTESYR
PtLOH1a  ------------------------------------------MGFMEYVKSIEWEHESYP
PtLOH1b  ------------------------------------------MGFMEYAKSIQWEHESYP
VvLOH1   ------------------------------------------MGLLESAASINWEHESFP
BrLOH1   ------------------------------------------MGFFESVKSINWEHESFP
AtLOH1   ------------------------------------------MGLFESVKSIDWEQESFP
AtLOH3   ------------------------------------------MGLLESVKSINWEHESSP
AlLOH3   ------------------------------------------MGLLESVKSINWEHESSP
OcLOH1   ------------------------------------------MGFLDLMNPIDWEYESYP
OcLOH3   ------------------------------------------MGFLEMVKSVDWEQESYS
GmLOH1   ----------------------------------------MTTMSSLSLSLDWHNESYP
GmLOH3   ------------------------------------MGTWVLQQVTSIDWNWNHESYP
RcLOH3   ------------------------------------------MGVVGTNGFINWESESYP
PtLOH3   ------------------------------------------MGVLGINNLIDWESESYP
AtLOH4   ----------------------------------------MDLKLLSRPDWDQESYP
AlLOH4   ----------------------------------------MDLKLLSR-DWDHESYP
HsCerS2  VNLTWADLED-RDGRVYAKASDLYITLPLALLFLIVRYFFELYVATPLAALLNIKEKTRL
```

```
HsCerS3  PTIKWSDLED-HDGLVFVKPSHLYVTIPYAFLLLIIRRVFEKFVASPLAKSFGIKETVRK
HsCerS4  PNVTWTELED-RDGRVYPHPQDLLAALPLALVLLAMRLAFERFIGLPLSRWLGVRDQTRR
HsCerS5  ENVSWADLEGPADGYGYPRGRHILSVFPLAAGIFFVRLLFERFIAKPCALCIGIEDSGPY
HsCerS6  HNVTWADLKN-TEEATFPQAEDLYLAFPLAFCIFMVRLIFERFVAKPCAIALNIQANGPQ
HsCerS1  ------------------MAAAGPAAGPTGPEPMPSYAQLVQRGWGSALAAARGCTDCGW
ScLAG1   DSKKDSDLLWKVWFSYREMNYRHSWLTPFFILVCVYSAYFLSGNRTESNPLHMFVAISYQ
ScLAC1   ATKNDSDLVKKIWFSFREISYRHAWIAPLMILIAVYSAYFTSGNTTKTNVLHRFVAVSYQ

SlAsc-2  AVSHLFYAIFFAFGFVIVRLFLDRFIFRRLAVLLLRLGTTHLRNDEATRG-----KIVKC
PtLOH2   NPSHFLLPIYFAFGFFLARFILDRFIFRKLAIWLLYSKAKAISSRIDEAT------IVKC
AtLOH2   EVWHFQIAVYFAFGFFFLRLVLDRYVFQRIALWLLSTGSAPIKLNDAATRA----KIVKC
SbLOH2   GGEAVSVALLFSLAFFCARLLLDRLVYKPLAVYLFNTKASKLMNDEARQA-----KIVKF
SlAsc-1  EYQDLIFLLFFALFFPVLRFILDRFVFEALAKRMIFGKKTVVNINGREERK----KINKF
SlAsc-3  EYKDLIFIPFFALFFPILRFILDRLVFEALAKRMICGKDAKVIKNGSSIKRK---KMNKF
PtLOH1a  GYEDCIVLPLFALFFPFVRFFLDRFVFQKVAQDLIFGKEHQTLDVQSDERRK---KIRKF
PtLOH1b  AYEDYIVLPLFSLFFTFVRFFLDRFVFQKLAQRLIFGKEHQMLDAQPDERRK---KIGKF
VvLOH1   EYGDFVALPVFAFFFFSVRFFLDRFVFQKLGRILIFGKGGQQLDVGVDEKRK---KLRKF
BrLOH1   TYQDFVCLPLFAVFFPSIRFLLDRFVFEKVGRLLIYGKQSPKKNDKKT-------KIRKF
AtLOH1   TYQDLGFLPLFAVFFPTIRFLLDRFVFEKLASLVIYGRMSTNKSDNIKDRKKNSPKVRKF
AtLOH3   VYQDFRVLPLFAVFFPSIRFLLDRFVFEKLAKYLIYGKHRQDMGDDTTERKK---KIRKF
AlLOH3   VYQDFRVLPLFAVFFPTIRFLLDRFVFEKLAKHLIYGKHRQDMGDDTTERNK---KIRKF
OcLOH1   QYEDFLVLPLFALFFPTVRFLLDRFVFEKVGRRLIYRKGVQEVENETYEQKK---KIRKF
OcLOH3   QYEDFIVLLFFVLFFPTVRFFLDIFVFEKVSRRLMFGKGMQVVANESEERKK---KIRKF
GmLOH1   AYHDFYLLPIFALFFPSLRFFLDRFIFEKVARRLIFGKGHAALDYQTDERRK---KISKF
GmLOH3   DFRDFSVIPFFALFFPSLRLLLDTFLFEQVARRLIFGKGHKKMDFQTLERKK---KISKF
RcLOH3   EAIDFSAVPFFALFFPSVRLFLDTYVFEKLARRLIFGKASTSTDVATHENRK---KINKF
PtLOH3   VATDFIAIPLFAVFFFSVRFVLDKYVFECSARRFIFGKGHVTVDVGKHGNRK---KVNKF
AtLOH4   DSSDFLVLIFFAPFFLFLRLILDRCIFERVARRLVVPKGLCA---DSNERRK---KVVKF
AlLOH4   AFSDLWVLIFFAPFFLFLRLILDRFIFERVARRLVVPRGHYG---DSNERRK---KIVKF
HsCerS2  RAPPNATLEHFYLTSGKQPKQVEVELLSRQSGLSGRQVERWFRRRRNQDRPS---LLKKF
HsCerS3  VTP-NTVLENFFKHSTRQPLQTDIYGLAKKCNLTERQVERWFRSRRNQERPS---RLKKF
HsCerS4  QVKPNATLEKHFLTEGHRPKEPQLSLLAAQCGLTLQQTQRWFRRRRNQDRPQ---LTKKF
HsCerS5  QAQPNAILEKVFISITKYPDKKRLEGLSKQLDWNVRKIQCWFRHRRNQDKPP---TLTKF
HsCerS6  IAPPNAILEKVFTAITKHPDEKRLEGLSKQLDWDVRSIQRWFRQRRNQEKPS---TLTRF
HsCerS1  GLARRGLAEHAHLAPPELLLLALGALGWTALRSAATARLFRPLAKRCCLQPR---DAAKM
ScLAG1   VDGTDSYAKGIKDLSFVFFYMIFFTFLREFLMDVVIRPFTVYLNVTSEHRQK------RM
ScLAC1   IGDTNAYGKGINDLCFVFYYMIFFTFLREFLMDVVIRPFAIRLHVTSKHRIK------RI

SlAsc-2  SESMWKFAYYATIEFCVLKVAYHEPWFLDVKGYFSG-----WPNQELTAGIKLIYMCQCG
PtLOH2   SESMWKLTYYATVEICVLKITCNEPWFRDTKEYFRG-----WPHQELGFPIMLFYMCQCG
AtLOH2   KESLWKLLYYAACDFFVLQVIYHEPWARDIKLYFHG-----WPNQELKLSIKLYYMCQCG
SbLOH2   SESSWKLTYYASVQAWVLMIIKQEPWSLDMMQYFDG-----WPNQPIASSLMLFYMCQCG
SlAsc-1  KESAWKFVYFLSAELLALSVTCNEPWFTDSRYFWAGPGDVVWPNLKMKLKLKLLYMYAGG
SlAsc-3  KESAWKFMYFLSAEIFALYVTYNEPWFTNTRYYWTGPGDQVWPDLKMKLKLKGWTMYAGG
PtLOH1a  KESAWKCIYFLSSEILVLCVTYDEPWLVNTKYFWVGPGSQAWPDQKMKLKLKAVYMYAAG
PtLOH1b  KESAWKCIYFLSAEILVLYVTYDEPWFGNTKYFWVGPGSQVWPDQKMKLKLKGAYMYAAG
VvLOH1   KESAWKCVYFLSAELLALSVTYDEPWFTNTKYFWVGPGNQVWPDQQIKLKLKGLYMYCGG
BrLOH1   KESAWKCIYYLSAEVLALSVTYNEPWFTDTLYFWIGPGDQIWPNQQMKIKLKFLYMYTAG
AtLOH1   KESAWKCIYYLSAELLALSVTYNEPWFSNTLYFWIGPGDQIWPDQPMKMKLKFLYMFAAG
AtLOH3   KESAWKCVYYLSAEILALSVTYNEPWFMNTKYFWVGPGDQTWPDQQTKLKLKLLYMFVAG
AlLOH3   KESAWKCVYYLSAEILALSVTYNEPWFMNTKYFWVGPGDQTWPDQQTKLKLKLLYMFVAG
OcLOH1   KESAWKCVYYLSAEILALAVTYNEPWFTKTKYFWLGPGNQVWPDQAYKLKLKGLYMFVGG
OcLOH3   KESAWKCVYFLSADFFALAATYKESWFTNTKHFWEGPGNQAWPDQKYNLKLKGLYMYTGG
GmLOH1   KESAWKCVYYLSAEILALSVTYDEPWFTNTINFWVGPRTQVWPDQKIKLKLKAVYMYAAG
GmLOH3   MESAWKCVYFLSAEIFALAVTYDEPWFTDTRYFWVGPGNQIWPDQKIKLKLKVLYMYAAG
RcLOH3   KESAWKYIYFSSAEILALSVSYNEPWFTNTKYFWVGPEDQIWPDQKLKLKLKGHYMFVAG
PtLOH3   KESAWKCVYFLCAEILALYVSYDEPWFTNTKYFWVGPGDQVWPDQKLKFELKVLYMYAGG
```

```
AtLOH4   KESAWKCLCSFSVEAFALYVTYKEPWFKDTRSFWLGPGDQVWPDQKIKLKMKGMYMFVGG
AlLOH4   KESAWKCLCSFSVEALALYVTYKEPWFKDTRCFWLGPGDQIWPDQKIKRLKMKGMYMFVG
HsCerS2  REASWRFTFYLIAFIAGMAVIVDKPWFYDMKKVWEG-----YPIQSTIPSQYWYYMIELS
HsCerS3  QEACWRFAFYLMITVAGIAFLYDKPWLYDLWEVWNG-----YPKQPLLPSQYWYYILEMS
HsCerS4  CEASWRFLFYLSSFVGGLSVLYHESWLWAPVMCWDR-----YPNQTLKPSLYWWYLLELG
HsCerS5  CESMWRFTFYLCIFCYGIRFLWSSPWFWDIRQCWHN-----YPFQPLSSGLYHYYIMELA
HsCerS6  CESMWRFSFYLYVFTYGVRFLKKTPWLWNTRHCWYN-----YPYQPLTTDLHYYYILELS
HsCerS1  PESAWKFLFYLGSWSYSAYLLFGTDYPFFHDPPSVFYD--WTPGMAVPRDIAAAYLLQGS
ScLAG1   LEQMYAIFYCGVSGPFGLYIMYHSDLWLFKTKPMYRT----YPVITNPFLFKIFYLGQAA
ScLAC1   MEQMYAIFYTGVSGPFGIYCMYHSDLWFFNTKAMYRT----YPDFTNPFLFKVFYLGQAA

SlAsc-2  FYL-YSIAALVVWETRRKDFAVMMSHHIVTVFLISSSYILSFFRIGIVILALHDGSDVFL
PtLOH2   FYI-YSIAALLIWETRRKDFSVMMSHHVITVILIGYSYSTSFFRIGTIICAVHDASDVFL
AtLOH2   FYV-YGVAALLAWETRRKDFAVMMSHHVITIILLSYSYLTSFFRIGAIILALHDASDVFM
SbLOH2   FYI-YSIGALVAWETRRKDFAVMMSHHVITSTLIGVSYLTGFFRIGTIILALHDASDVFL
SlAsc-1  FYF-YSIFATLYWETRRYDFAAQIIHHVTTVSLIVLSYVYGFARIGSVVLALHDGSDVFM
SlAsc-3  FYL-YSIFALIYWETRRSDFAAHMIHHITSVSLILLSYIFGMARAGSMAALIHDGSDVLM
PtLOH1a  FYT-YSIFALIFWETRRSDFGVSMSHHVATVILIVLSYILRFGRVGSVVLAIHDASDVFL
PtLOH1b  FYT-YSIFALIFWETRRSDFGVSMSHHVATVILIVLSYILRFGRAGSIVLAIHDASDVFL
VvLOH1   FYT-YSIFALIFWETRRSDFGVSMGHHVATFILIVLSYIFRFARVGSVVLALHDASDVFL
BrLOH1   FYT-YSIFALIFWETRRSDFGVSMGHHITTVILIVLSYICRFSRAGSVVLALHDASDVFL
AtLOH1   FYT-YSIFALVFWETRRSDFGVSMGHHITTLVLIVLSYICRLTRAGSVILALHDASDVFL
AtLOH3   FYT-YSIFALVFWETRRSDFGVSMGHHIATLILIVLSYVCSFSRVGSVVLALHDASDVFL
AlLOH3   FYT-YSIFALIFWETRRSDFGVSMGHHIATLILIVLSYVCSFSRVGSVVLALHDASDVFL
OcLOH1   FYT-YSIFALIFWETRRSDFGVSMSHHVATFILIVLSYVLRFARAGSVVLALHDASDVFL
OcLOH3   FYT-YSIFALIFWETRRSDFGVSMGHHVASSVLIVLSYVF-----GSVVLALHDATDVFL
GmLOH1   FYS-YSIFALIFWETRRSDFGVSMSHHVATVILIVLSYIFRFARVGSVVLALHDASDVFL
GmLOH3   FYT-YSILALVFWETKRSDFVVSMGHHVITVILIVLSYIFRFVRVGSVVLALHDASDVFI
RcLOH3   FYI-YSIFALIFWETRRSDFAVSMAHHVATVILLVMSYILRFARVGSIVLALHDVCDGFL
PtLOH3   FYT-YSIFALVFWETRRSDFGVSMGHHIVTVFLIVLSYILRFGRVGAVVLALHDATDVFM
AtLOH4   LNV-YAFFALFFWETRRSDFKVMLVHHIVTSFLIILSYVFRFARIGSVILALHEISDVFL
AlLOH4   GLNVYAFFALFFWETRRSDFKVMLVHHIVTSFLIILSYVFRFARIGSVILALHEISDVFL
HsCerS2  FY--WSLLFSIASDVKRKDFKEQIIHHVATIILISFSWFANYIRAGTLIMALHDSSDYLL
HsCerS3  FY--WSLLFRLGFDVKRKDFLAHIIHHLAAISLMSFSWCANYIRSGTLVMIVHDVADIWL
HsCerS4  FY--LSLLIRLPFDVKRKDFKEQVIHHFVAVILMTFSYSANLLRIGSLVLLLHDSSDYLL
HsCerS5  FY--WSLMFSQFTDIKRKDFLIMFVHHLVTIGLISFSYINNMVRVGTLIMCLHDVSDFLL
HsCerS6  FY--WSLMFSQFTDIKRKDFGIMFLHHLVSIFLITFSYVNNMARVGTLVLCLHDSADALL
HsCerS1  FYG-HSIYATLYMDTWRKDSVVMLLHHVVTLILIVSSYAFRYHNVGILVLFLHDISDVQL
ScLAG1   FWAQQACVLVLQLEKPRKDYKELVFHHIVTLLLIWSSYVFHFTKMGLAIYITMDVSDFFL
ScLAC1   FWAQQACILVLQLEKPRKDHNELTFHHIVTLLLIWSSYVFHFTKMGLPIYITMDVSDFLL

SlAsc-2  EAAKVFKYSEKELGASVLFGCFAVSWFPLRLVFFPFWVIRSSSYYLCEVLKLSESYD---
PtLOH2   EAAKVFKYSGKELSASILFGLFAISWVILRLVFFPFWIIKATSYELVEFLDLSLAYDK--
AtLOH2   ETAKIFKYSEKEFGASVCFALFAVSWLLLRLIYFPFWIIRATSIELLDYLDMTSA-----
SbLOH2   ETAKLCKYTEKELGASLFFGLFAISWLLLRLIYFPFWIIKASSYHSIAFLRKLDEF----
SlAsc-1  EIAKMSKYSGFDLIADIFFSLFALVFTSLRIICYPFWIIRSTCYELLYVLDIQKER----
SlAsc-3  EIAKMSLYSGFHSVADISFALFALSWLLLRLIYFPFFIIYSTSYEVLFIVDKEKQ-----
PtLOH1a  EVGKMSKYSGAEGVASFAFILFVLSWILLRLIYYPFWVLWSTSYEVLLILDKEK------
PtLOH1b  EVGKMSKYSGAEGIASFAFILFVLSWILLRLIYYPFWVLWSTSYEVLLNLDKEK------
VvLOH1   EVGKMSKYKGAETTASISFILFVLSWIVLRLIYYPFWILRSTSYEVILTLDKEK------
BrLOH1   EVGKMSKYSGFEGIAAFSFVLFALSWVLLRLIYYPFWILWSTSYQIIMTVDKEK------
AtLOH1   EIGKMSKYCGAESLASISFVLFALSWVVLRLIYYPFWILWSTSYQIIMTVDKEK------
AtLOH3   EVGKMSKYSGAERIASFSFILFVLSWIILRLIYYPFWILWSTSYEVVLELDKDK------
AlLOH3   EVGKMSKYSGAERIASFSFILFVMSWIILRLIYYPFWILWSTSYEVVLELDKDK------
OcLOH1   EVGKMSKYSGAEAIASISFVLFVLSWVVLRLIYYPFWILWSTSYEVIQTVDKEK------
OcLOH3   EVGKMSKYSGAETLASCSFVLFVVSWVILRLIYYPFWILWSTSCEIIPFLDKDT------
GmLOH1   EIGKMSKYSGAETMASFAFILFVLSWIVLRLIYYPFWILWSTSYEVLLTLDKEK------
```

```
GmLOH3   ETGKMSKYSGAETTASIAFILFVLCFTVTRIIYYPFWILRSTSYEVVHALKMD-------
RcLOH3   EIAKMSRYSGYEWISSIFFVLFVLSWTIFRIIYYPFWILRSTSYEVVLTLDMKK------
PtLOH3   EIAKMSKYSGYELMASVFFLLFVLFWTILRIIYYPFWILRSTSYEIVSALNKEK------
AtLOH4   EIGKMCKYSGAETMTSVSFVLFFLSWTTLRLIYYPFWILWSTSYESIKVKTEYWDKKHLM
AlLOH4   EIGKMCKYSGAEAMTSVSFVLFFLSWTALRLIYYPFWILWSTSYESIKVKMEYWDKKNLM
HsCerS2  ESAKMFNYAGWKNTCNNIFIVFAIVFIITRLVILPFWILHCTLVYPLELYPAFFG-----
HsCerS3  ESAKMFSYAGWTQTCNTLFFIFSTIFFISRLIVFPFWILYCTLILPMYHLEPFFS-----
HsCerS4  EACKMVNYMQYQQVCDALFLIFSFVFFYTRLVLFPTQILYTTYYESISNRGPFFG-----
HsCerS5  EAAKLANYAKYQRLCDTLFVIFSAVFMVTRLGIYPFWILNTTLFESWEIIGPYAS-----
HsCerS6  EAAKMANYAKFQKMCDLLFVMFAVVFITTRLGIFPLWVLNTTLFESWEIVGPYPS-----
HsCerS1  EFTKLNIYFKSRGGSYHRLHALAADLGCLSFGFSWFWFRLYWFPLKVLYATSHCSLRTVP
ScLAG1   SLSKTLNYLNSVFTPFVFGLFVFFWIYLRHVVNIRILWSVLTEFRHEGNYVLNFATQQYK
ScLAC1   SFSKTLNYLDSGLAFFSFAIFVVAWIYLRHYINLKILWSVLTQFRTEGNYVLNFATQQYK

SlAsc-2  ------TMIYYFFNTMLLTLLVFHIYWWILIYSMIMKQLRNRGQVGEDIRSDSEDDD---
PtLOH2   -------LLYYVFNTMLLMLLVFHIYWWILIYSMIMRQLRNRGRVGEDIRSDSEDDE---
AtLOH2   ----EGTLMYYSFNTMLLMLLVFHIYWWYLICAMIVRLLKNRGKVGEDIRSDSEDDDD--
SbLOH2   -----PTALYYILNTMLLTLLVFHMYWWKLICLMIMRQLNNKGQVTDDVRSDSEDDE---
SlAsc-1  ---TTGIILYFVFNALLICLLVLHLFWFKIILRMVKNQILSRGHITDDVREDSESDDD-H
SlAsc-3  -QNINGIILYFVINSMLICLLLLHIYWWTLICRVIINIL-KKGQF-DDVRSDSESESDED
PtLOH1a  -HPVDGPIYYYVFNTLLYCLLFLHVYWWVLIYQMLAKQIQARGHLSDDVRSDSEGEDE-H
PtLOH1b  -HAVDGPIYYYVFNTLLYGLLVLHIYWWVLMYRMLVKQIQARGQLSDDVRSDSEGEDE-H
VvLOH1   -HAVEGPIYYYLFNTLLFCLLVLHIYWWVLMYRMLVKQVQARGQLSDDVRSDSEDEDE-H
BrLOH1   -HPIEGPIYYYMFNTLLFCLLVLHIFWWVLIYRMLVKQVQDRGKLSEDVRSDSESDDE-H
AtLOH1   -HP-NGPILYYMFNTLLYFLLVLHIFWWVLIYRMLVKQVQDRGKLSEDVRSDSESDDE-H
AtLOH3   -HPIEGPIYYYMFNTLLYCLLVLHIYWWVLMYRMLVKQIQDRGKLSEDVRSDSEGEDE-H
AlLOH3   -HPIEGPIYYYMFNTLLYCLLVLHIYWWVLMYRMLVKQIQDRGKLSEDVRSDSEGEDE-H
OcLOH1   -HRADGPIYYYVFNSLLFSLLVLHIYWWVLMYRMLVKQIQARGRVSEDVRSDSEDEDE-H
OcLOH3   -HKVDGPIYYYIFNTLLFSLLVLHIYWFVLMFRMLVDQIKAGGQVSGDVRSDSEDEET-Q
GmLOH1   -HRVDGPIYYYVFNSLLYCLLVMHIYWWVLIYRMLVKQIQARGKVSEDVRSDSEDEDA-H
GmLOH3   --LVDGPLYYYVFNSLLYFLQVLHIYWWVLMLRMLVKQIQEKGKVSEDIRSDSEDEDE-H
RcLOH3   -HMVDGPLNYYLFNTLLFCILVFNIYWWILMVRMVVEQIKARGKVSDDVRSDSEGEDE-H
PtLOH3   -QMVDGSIYYYLFNTLLFSLLVLHIYWWILMVGMVMAQIQAGGQVSDDVRSDSEGEDD-H
AtLOH4   ETGPPLILFYYVFNTLLYCLQILHIYWWILIYRVLISQIRAKGKVAKDIRSDSEGEDDEH
AlLOH4   ETGPNLMVFYYVFNTLLYCLQILHIYWWILIYRVLISQIRAKGKVAKDIRSDSEGEDDEH
HsCerS2  ---------YYFFNSMMGVLQLLHIFWAYLILRMAHKFIT--GKLVEDERSDREETESSE
HsCerS3  ---------YIFLNLQLMILQVLHLYWGYYILKMLNRCIF--MKSIQDVRSDDEDYEEEE
HsCerS4  ---------YYFFNGLLMLLQLLHVFWSCLILRMLYSFMK-KGQMEKDIRSDVEESDSSE
HsCerS5  ---------WWLLNGLLLTLQLLHVIWSYLIARIALKALI-RGKVSKDDRSDVESSSEEE
HsCerS6  ---------WWVFNLLLLLVQGLNCFWSYLIVKIACKAVS-RGKVSKDDRSDIESSSDEE
HsCerS1  D-----IPFYFFFNALLLLLTLMNLYWFLYIVAFAAKVLTGQVHELKDLREYDTAEAQSL
ScLAG1   C-----WISLPIVFVLIAALQLVNLYWLFLILRILYRLIW-QG-IQKDERSDSDSDESAE
ScLAC1   C-----WISLPIVFVLIGALQLVNLYWLFLIFRVLYRILW-RG-ILKDDRSDSESDEESD

SlAsc-2  ----------------------------------------
PtLOH2   ----------------------------------------
AtLOH2   ----------------------------------------
SbLOH2   ----------------------------------------
SlAsc-1  KD--------------------------------------
SlAsc-3  EHKQS-----------------------------------
PtLOH1a  ED--------------------------------------
PtLOH1b  ED--------------------------------------
VvLOH1   ED--------------------------------------
BrLOH1   ED--------------------------------------
AtLOH1   ED--------------------------------------
AtLOH3   ED--------------------------------------
AlLOH3   ED--------------------------------------
```

```
OcLOH1   ED----------------------------------------
OcLOH3   DD----------------------------------------
GmLOH1   EHED--------------------------------------
GmLOH3   KHEE--------------------------------------
RcLOH3   DD----------------------------------------
PtLOH3   DD----------------------------------------
AtLOH4   QD----------------------------------------
AlLOH4   HD
HsCerS2  GEEAAAGGGAKSRPLANGHPILNNNHRKND------------
HsCerS3  EEEEEEATKGKEMDCLKNGLRAERHLIPNGQHGH---------
HsCerS4  EAAAAQEPLQLKNGAAGGPRPAPTDGPRSRVAGRLTNRHTTAT
HsCerS5  DVTTCTKSPCDSSSSNGANRVNGHMG-GSYWAEE---------
HsCerS6  DSEPPGKNPHTATTTNGTSGTNGYLLTGSCSMDD---------
HsCerS1  KPSKAEKPLRNGLVKDKRF------------------------
ScLAG1   NEESKEKCE--------------------------------
ScLAC1   ESSTTPTDSTPTKKDI--------------------------
```